Universidade do Minho
Escola de Engenharia

Héloïse le Forestier de Quillien

Development of a multiaxial fabric out of untwisted flax slivers for high-performance composites

Dissertação de Mestrado

Mestrado Integrado em Engenharia Têxtil

Trabalho efetuado sob a orientação de

Professora Ana Maria Moreira Ferreira Rocha

Carsten Uthemann

Setembro 2018

Foreword

This work was carried out at ITA, the Institute of Textile Technology of RWTH Aachen University. It's part of a two-year project, funded by AiF, the German Industrial Research Association, and in collaboration with Puk, the Institute of Polymer Materials and plastic Engineering of TU Clausthal University. The aim of the project is to develop a high-performance natural fiber composite material for structural parts.

Acknowledgements

I would like to express my deep gratitude to Carsten Uthemann, my research supervisor, for his guidance, time, encouragement and useful critiques for this research work.

I would like to thank Markus Wensing, master student at ITA, for his help, explanations and support.

My grateful thanks are also extended to Stefan Hesseler, Lukas Lechthaler, Oscar Bareiro and Gözdem Dittel, PhDs at ITA, for their welcoming and constant support!

I would also like to thank Niklas Birk, for his help in the evaluation of partial solutions for the weft-insertion system, and Monika Steffens, head of the textile test laboratory, for helping me with the characterization of the flax slivers.

I would also like to extend my thanks to the staff of the library at ITA for helping me in finding useful resources.

A big thank you also to Professor Manuela Ferreira, for her support, Professor Rosa Vasconcelos, for her care, and Professor Ana Maria Moreira Ferreira Rocha, for accepting to supervise my work.

Finally, I wish to thank my universities, Minho University and ENSAIT, for the valuable education I had there, helping me find my way professionally, and also the ERASMUS, MERMOZ and CROUS organizations, for the financial support of my studies.

Abstract

Flax fibers represent an ecological alternative for glass and carbon fiber reinforced plastics (FRP). Although flax fibers have valuable properties for applications in FRP, they are currently not fully exploited. Today, flax FRP are mostly used in components with low-mechanical loads. This research presents a solution that could enable the application of flax fiber in the FRP industry for structural components. The solution presented here is the production of a multiaxial fabric reinforcement out of untwisted flax fiber slivers. This fabric allows to maximize the potential of flax fibers, exploiting the mechanical properties of flax fibers and skipping the spinning process that is expensive and has an important ecological footprint. However, in order to process the untwisted flax slivers into a multiaxial fabric, the multiaxial warp-knitting machine has to be adapted. The aim of this work is the investigation and validation of a new weft-insertion system, adapted for the processing of untwisted flax slivers. Untwisted flax slivers are hard to handle, they tend to get loose or break during production. In this research, different guiding and spreading systems are presented and evaluated. After evaluating all the solutions on the basis of implementability, costs and installation space, a system with guiding rollers and an air spreading device method were selected for further testing. A test stand was constructed, allowing to validate the solution and to determine the influencing parameters of the guiding and spreading of the slivers. After a kinematic study of the multiaxial warp-knitting machine, the construction of the new system was initiated. But the new system could not be incorporated to the machine over the project period, as the construction took longer than planned. It was therefore not possible to produce the multiaxial flax fabric.

Resumo

As fibras de linho representam uma alternativa ecológica para compósitos com fibra de vidro e carbono. Embora as fibras de linho tenham propriedades valiosas para aplicações em compósitos, elas atualmente não são totalmente aproveitadas. Hoje, compósitos de linho são usados principalmente em componentes com baixa carga mecânica. Esta pesquisa apresenta uma solução que poderia permitir o emprego de fibra de linho na indústria de compósitos para componentes estruturais. A solução apresentada aqui é a produção de um reforço de tecido multiaxial a partir de fitas de linho sem torção. Este tecido permite maximizar o potencial das fibras de linho, explorando as propriedades mecânicas da fibra e evitando o processo de fiação que é caro e tem um importante ônus ecológico. No entanto, a fim de processar as fitas de linho sem torção em um tecido multiaxial, a máquina de produção destes tecidos tem de ser adaptada. O objetivo deste trabalho é a investigação e validação de um novo sistema de inserção de trama, adaptado para o processamento de fitas de linho sem torção. Fitas de linho sem torção são difíceis de manusear, elas tendem a quebrar durante a produção. Nesta pesquisa, diferentes sistemas de condução e espalhamento são apresentados e avaliados. Depois de avaliar todas as soluções com base na viabilidade, custos e espaço de instalação, um sistema de rolos de condução e um dispositivo de espalhamento de ar foram selecionados para testes adicionais. Uma bancada de testes foi construída, permitindo validar a solução e determinar os parâmetros de influência de condução e espalhamento das fitas. Depois de um estudo cinemático da máquina de tecido multiaxial, a construção do novo sistema foi iniciada. Mas o novo sistema não pôde ser incorporado à máquina durante o período do projeto, pois a construção levou mais tempo do que o planejado. Portanto, não foi possível produzir o tecido de linho multiaxial.

Table of Contents

Table of Tables

Table of Figures

List of abbreviations and acronyms

CFRP: Carbon Fiber Reinforced Plastics

FFRP: Flax Fiber Reinforced Plastics

FRP: Fiber Reinforced Plastics

GFRP: Glass Fiber Reinforced Plastics

NFRP: Natural Fiber Reinforced Plastics

UD: Uni-directional

1 Introduction

Due to global warming, there is an increasing interest towards reducing CO_2 emissions and improving resource efficiency (Ruth Heuss *et al.*, 2012). Legislation is increasingly being introduced to drive industries to aim for energy and CO_2 reduction. For example, in 2016, the EU set mandatory emission reduction targets. By 2016, the average car emission should be of 118,1 g of CO_2/km travelled and the target keeps increasing, as the average car emission targeted for 2021 is of 95 g of CO_2/km travelled (EC (European Commission), 2009). If the average CO_2 emissions exceed the limit value, the manufacturer has to pay a penalty according to the excess of emission. To respond to those restrictions, industries are in quest of solutions. For example, the transportation sector is increasingly looking for ways to reduce weight, as it decreases the fuel consumption. In fact, a weight reduction of 10 kg for a car means a reduction of 1 g of CO_2/km travelled (Faurecia, 2016).

A promising approach for weight reduction lies in the application of fiber reinforced plastics (FRP)(ICICI, 2015), which can be lighter and have similar or even better mechanical properties than conventional materials such as steel or aluminum (JEC, 2012). Carbon fiber reinforced plastics (CFRP) for example can save up to 60 % of weight compared to steel and 30 % compared to aluminum (Robert Crow, 2015). Nevertheless, the production of conventional reinforcement fibers such as carbon or glass fibers requires high amounts of energy, which in return leads to high CO_2 emissions, when using fossil fuels (Deng and Tian, 2015).

By using natural fiber reinforced plastics (NFRP), energy savings of approx. 40 % can be achieved compared to glass fiber reinforced plastics (GFRP). Also, natural fibers, compared to glass fibers, have the advantage of being renewable, recyclable, bio-degradable and nontoxic, they have lower density and better specific stiffness properties (see Figure 1) (JEC, 2012; Shah, Schubel and Clifford, 2013).

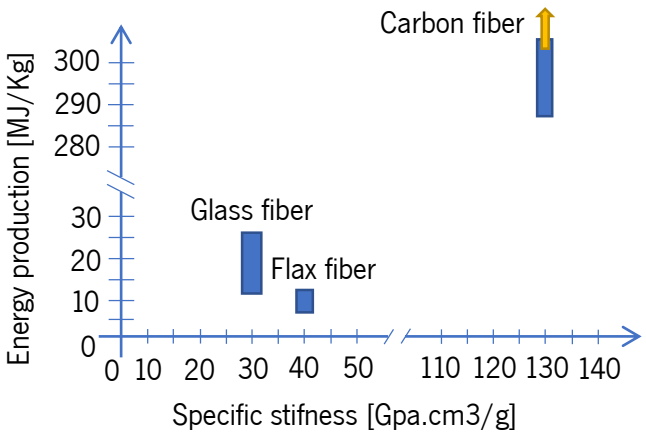

Figure 1 Comparison of carbon, glass and flax fiber energy for production and specific stiffness (JEC, 2012)

Despite its promising properties, NFRP are mainly used for non-structural components with low mechanical properties. This is due to the fact that the potential of the natural fiber is currently not being fully exploited. Conventional reinforcement fabrics are generally produced on the basis of twisted yarns. The twisting, however, does not allow the fibers to be fully aligned in the load direction, which reduces the mechanical properties of the composite.

One solution for improving the mechanical properties, is the production of reinforcement fabrics out of untwisted natural fiber slivers (Figure 2). At the same time, the cost and time intensive spinning process can be saved, making the process more efficient (Dissanayake *et al.*, 2009).

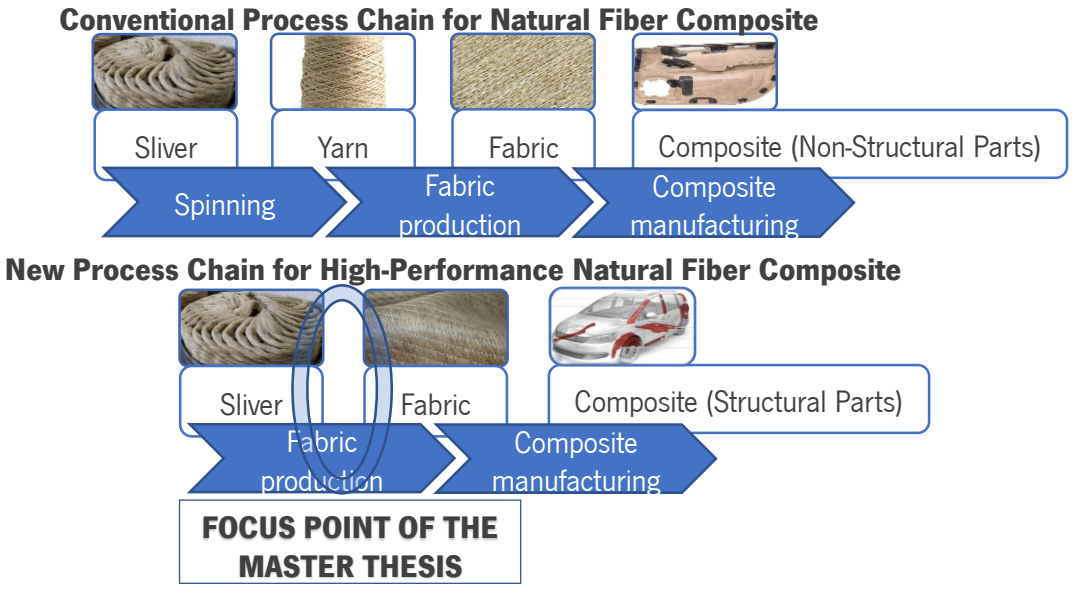

Figure 2 Focus point of master thesis

When working with slivers, the most adapted reinforcement architecture is the multiaxial fabric (Cherif, 2015). However, conventional machines to produce multiaxial fabrics are only adapted for the processing of yarns or continuous fibers – such as carbon, glass, etc. Within the scope of this master thesis, the focus lies on the analysis of the potential of NFRP in substituting GFRP and, hence, the identification of an adapted lay-up concept for the processing of untwisted flax slivers.

The first step of the following work is a comprehensive state of the art regarding FRP, especially CFRP and GFRP, in order to identify the deficits of the FRP market. The second step is an investigation of the potential of NFRP and how they could respond the deficits of the market. The investigated solution is the production of multiaxial fabrics out of flax slivers. Thereupon, so as to adapt the processing of flax slivers with the multiaxial with weft-insertion machine, a new weft-insertion system is conceived, following the

Guidelines VDI 2221 (Systematic approach to the development and design of technical systems and products with the realization). Primarily, a requirements list is set up, and from it, derives a function structure to ponder possible solutions. Once the possible solutions for the weft-insertion system are explored and combined, by means of a morphological box, the solution concepts are further elaborated and evaluated until the most practical concept is selected. A test stand of the concept is built and tested for validation and the project is concluded with the reached objectives.

2 State of the art

2.1 Fiber Reinforced Plastics

Over the past few years, FRP have gradually taken a huge importance in the industry, mostly in the replacement of steel reinforcements. In fact, although FRP are pricier than steel, they present many advantages such as lightness, insensitiveness to corrosion, high strength and other advantages, which will vary accordingly to the nature of FRP (Nad, Kolleger and Horvatits, 2007).

Fiber reinforced plastics are composites. A composite material is a material which is composed of at least two distinct phases, with different properties. In the case of FRP, those phases correspond to the polymer matrix and the fiber reinforcement, illustrated in Figure 3 (Autar K. Kaw, 2006):

- **Polymer matrix**: The matrix transmits the forces to the fiber reinforcement and protects it. It also defines the shape of the composite part (Autar K. Kaw, 2006);
- **Fiber reinforcement**: The reinforcement is responsible for the mechanical properties of the material; including stiffness and strength (Autar K. Kaw, 2006).

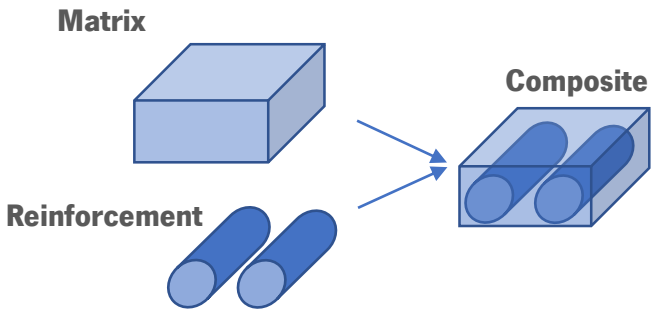

Figure 3 Composite structure

FRP have also a third important phase to consider: the **interphase**. Given the presence of different phases with different properties, a good junction between the phases is essential to ensure good mechanical characteristics for the composite material (Soulat, 2015).

The type of reinforcing fiber is decisive for the mechanical performances of the composite part. When selecting the fiber, the mechanical properties of the fibers are not the only factor to take into consideration, as it is also important to consider the cost and disposability of the fiber.

The most common fibers in composites for structural applications are carbon fibers and glass fibers:

- **Carbon fibers** are the second most used fibers within the composite industry, with a global demand, in 2015, of 91 thousand tones (Kühnel and Kraus, 2015). They have very good mechanical properties but are expensive and therefore are mostly used for 'high-end' applications (ex: aerospace industry);
- **Glass fibers** represent 95 % of the total volume of composites production, with a global demand, in 2016, of more than 4,5 million tones (Mazumdar *et al.*, no date; Dr Elmar Witten, 2014). They are used for applications in which the mechanical loading is moderate and when the cost of product must be limited.

Both reinforcements are further described in the following parts of the work.

2.2 Carbon fiber reinforced plastics

Carbon fibers first patent was deposited in 1877, by Thomas Alva Edison, who used carbon fibers in electric lamps. By then, carbon fiber had poor mechanical properties. It was only around 1950 that the mechanical properties were highly improved and that the first applications were found in the composite industry (NPTEL, 2013b). Carbon fibers can be classified in three different groups of properties; Standard Modulus, Intermediate Modulus and High Modulus, shown in Table 1. Standard modulus carbon fibers are the most produced ones (representing 80-90 % of the market) (Das *et al.*, 2016).

Table 1 Carbon Fiber Types (Das *et al.*, 2016)

Type	Modulus (Gpa)	Strength (Mpa)	Tow Size (K)
Standard Modulus	230	3500	12 – 50
Intermediate Modulus	400	5000	3 – 24
High Modulus	500	3500	1 – 12

CFRP are very durable. They have very good mechanical properties (high specific strength, high specific stiffness). They possess a good strength to weight ratio. Also, they have good chemical stability, low thermal expansion and high vibration resistance (NPTEL, 2013b), (University of Arkansas, 2016), (Barnes and Composites World, 2016).

2.2.1 Carbon fiber production

Carbon fibers are made out of precursors, mainly polyacrylonitrile (PAN), by 90 %, and petroleum pitch precursors. Precursors are organic polymers that form long strings of molecules bounded by carbon atoms. The composition of the precursor is very diverse, each company having their own composition (ZOLTEK, 2018). To manufacture the carbon fiber, there are six main process steps (Figure 4):

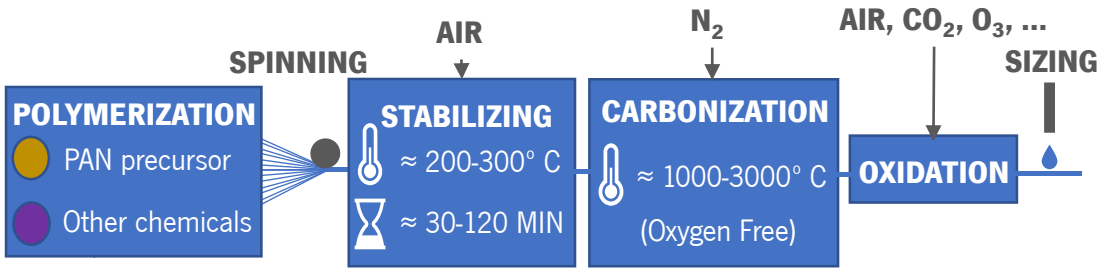

Figure 4 Carbon fiber production

- **Polymerization:** The chemical polymerization of the precursor material;
- **Spinning:** The production of the precursor, generally by a wet spinning process (Energetics Incorporated, 2016);
- **Stabilization:** The chemical preparation of the precursors before the carbonization, in order to thermally stabilize the linear atomic bonds. The fibers are heated in air to about 200-300 °C for 30-120 minutes, causing the fibers to react with oxygen molecules and allowing a rearrangement of the atomic bonds (ZOLTEK, 2018);
- **Carbonization:** The burn off of non-carbon atoms. The fibers are heated within furnaces, in an oxygen-free atmosphere, to about 1000-3000 °C for several minutes. When the non-carbon atoms are burned off, the remaining carbon atoms are tightly bonded, forming carbon crystals aligned along the fiber axis (McConnell, 2008; Energetics Incorporated, 2016; ZOLTEK, 2018).
- **Oxidation:** The addition of oxygen atoms to the surface of the fiber in order to give better bonding properties to the fibers. The fibers are immersed in several gases; air, carbon dioxide or ozone. The resulting PAN fiber is composed of 50-65 % of carbon molecules and the rest is hydrogen, nitrogen and oxygen molecules (McConnell, 2008; ZOLTEK, 2018).
- **Finishing (Sizing):** The fibers are coated to protect them from eventual damage during processing and to enhance the fibers bonding properties. The coating materials are chosen according to the resin material used for the composite. The coats can be made out of epoxy, polyester, nylon, urethane and other materials (Energetics Incorporated, 2016; ZOLTEK, 2018).

2.2.2 Current applications

CFRP can be found in various applications in the industry. Due to the very high mechanical properties, they are mainly used for structural high-end applications. According to the mechanical properties of the carbon fibers, CFRP can be found in different applications (Table 2).

Table 2 Carbon fiber types by application (Das *et al.*, 2016)

Type	Application
Standard Modulus	Automotive, Aerospace
Intermediate Modulus	Pressure Vessels, Wind Turbine Blades, Aerospace
High Modulus	Aerospace

They are mainly found in aerospace and defense applications, representing 30 % of the CFRP market (Figure 5), but also in automotive, marine, sports goods, civils constructions, biomedical applications and others (NPTEL, 2013b).

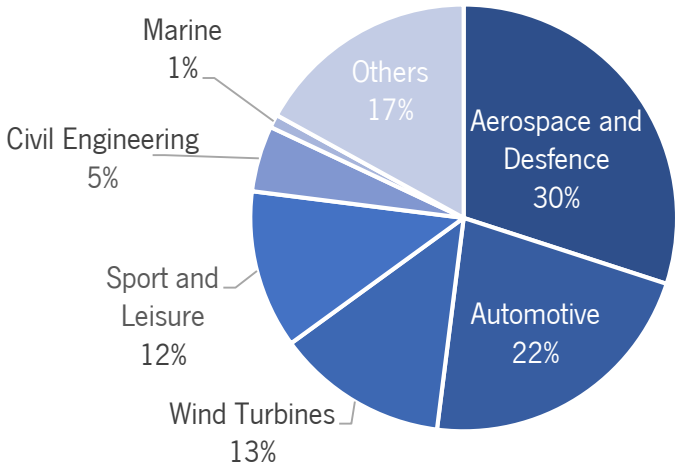

Figure 5 CFRP demand by application (Kühnel and Kraus, 2015)

2.3 Glass fiber reinforced plastics

The patent on glass fiber was deposited in 1933 by employees of Owens-Illinois Glass Co. (Tuf-Bar, 2018b) and since then, glass fibers have grown rapidly in the FRP market, representing 95 % of the total volume of composites production in the world (Dr Elmar Witten, 2014).

Glass fibers can present different characteristics, accordingly to the type of glass fiber (Table 3). E-Glass fibers are the most exploited (90 % of the GFRP market) (Wallenberger, Watson and Hong, 2001).

Table 3 Glass Fiber Types (Wallenberger, Watson and Hong, 2001) (NPTEL, 2013a)

Type	Property/Characteristic
E-Glass	Low electrical conductivity
S-Glass	High strength
C-Glass	High chemical durability
M-Glass	High stiffness
A-Glass	High alkali or soda lime glass
D-Glass	Low dielectric constant

GFRP are light and have good mechanical properties (high flexural strength, high tensile strength, high compressive strength). They present resistance to most chemicals and are non-conductive. GFRP are cost-effective, they need low maintenance and are durable (Stromberg, 2012; Antop Global Technology Co., 2017; Tuf-Bar, 2018a).

2.3.1 Glass fiber production

Glass fibers are made from Silica (SiO_2) sand which is melted at 1720 °C. When heated at higher temperatures then 1200 °C, SiO_2 crystalizes and becomes quartz. To prevent this from happening, SiO_2 is heated to 1720 °C and cooled quickly, producing an amorphous and randomly orientated atomic structure that becomes glass (Composites World, 2009).

In order to manufacture glass fiber, there are five main process steps, illustrated by Figure 6 :

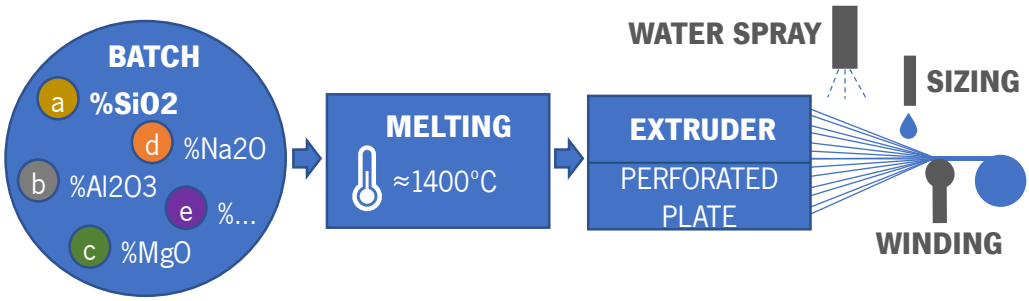

Figure 6 Glass fiber production process (Composites World, 2009; NPTEL, 2013a; Saint-Gobain, 2018)

- **Batching:** The batch is composed of SiO_2 with a mixture of different materials. By adding additives, the process can be done at lower temperatures. The additives are selected in order to facilitate the processing or to give a specific characteristic to the fiber. For example, for E-Glass, Boron Oxide (B_2O_3) can be added to prevent clogging of the nozzles during the spinning. For S-Glass, a mixture of SiO_2-Al_2O_3-MgO with a high percentage of SiO_2 is formulated in order to increase the tensile strength of the resulting glass fiber (Composites World, 2009);
- **Melting:** The mixture from the batch is melted in furnaces at high temperatures, approx. 1400 °C. The molten glass goes into the refiner at lower temperature, approx. 1370 °C (Composites World, 2009);
- **Spinning**: The molten glass is extruded through a platinum/rhodium alloy with 200 to 8000 orifices. The temperature is controlled to maintain glass viscosity constant. The filaments are cooled down by water jets at the exit. The extruded molten glass is then mechanically drawn by a high-speed winder, into filaments with a diameter ranging from 4 µm to 34 µm (Composites World, 2009).
- **Coating:** The fibrous elements are sized by lubricants, binders and/or coupling agents. Lubricants protect the fibers from eventual damage during the process. Coupling agents enhance the fibers compatibility with certain resins (Composites World, 2009).
- **Drying/Packaging:** The filaments are collected, forming a glass strand of 51 to 1624 filaments. They are dried in an oven and are processed into chopped fiber, roving or yarn (Composites World, 2009).

2.3.1 Current applications

GFRP are used for applications in which the mechanical stress is moderate and when the product costs must be limited. They can be found in many sectors such as in the automotive industry, in car motors, rubber tires, structural parts - such as the chassis (NPTEL, 2013a). Also, in civil engineering, in highway applications (bridges, overpasses, ...), mining and tunneling, marine applications (seawalls, retaining walls, ...) and transport structures (bus stops, runways, ...) (Tuf-Bar, 2018b).

2.4 Disadvantages

2.4.1 Carbon fiber reinforced plastics

The manufacturing process for CFRP is very wasteful. CFRP are hard to recycle and approximately a third of the production ends up in landfill. The processes for recycling CFRP are expensive and recent (ELG Carbon Fibre Ltd, 2018). Also, CFRP are very expensive. Carbon fiber can cost more than 10 €/kg (Laboratory, 2012) - 10 times more expensive than glass fiber. Carbon fibers require high amounts of energy to produce. In fact, the total energy consumption to produce carbon fiber (from PAN precursor), can vary from **286 MJ/kg**, for standard-modulus carbon fibers, to **1134 MJ/kg**, for high-modulus carbon fibers (Suzuki and Takahashi, 2005; Song, Youn and Gutowski, 2009; Das and Warren, 2014; Sunter *et al.*, 2015; Energetics Incorporated, 2016).

The most energy consuming process is the oxidation and carbonization, as illustrated in Figure 7.

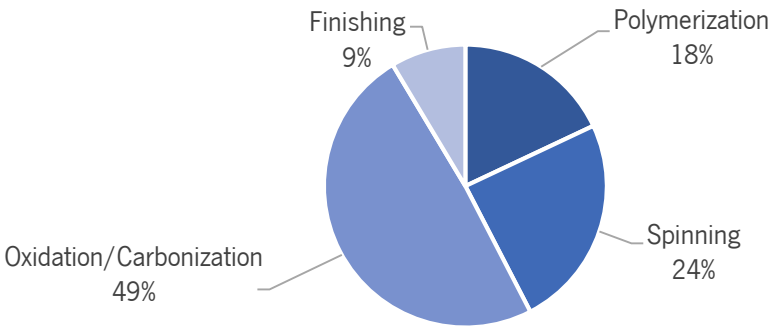

Figure 7 Energy consumption by sup-process for carbon fiber production (Energetics Incorporated, 2016)

2.4.2 Glass fiber reinforced plastics

Glass fibers require high amounts of energy and CO_2 to produce. In fact, the total amount of energy consumption can vary from **10,74** to **25,80 MJ/kg** (Table 4). The most energy consuming process is melting and refining.

Table 4 Energy consumption for E-glass fiber production (MJ/Kg) (Ruth, 1997; Diener and Siehler, 1999; DOE, 2002; Rue *et al.*, 2007; Worrell *et al.*, 2008; Song, Youn and Gutowski, 2009; Dai *et al.*, 2015)

Energy consumption for E-glass fiber production (MJ/Kg)							
Processing steps	Ruth, 1997	Worrell, 2008		DOE, 2002	Diener, 1999	Young, 2009	Rue, 2007
Batch preparation	1,21	1,16	1,16	0,72	—	—	0,72
Melting and refining	10,43	5,91	11,08	8,86	—	—	6,86
Forming	7,64	2,64	5,28	7,60	—	—	1,58
Post-forming	2,89	3,48	3,48	4,11	—	—	1,58
Total	**22,18**	**13,19**	**21,00**	**21,29**	**25,80**	**13-32**	**10,74**

2.4.3 Alternative

With the increasing concern of the industries in improving the environmental impact of their products by reducing energy and CO2 emissions, CFRP and GFRP present relevant solutions: They are light, very performant and can replace steel or aluminum in many applications. But both need a lot of energy and CO_2 to produce, they are hard to recycle and are produced from non-renewable sources. Also, in 2005, the EU set a directive that automotive components should be recycled and reused by at least 85 % by 2015 (JEC, 2012).

Natural fibers seem to respond to the composite market needs (Autar K. Kaw, 2006). They need less energy and CO_2 to produce, they are renewable, recyclable, bio-degradable, nontoxic and have good mechanical properties, equivalent to glass fibers in stiffness for example (JEC, 2012; Shah, Schubel and Clifford, 2013). In the following part of this thesis, the potential of NFRP in the composite industry is analyzed.

3 Analysis of the potential of natural fiber reinforced plastics

Natural fibers have already been used as composites not less than one century ago, some airplanes seats and fuel tanks were made with natural fibers and polymeric binders (Bledzki and Gassan, 1999; Sparnins, 2006). However, the industry has not given as much interest to natural fibers as to glass fibers, which presents many benefits, such as lower costs and larger-scale production. Yet, interest in natural fibers has recently aroused, due to the potential regarding weight saving, low raw material price and ecological advantages (FlexForm Technologies, 2013). The market for NFRP is forecasted to hugely grow from 2015 to 2024 (Figure 8) (Grand View Research, 2016).

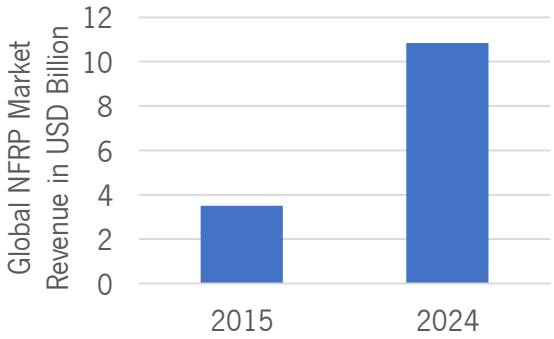

Figure 8 Global NFRP market revenue forecast (Grand View Research, 2016)

3.1 Natural fibers

To examine the potential of natural fibers in composites structures, it is important to analyze their mechanical properties. Some properties of natural fibers are regrouped in Table 5.

Table 5 Natural fibers mechanical properties [50]

Fibre	Density (g/cm^3)	Diameter (µm)	Tensile Strength (MPa)	Young's Modulus (GPa)	Specific strength (MPa/g/cm^3)	Elongation at break (%)
Flax	**1,52**	**40 - 600**	**345 - 1500**	**27,6-85**	**227 - 986,8**	**2,7 - 3,2**
Hemp	1,51	25 - 500	690	**70**	457	1,6
Ramie	1,55	/	400 - 938	**61 - 128**	258,1 - 605,2	1,2 - 3,8
Coir	**1,1 - 1,46**	100 - 460	131 - 220	4 - 6	119,1 - 150,7	**15 - 40**
Cotton	1,5 - 1,6	**12 - 38**	287 - 800	5,5 - 12,6	191,3 - 500	7 - 8

The most relevant fiber to work with is flax fiber. It has in average, the best tensile strength and specific strength and has good elastic modulus (Young modulus). In the following parts of the work, flax fiber will be the main focus of study and will be further analyzed.

3.2 Flax fibers

Flax fiber is considered as an eco-friendly natural fiber. It needs less water and energy to produce than cotton for example. Also, the whole plant can be used, there is no waste or residual product. Long fibers are used for fabrics, short fibers for non-woven fabrics, straws for agricultural harvesting, seeds for paint or resin oils and bagasse for feeding animals (Groupement National Interprofessionnel des Semences (GNIS), 2006).

3.2.1 Fiber production

Flax is a plant, member of the Linaceae family. It is generally cultivated in temperate climate with slight humidity. In Europe, it grows from April to June and reaches maturity by August. It can reach 1,2 m in height and has a thin stem of 1 to 3 mm thickness. Once the plant is fully matured, the plant is pulled out, not cut, allowing to exploit the whole plant length (Mosiniak and Prat, 2005).

To exploit the fibrous parts of the plant, the woody parts of the plant stems must be separated from the fibrous parts. To do so, the following operations are held:

- **Retting:** Dissolving or rotting of the cellular tissues and pectins surrounding the bast-fiber bundles, by means of micro-organisms and moisture. The main method for retting is “water retting”. The flax is submerged in water, which swells the inner cells and thus increases the moisture absorption and decay (by producing bacteria in the flax). It helps the future separation of the woody part from the fibrous part (‘Retting’, 2009).
- **Scutching:** Separation of the impurities (ex: woody part), from the fibers. There are two methods for scutching; hand scutching (the flax is scraped by a knife) and machine scutching (the stalks are crushed between two metal rollers) (‘Scutch’, 1989).
- **Combing (or Heckling):** Splitting and straightening of the fibers, removing the remaining impurities and separates the short fibers to the long fibers (‘Heckle’, 1989). The flax is drawn through heckling combs, which allows to straighten and clean the fibers and forms slivers. The short fibers form tows that are used for low grade yarns and the long fibers are used for high quality yarn.

- **Draw frame:** After the combing operation, in order to prepare the sliver to be spun, the slivers need to be drafted. The drafting step is the main influencer of the yarn quality. It allows to improve the fiber orientation, evenness and reduces the cross-section of the sliver. The most common process for drafting is: the roller drafting (Lord, 2003). It is executed by fixing the fibers to a series of roller pairs, with steel bottom rollers and coated top rollers (Figure 9). The speed of the roller pairs increases from roller pair to roller pair, ensuing that the fibers slide from each other and are drawn apart. In Figure 9, the zone (B) is the break draft zone, which prepares and straighten the fibers for the main draft zone (A).

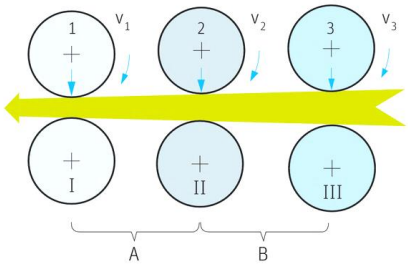

Figure 9 Roller drafting arrangement (Klein, 2016a)

- **Coiling:** The slivers coming from the drafting system pass through a condenser that produces lateral fiber migration and enhances the sliver cohesion. The sliver passes through a trumpet, which further condenses the sliver. Take-up rolls discharge the sliver into a can, in a determined pattern (Lord, 2003). The staple fiber slivers are usually stored in delivery cans and later spun.

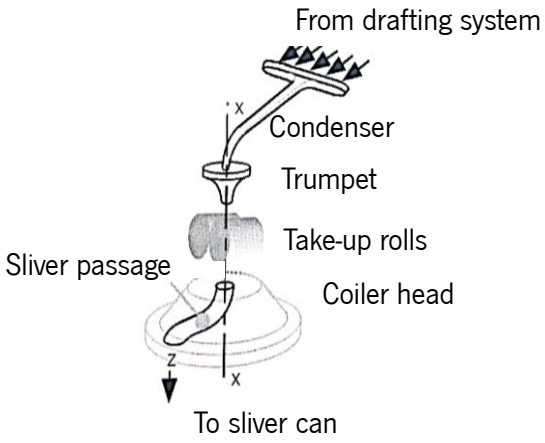

Figure 10 Sliver coiling

- **Roving frame:** Attenuates the sliver by drafting the sliver between 5 to 30 times. The resulting strand has low coherence and twist is applied, from 25 to 70 turns per meter (Klein, 2016a).

- **Spinning:** draws the roving until the required count, twists the bundle of fibers to give tenacity and winds up the yarn for storage and future processing (Klein and Rieter Machine Works, 2008).

3.2.2 Advantages of flax fibers

Flax fibers have very competitive mechanical properties compared to synthetic fibers (Delft University, 2001; JEC, 2012);

- The **density** of flax fiber is of 1.4 g/cm³ and glass fiber is of 2.55 g/cm³.
- For **stiffness**, flax fibers are almost equivalent to glass fibers.
- For the **specific stiffness in tension**, flax fibers are better than glass fibers.
- For the **specific stiffness in bending**, flax fibers almost reach carbon fibers performance.
- For the **strength** performance, flax fibers are 1/2 that glass fibers and 1/3 that of carbon fibers. However, when considering the density of flax fibers, the specific properties compare well with those of glass fibers.

The mechanical properties of flax, glass and carbon fibers are given in Table 6:

Table 6 Comparison mechanical properties flax, glass and carbon fibers (Kozlowski, 2012)

Fibre	Density (g/cm³)	Diameter (µm)	Tensile Strength (MPa)	Young's Modulus (GPa)	Specific strength (MPa/g/cm³)	Elongation at break (%)
Flax	1,52	40-600	345-1500	27,6-85	227-986,8	2,7-3,2
E-Glass	2,55	<17	3400	73	1333,3	2,5
Carbon	1,78	5-7	4000	230-240	2247,2	1,4-1,8

Flax fibers have **higher vibration damping properties** than glass fiber, thus allowing to minimize noise in the car interior, for example, and consequently creating comfort zones. They have also good **natural optics** characteristics, thus optically upgrading visible components and increasing environmental awareness. Furthermore, compared to glass fibers, flax fibers present the advantage of not being abrasive, safe to handle and having low tendency to splinter in the composite (Rinberg, 2012; Verpoest, 2012; Pico, D.; Wilms, C.; Seide, G.; Gries, T.; Tiesler, H.; Kleinholz, 2016).

Consequently, flax fibers have huge potential for replacing glass fibers as they are relatively similar and better properties.

3.2.3 Energy Consumption

Giving the importance of energy and CO_2 emission for producing carbon fibers and glass fibers, natural fibers are seen as a solution to lower the consumption rate of the composite industry.

Many different studies can be found concerning the data for energy consumption for the flax fiber production. The energy consumption varies between **6,5** to **12,21 MJ/kg**, (Turunen and Van der Werf, 2008; Dissanayake *et al.*, 2009; Song, Youn and Gutowski, 2009).

Table 7 Energy consumption for flax fiber and yarn production [MJ/kg] (Turunen and Van der Werf, 2008; Dissanayake *et al.*, 2009; Song, Youn and Gutowski, 2009)

Energy consumption for flax fiber and yarn production (MJ/Kg)		
	Turunen, 2008	Young, 2009
Warm water retting	0,59	–
Scutching	9,39	–
Hackling	2,23	–
Total fiber	**12,21**	**6,5**
Spinning	23,90	–
Total yarn	**36,11**	–

The wet spinning process represents 66 % of the total energy consumption for the production of a flax yarn (Figure 11).

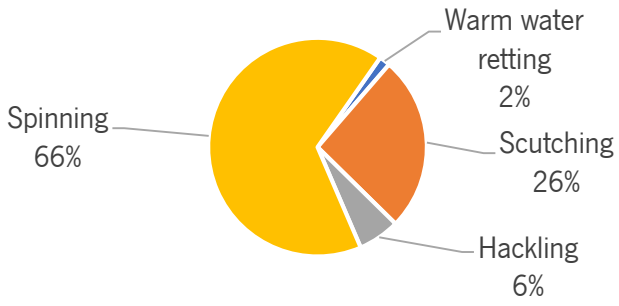

Figure 11 Energy consumption for a flax yarn by sub-process

NFRP have therefore, huge potential, but today, they are mainly used for non-structural components with low mechanical loads. The following part covers the current applications of NFRP.

3.3 Current applications of natural fiber reinforced plastics

The NFRP market is rapidly growing and many projects aiming to integrate NFRP in the composite industry and different applications can be found today. NFRP are employed in the automotive industry (Figure 12), in personal equipment (such as glasses), home improvement and decoration items (such as chairs or tables), in sports goods (such as helmets or skis) (Ticoalu, Aravinthan and Cardona, 2010; JEC, 2014; Sanjay *et al.*, 2016).

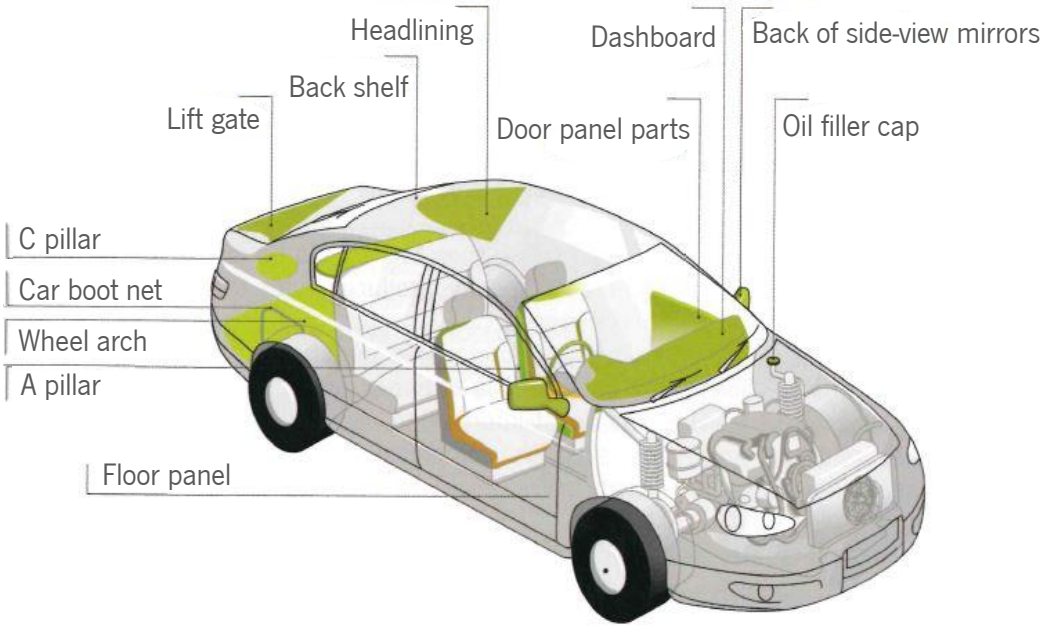

Figure 12 Example of NFRP applications in the automotive industry (JEC, 2014)

NFRP can be found in interior hidden parts of cars, such as door panels, roof, seat shells, dashboards. The most used reinforcement structure for NFRP are non-woven mats, with low weight and moderate mechanical properties.

For structural components, the applications are low, they can be found in prototypes and research projects for the industry. Recently, Jaguar integrated NFRP in the floor of one of its cars, the F-Type convertible, by using a "100 % renewably sourced panel consisting of a honeycomb paper core with skin layers of non-woven flax mats that were pre-impregnated with a sugar-based thermoset resin" (JEC, 2014). Alternatively, a chassis prototype for cars was made out of a UD flax fiber composite (JEC, 2014).

3.4 Disadvantages of natural fibers

Natural fibers are incompatible with synthetic polymers, therefore an additional chemical treatment is needed during manufacture - such as acetylation, bleaching, mercerization, oxidation and others (Ahmad, Choi and Park, 2015) (Summerscales and Grove, 2014). Secondly, the conditions of processing are restricted because of the natural fibers sensitivity to temperature. Natural fibers are therefore mostly used in combination with thermoplastics, but, the choice of polymers remains limited (Summerscales and Grove, 2014). Existing studies are looking to improve the incorporation of natural fibers at higher temperatures by either improving the thermal resistance of the fibers or by reducing the melting point of the resin, but overall, there's still a need for further research (Leong *et al.*, 2014).

Also, the production capacity of flax fiber is small compared to glass fiber production. In fact, in 2016, the flax fiber production was of 800 thousand tonnes whereas the glass fiber was of more the 5 million tonnes (Food and Agriculture Organization of the United Nations, 2016; Statista, 2018).

In spite of the limitations mentioned above, there is one major limitation for natural fiber integration in composite applications (with the existing production technologies) (Ramaswamy, R.; Aslan, B.; Raina, M.; Gries, 2012) : The **negative influence of twist**.

Because natural fibers are staple fibers, the fibers need to be processed in the form of yarns so that they have enough cohesion and tensile strength for being processed. However, while twist is necessary for processing, it has negatives effects on the final characteristics of the composite.

In fact, for the reinforcement, twisted yarns are source of obliquity and misalignment from which results stress concentrations and therefore affects the mechanical properties of the composite. The higher the twist angle of the yarn, the lower is the stiffness of the resulting composite, as shown in Figure 13.

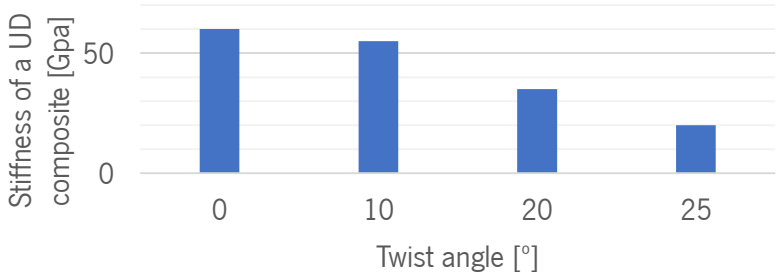

Figure 13 Influence of the twist angles on the stiffness of a uni-directional (UD) composite with flax yarn reinforcement (JEC, 2012)

Besides affecting the mechanical properties, twisted yarns increase the density of the fabric, reducing the permeability and therefore affecting the impregnation of the reinforcement. The higher the angle of the twist the worse is the impregnation, leading to an increase of process time and weakening the composite properties (Goutianos *et al.*, 2006; Shah DU, Schubel PJ, Clifford MJ, 2011; Lomov, S. V.; Baets, 2012; Verpoest, 2012). Lastly, spinning natural fibers is a very costly and energy consuming process (Dissanayake NPJ, 2009). In fact, the price of flax fabric production can reach more than 15 €/kg (Lewin M., 2007). The spinning process is the main cost driver for the conventional manufacturing, representing 48 % of the total cost of production of a natural fiber yarn (International Textile Manufacturers Federation (Hrsg.), 2012; Shah, Schubel and Clifford, 2013). Natural fibers are therefore not competitive enough to substitute glass fibers fabrics with a production cost of approx. 7,3 €/kg.

3.5 Solution approach

As enlightened in the previous parts, natural fibers have huge potential in the composite industry. In Table 8, a review of the main properties of interest for FRP, for natural fibers and synthetic fibers is presented.

Table 8 Potential of natural fibers in FRP applications (Sanjay *et al.*, 2016)

Properties	Natural fibers	Synthetic fibers
Technical		
Density	Low	Moderate
Mechanical properties	Moderate	High
Moisture sensitivity	High	Low
Thermal sensitivity	High	Low
Environmental		
Production, energy	Low	High
Resource, sustainability	Infinite	Limited
Health aspects	Good	Moderate
Recyclability	Good	Moderate

Currently, the application of NFRP is limited to components with low mechanical stress, such as door inner linings in automobiles (Shah, Schubel and Clifford, 2013; Steuernagel, 2014). In their unprocessed state, flax fiber have the potential to be used in highly stressed components thanks to their higher specific rigidity and comparable specific strength to glass fibers (Shah, Schubel and Clifford, 2013).

Working with non-twisted flax sliver compared to flax yarn seems to be the most relevant solution (Song, Youn and Gutowski, 2009; JEC, 2012; Cherif, 2015):

- Better mechanical properties of the composite with non-twisted fibers;
- Shorter process time for processing;
- Lower production cost;
- Low energy and CO_2 emission consumption.

Untwisted flax slivers are complicated to handle because of the low-cohesion of the fibers. Braiding, knitting or weaving is therefore not possible, since those systems are high-stress processes. In order to work with flax slivers, the most adapted reinforcements to work with are UD prepregs or multiaxial fabrics (Cherif, 2015). The following parts of the work will focus on the production of a multiaxial fabric reinforcement out of untwisted flax sliver.

4 Analysis of the multiaxial fabric production process

4.1 Multiaxial fabrics

According to the European Standard EN 13473 a multiaxial fabric (Figure 14) is defined as "a textile structure constructed out of one or more laid parallel non-crimped not-woven thread plies with the possibility of different orientations, different thread densities of the single thread plies and possible integration of the fiber fleeces, films, foams or other materials, fixed by loop systems or by chemical binding systems. The threads can be orientated parallel or alternating crosswise. These products can be produced on machines with insertion devices (parallel-weft or cross-weft) and warp-knitting machines or chemical binding systems." (*NF EN 13473: Spécifications pour les tissus multi-axiaux multicouches*, 2001)

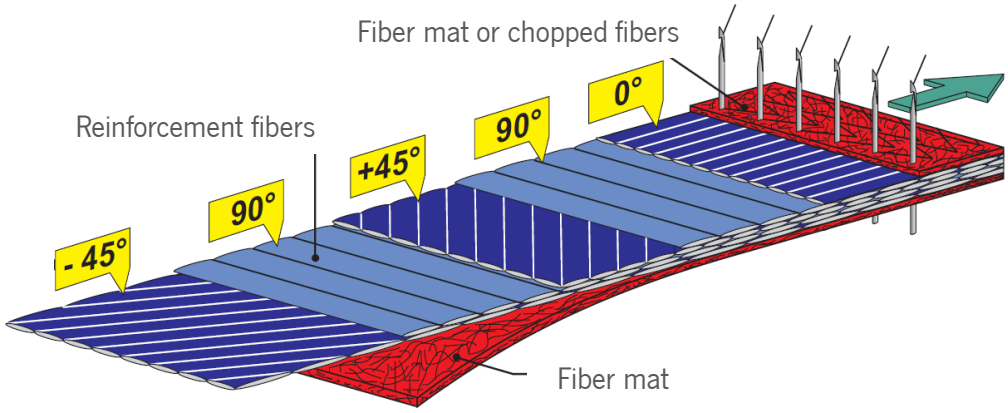

Figure 14 Schematic set-up of a multiaxial warp-knitted multiaxial fabric (Cnc, 2003)

A multiaxial warp-knitted fabric is a stacking of layers of unidirectional fibers. Each layer can have different orientations and the final reinforcement is fixed by a loop system. This structure has many advantages;

- Good resin impregnation thanks to the straight disposition of the yarns and the presence of stitches, which allows good vertical diffusion (Seu, 2014);
- Full exploitation of fiber mechanical properties thanks to the straight disposition of the yarns (Seu, 2014). In fact, the structure has no crimp, which allows better mechanical results for the composite. Crimp has been shown to create complex elastic coupling and stress distribution which results in stiffness and strength decrease of the resulting composite (Bogetti TA, Gillespie JW, 1992; Hipp P, 1992; Jensen D, 1993; Pai SP, 2001; Henry TC, Bakis CE, 2015; HENRY, Todd C., RIDDICK, Jaret C., EMERSON, Ryan P., 2015).

4.2 Production

For producing a multiaxial fabric, the warp-knitting with multiaxial weft insertion machine is the most adapted and used one in the industry today (Schnabel and Gries, 2011a). This machine was patented in 1983 by the LIBA Maschinenfabrik Gmbh (LIBA Maschinenfabrik Gmbh, 1983) and has since then evolved in various versions. In the following part, the production process is further described.

4.2.1 Principle

The warp-knitting with multiaxial weft insertion machine in composed of a beam with multiple pillar threads (forming a 0° angle layer), creels with a transport system for the weft-insertion, a warp-knitting unit and a take-up unit.

The machine transport system carries the loose fiber layers to the warp-knitting module, where pillar threads are also carried. The weft and pillar threads are then fixed together by warp-knitting yarns and the multiaxial fabric is cut out of the transport chain and wound up (Figure 15) (Schnabel and Gries, 2011b).

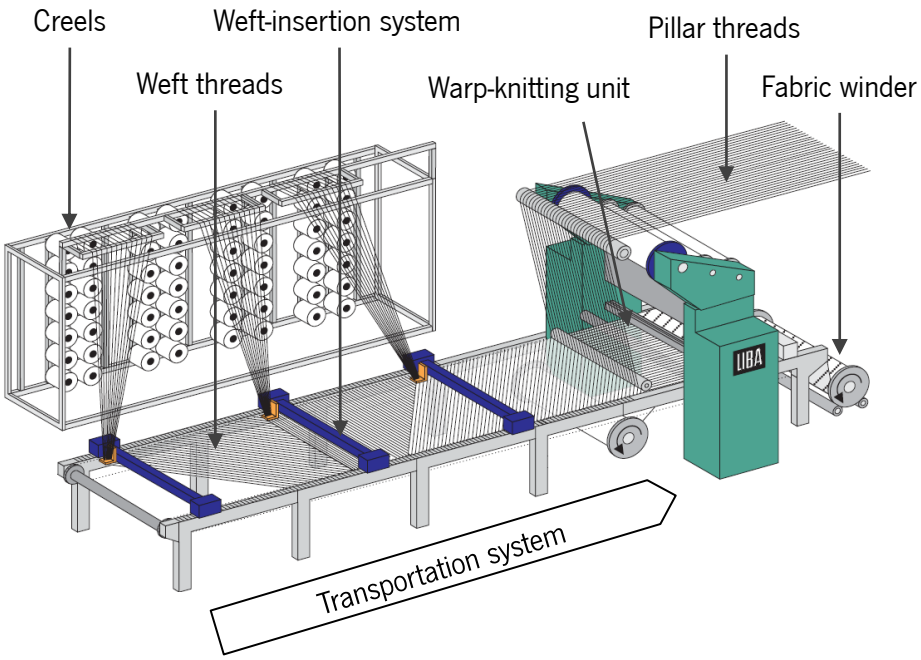

Figure 15 Tricot Machine with Multiaxial Weft Insertion COPCENTRA MAX 3 CNC (Cnc, 2003)

The machine has as many weft-carriage systems as needed and the angle of the weft layers can be varied (Cnc, 2003).

4.2.2 Weft carriage system

The weft carriage system carries the threads from the stationary creel to the transport system, swinging permanently between the two lay-in units, placed on both sides of the machine (Figure 16) (Schnabel and Gries, 2011b). The weft carriage system guides the threads, spaces them to a specific width while preserving the thread configuration. Once the thread arrives to the transport system, the weft carriage deposits the layers and fixes them to the weft lay-in unit (Schnabel and Gries, 2011b).

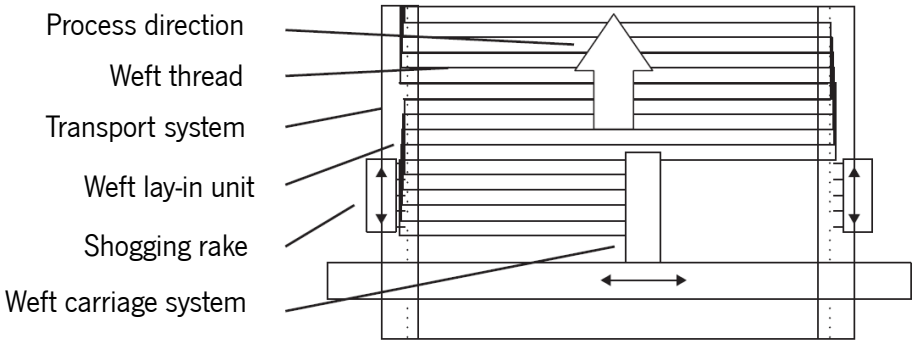

Figure 16 Schematics of the weft insertion system (Schnabel and Gries, 2011b)

There are two main types of weft-insertion portals (Figure 17):

- Stationary: The angle of the layer depends on the angle of the weft-insertion portal according to the direction of the process.
- Mobile: The angle of the layer depends on the transport system speed and the portal movement. The weft-insertion portal moves independently from the process direction.

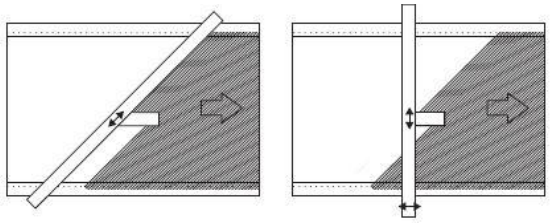

Figure 17 Stationary (left) and mobile (right) weft insertion portal (Schnabel and Gries, 2011a)

4.2.2.1 Weft thread transport system

The transport chain of the warp-knitting weft insertion machine consists of two main systems. For the COPCENTRA MAX 3 CNC, which can be found in ITA's laboratory, there's a hook chain along the transport chain. For the COPCENTRA MAX 5 CNC, there's a compiled clamp system added to the hook chain. The two systems are further explained in the following part.

4.2.2.2 Hook chain

In Figure 18, the weft carriage system with the hook chain is represented.

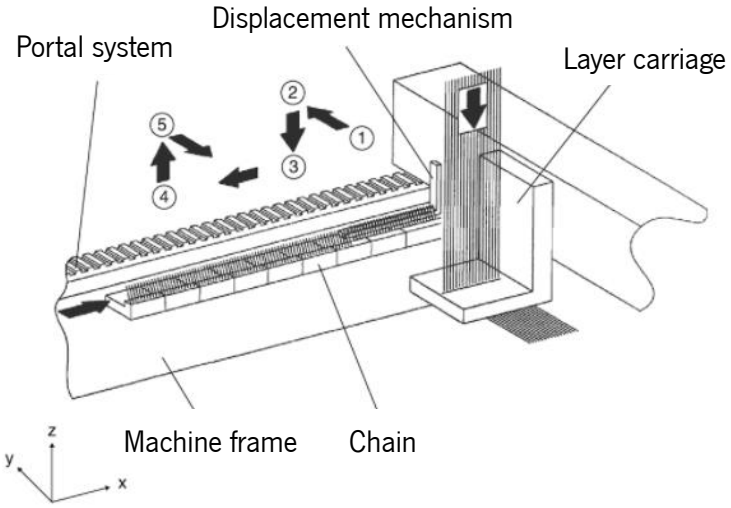

Figure 18 Movement of the weft carriage (Schnabel and Gries, 2011a)

When the weft threads are filled into the open transport hooks (1), the weft clamps close (2) automatically and fix the weft threads. The clamps move laterally while the weft carriage starts to move (3) to the opposite direction of the process, whereby the threads are fixed in the weft lay-in units. As soon as the weft threads are fixed, the weft-insertion device moves back up (4) and goes to the other side of the transport chain (5), continuing indefinitely with the same procedure (Schnabel and Gries, 2011b).

4.2.2.3 Hook chain combined with clamping system

In Figure 19, the weft carriage system with the hook chain and a clamping system is represented.

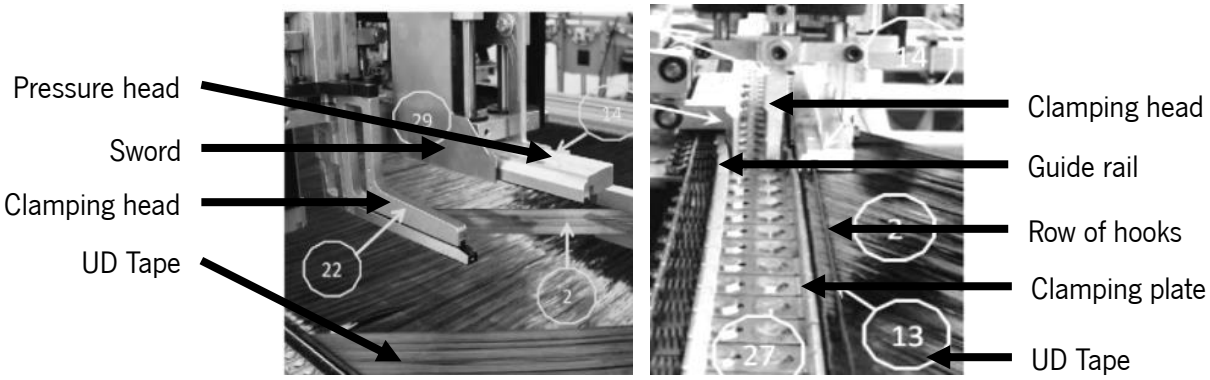

Figure 19 Clamping system (Schnabel and Gries, 2011a)

The tapes are pulled out from the creels, cut to a defined length and placed in the transport chain with the clamping device and a row of hooks.

When the tape is deposited threw the row of hooks, the guide rail opens the upper clamping plate, the clamping head opens, the UD tape is released, a sword cuts the tape and the UD tape is fixed by the clamping plate. The weft carriage moves back up and goes to the other side of the transport chain, repeating the same steps.

4.2.3 Warp-knitting module

In the warp-knitting module, the weft and pillar layers are fixed together with knitting loops (Figure 20). Generally, the gauges of the needles vary between 3,5 to 14 needles per inch. The weft and pillar thread sinkers fix the threads and places them the closest to the knitting elements (Schnabel and Gries, 2011a).

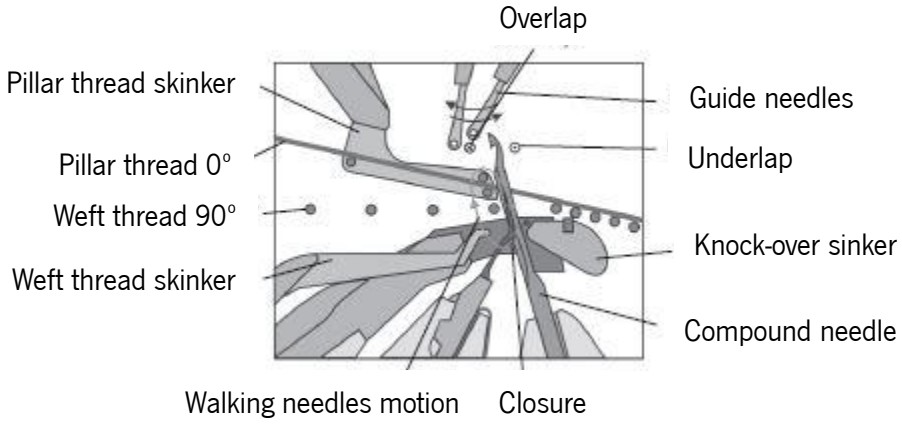

Figure 20 Knitting elements and walking needle (Schnabel and Gries, 2011a)

4.3 Challenge

The machine which will be considered is the 2007 multiaxial weft-insertion machine COPCENTRA MAX 3 CNC. Conventional machines for the production of multiaxial fabrics are adapted for the processing of yarns or continuous fibers – such as carbon, glass, aramid, etc. However, because of the low cohesion of untwisted flax slivers, the feeding system needs to be modified in order to be able to process them. Therefore, the objective of the following work will be to design an adapted lay-up system for the processing of untwisted flax slivers (Figure 21).

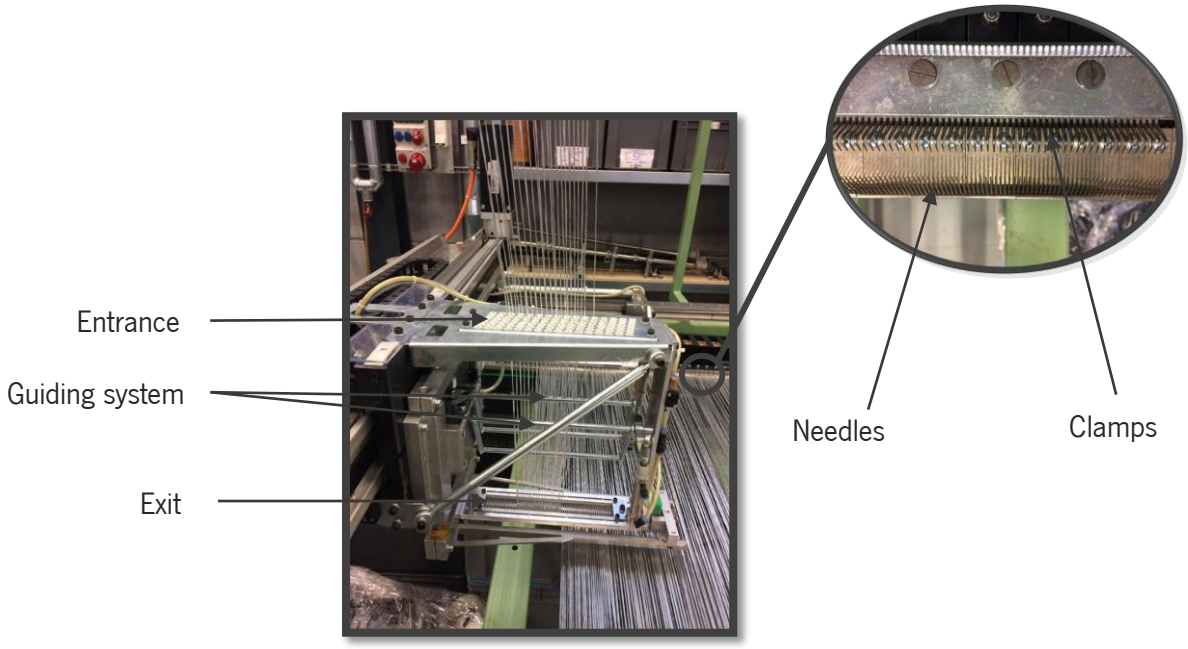

Figure 21 Weft insertion system

5 Conceptualization of a novel weft insertion system

In order to conceptualize a new design for the weft-insertion system, the guideline VDI 2221 (Systematic approach to the development and design of technical systems and products) gives a methodology for designing technical systems and products. The methodology is subdivided into 7 main steps, the identification and definition of the main task, from which results the requirements list, the determination of function structures, the identification of solution principles, their combination to solutions, their evaluation and validation until construction. (Figure 22).

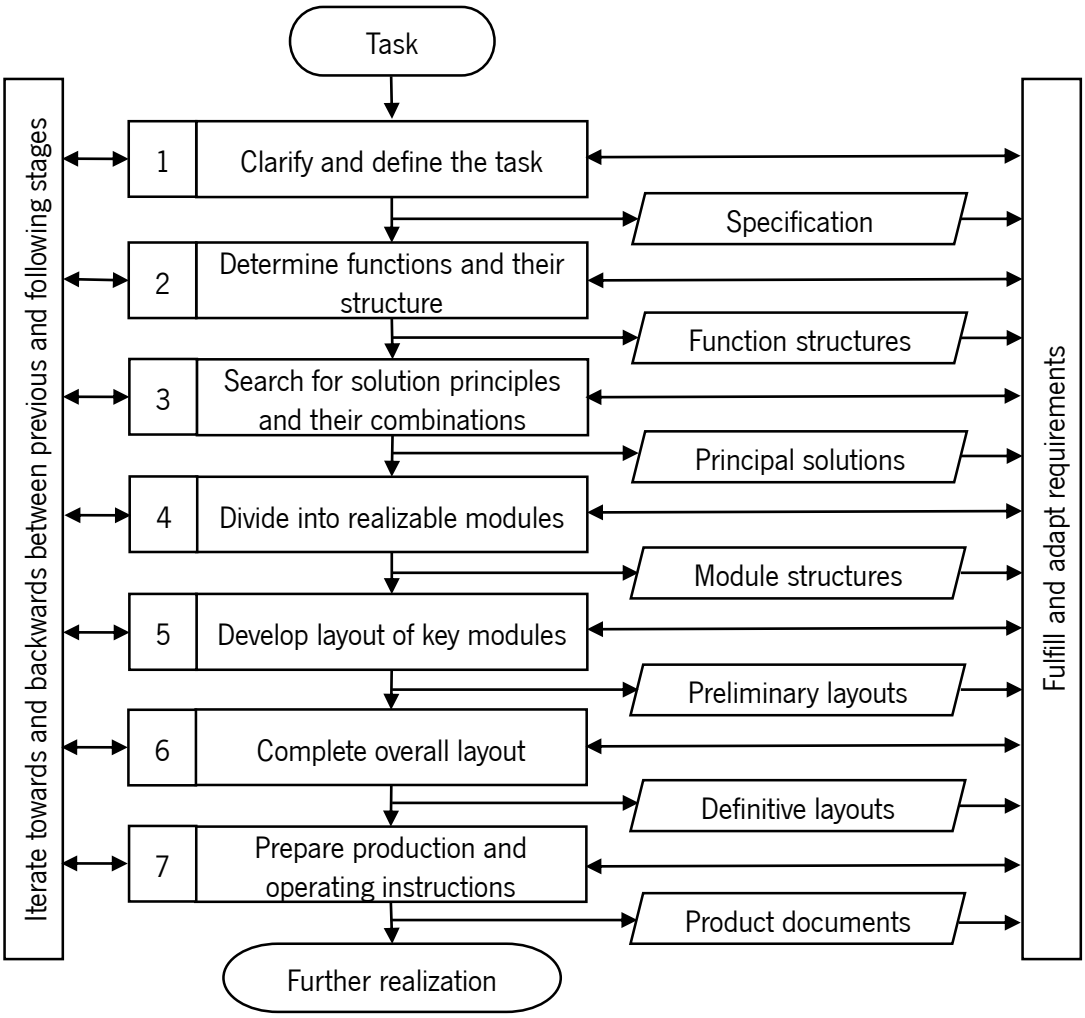

Figure 22 Guideline VDI 2221 (Jänsch, 2006)

5.1 Requirements list for the weft-insertion system

To design a new weft insertion system, the task needs to be clarified, the product needs to be investigated, its functionality and performance described, and the limitations discerned: identifying the requirements for the solution. A requirements list must be made to identify the objectives of the solution and the properties it should or should not have (Jänsch, 2006).

Here, the weft insertion system needs to be adapted to the processing of flax slivers. 5000 tex flax slivers from Safilin, Sailly-sur-la-Lys and 9000 Tex flax slivers from HessenLeinen GmbH, Zierenberg are used as raw material. The 5000 tex slivers were tested using the COPCENTRA MAX 3 CNC resulting in the following problems. The flax slivers tend to slip apart during the transportation from the creel to the laying of the sliver due to high tension. When clamping the slivers to the needle system, the sliver was loose, and the distribution of the sliver was uneven, the slivers overloaded the needle system, leading to material loss. For the definition of the requirements list, the current weft-insertion system, the kinematics of the machine and the processed slivers are analyzed.

5.1.1 Weft insertion system

The geometry of the weft insertion system needs to be calculated, as the size of the system gives the space limitation for the solution. The weft-insertion system is separated in three functions here, in Figure 23, the entrance, the guiding system and the exit.

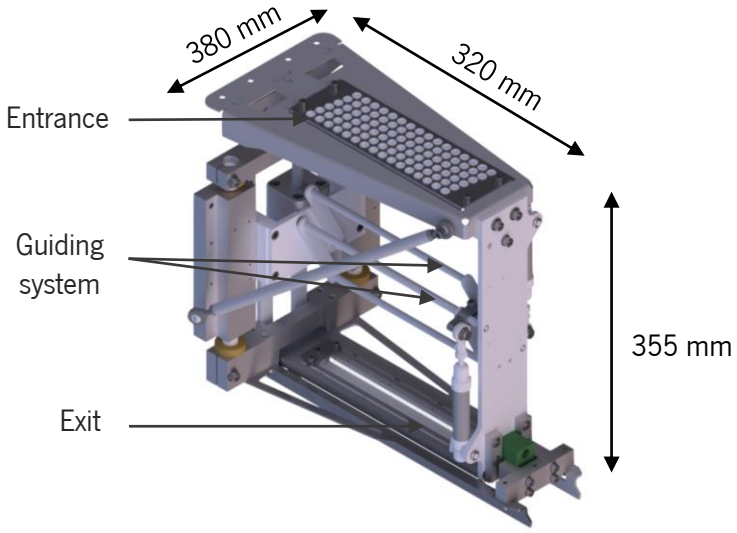

Figure 23 Weft insertion system of the COPCENTRA MAX 3 CNC

5.1.2 Sliver Characterization

To understand the problems occurring during the processing of the flax slivers in the weft insertion system, a sliver characterization is necessary. First, the fineness of the slivers is tested, then, because of the inhomogeneities of the sliver, the unevenness of the sliver and its average fiber length is also tested. Finally, given the tendency of the sliver to break under tension, a mechanical test of the slivers and its fibers is proceeded.

Two different flax slivers are tested, one from Safilin, in France, that we'll be referred as "F-Flax", and one from Hessen Leinen, in Germany, that we'll be referred as "G-Flax". For the sliver characterization, the slivers were conditioned and tested in a standard atmosphere of:

Temperature: 20 °C ±2 °C

Relative Humidity: 65 % ±2 %

5.1.2.1 Fineness

The fineness of a sliver in [Tex] is the weight in grams of 1000 meters of sliver.

$$Fineness[Tex] = \frac{Weight[g]}{Length[km]}$$

To find the title of the sliver, 5 measurements must be taken from different spots of the sliver. The fineness of the two flax sliver samples are presented in Table 9:

Table 9 Flax sliver fineness

Sample	G-Flax (Tex)	F-Flax (Tex)
1	8596,0	5288,9
2	9649,0	5087,7
3	8506,0	5033,9
4	8738,0	4960,6
5	9169,0	5113,8
Average	**8931,6**	**5097,0**

It is to expect that the evenness and mechanical properties of the G-Flax will be better than the F-Flax, since the fineness of G-Flax is higher (Klein, 2016b).

5.1.2.2 Unevenness

For textile products, the unevenness, also known as irregularity, is the variation in mass per unit length along the yarn (or slivers, rovings, ...) (NPTEL, 2012).

Unevenness is unavoidable for staple fibers, as it is not possible to keep a constant number of fibers in the cross section, however it is possible to minimize the unevenness.

Unevenness can affect the quality of the end-product:

- Strength of yarns (the more regular the yarn/sliver, the better strength it will have, the less it will break during processing);
- Fabric appearance, defects, feel;
- Fabric properties such as abrasion, soil retention, drape, absorbency, reflectance;
- Productivity (the lower the unevenness the lower incidents during processing, because of occasional break).

There are different methods for measuring the yarn unevenness. A visual examination is firstly made (Figure 24), showing that the unevenness of the G-Flax is higher than the F-Flax.

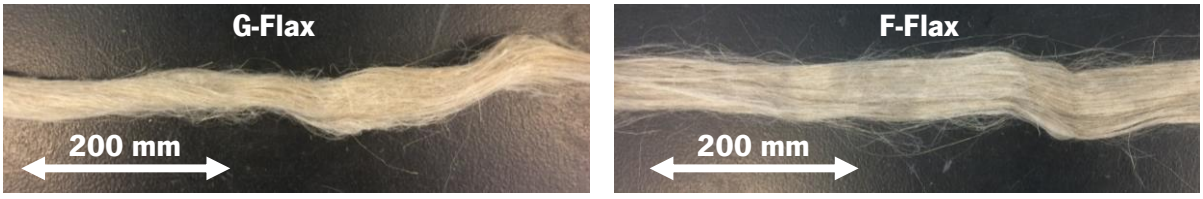

Figure 24 G-Flax and F-Flax

A further test is proceeded with the USTER 5. The USTER 5 determines the yarn evenness, imperfections, hairiness, diameter, shape, density for short and long staple yarns, roving or slivers. (USTER, 2016) It consists of a parallel plate air capacitor where the material passes through. The material changes the capacity of the capacitor, which is proportional to the mass per unit length, which are then processed by the USTER.

The results of the F-flax tested with the USTER 5 are shown in Figure 25 (more details in ANNEX 1).

Sample	U% %	CVm %	CVm 1m %	CVm 3m %
F-Flax	14,31	17,78	4,75	3,09
G-Flax	13,23	16,92	6,60	3,17

Figure 25 Unevenness results F-Flax A and B

U%: is the percentage mass deviation of unit length of material. It is caused by uneven fiber distribution along the length of the sliver.

CV%: is the coefficient of variation which defines. It is used when handling large quantities of data. The lower is the CV-value, the more even is the material.

In Figure 26 and Figure 27, the mass per unit along the length of the sliver is graphically represented, it shows the variability of the sliver. It's notable that the variability of the F-Flax is lower than the G-Flax, confirming the visual examination.

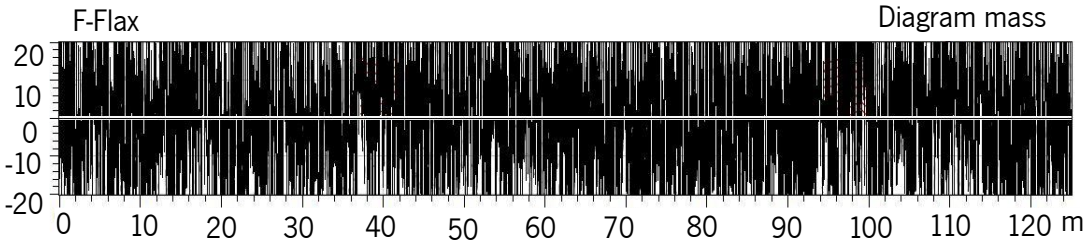

Figure 26 Diagram mass F-Flax

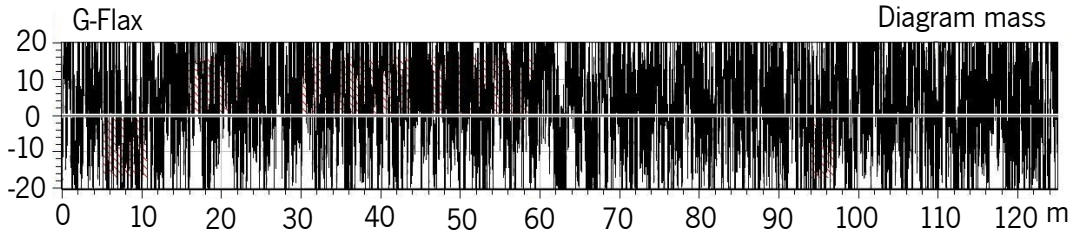

Figure 27 Diagram mass G-Flax

5.1.2.3 Fiber length

Giving the importance of the fiber length for machine settings, more than 200 fibers are measured to have an idea of the average fiber length. The fiber length varies between 30 mm and 400 mm. In Table 10, the average length and the standard deviation of the G-Flax and F-Flax are regrouped.

Table 10 Fiber length of F-Flax and G-Flax

Fiber length	F-Flax	G-Flax
Average fiber length [cm]	209,3	192,54
Standard deviation	81,95	75,26

It is important to note that the result is not reliable, the laboratory is not equipped to test fiber length and the differentiation between the single fiber and the fiber bundle is complicated. The values are not representative of the real value but give an estimated representation.

5.1.2.4 Mechanical properties of the sliver

The tensile strength of the sliver is measured with the STATIMAT 4U, with a load cell of 100 N, a gauge length of 240 mm and a pretension of 0 cN. The test is conducted for 10 samples of 240 mm length slivers. The detailed results can be found in ANNEX 2.

- **Force/Elongation diagram**: According to the diagrams, the rupture strength (moment were the fibers start to slide) for the F-Flax varies between 13,80 and 30,65 N and for the G-Flax between 7,82 and 14,10 N.

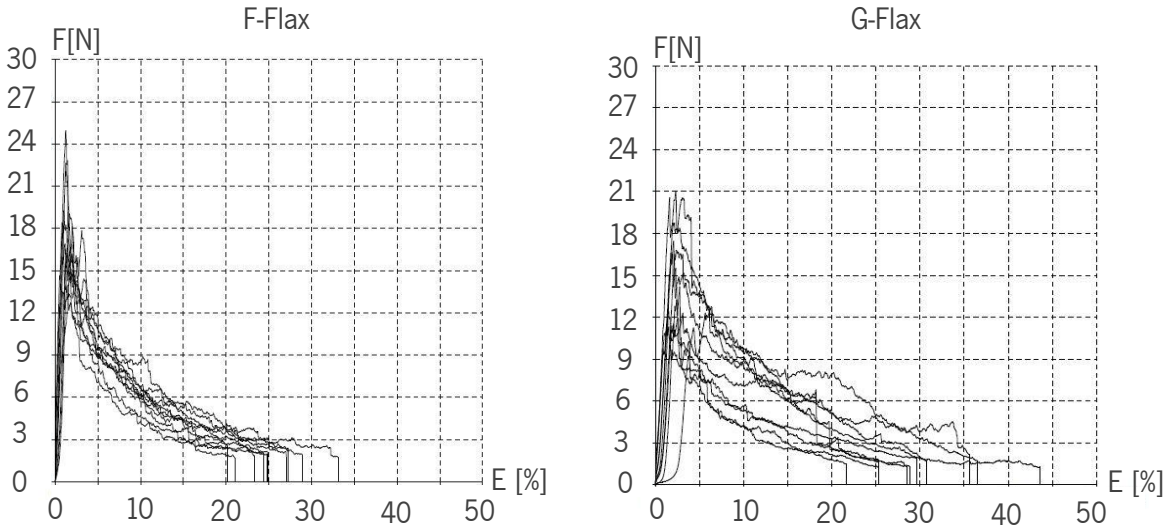

Figure 28 Fiber Force/Elongation diagram of F-Flax and G-Flax

- **Fmax:** The sliver tensile strength is on average, for F-Flax, **18,95 N** and for G-Flax, **10,32 N**. The variation coefficient is high, around 15 % for F-Flax and 20,57 % for G-Flax B, the values are not regular, which is to expect when working with natural fibers.

5.1.2.5 Mechanical properties of the fiber

The tensile strength of the fiber is measured with the FAVIMAT+ FIBRE TEST, with a pretension of 0,50 cN/Tex. The test is conducted for 50 samples of fibers of 25 mm for each material A and B. The detailed results can be found in the ANNEX 3.

- **Fmax:** The fiber tensile strength is on average, for F-Flax A, **150,51 cN**, and for G-Flax, **96,05 cN**. The variation coefficient is high, around 105,69 % for F-Flax and 82,82 % for G-Flax B, the values are not regular, which is to expect when working with natural fibers.

5.1.3 Sliver width determination

The aim is to produce a multiaxial fabric consisting of two layers with a weight per area for each layer of 150 g.m^{-2}. To achieve this with the 5000 Tex flax slivers, the following equation is used:

$$Sliver\ width = \frac{Fineness}{1000 \times Basis\ weight\ per\ layer \times \sin\frac{\alpha\pi}{180}}$$

α - layer angle [°]

The width of the sliver depends on the required layer angle:

- For a -45°/+45°, the width of the sliver has to be 4,71 cm (Figure 29);
- For a -90°/+90°, the width of the sliver has to be 3,33 cm.

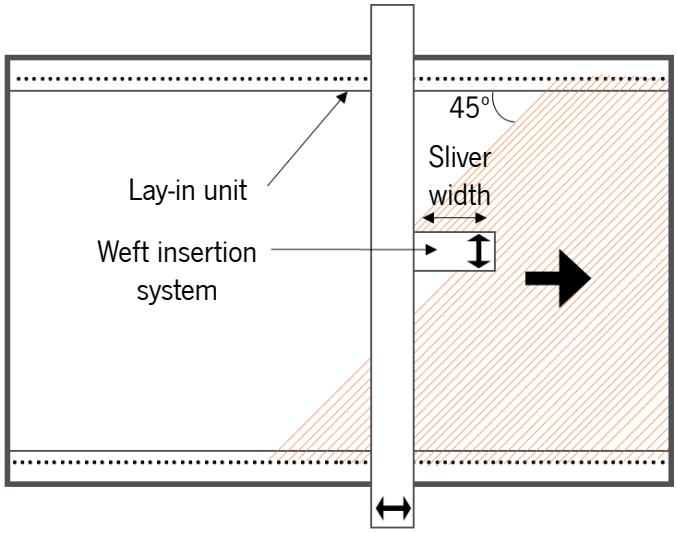

Figure 29 Laying of the sliver: width determination

5.1.4 Kinematics determination

The acceleration of the weft insertion system is measured with the acceleration sensor of a Samsung Galaxy S7 and the application "Physics Toolbox Sensor". The device is unprecise and measures the coordinates over time instead of the acceleration, which would have been more exact. The cellphone was attached to the carrier system and the machine was set up with a production speed of 25 m/hour.

5.1.4.1 Kinematics according to the x-axis and y-axis

The phone application provided the acceleration of the machine, a_x and a_y, expressed in [g], according to the time, in seconds (Figure 30).

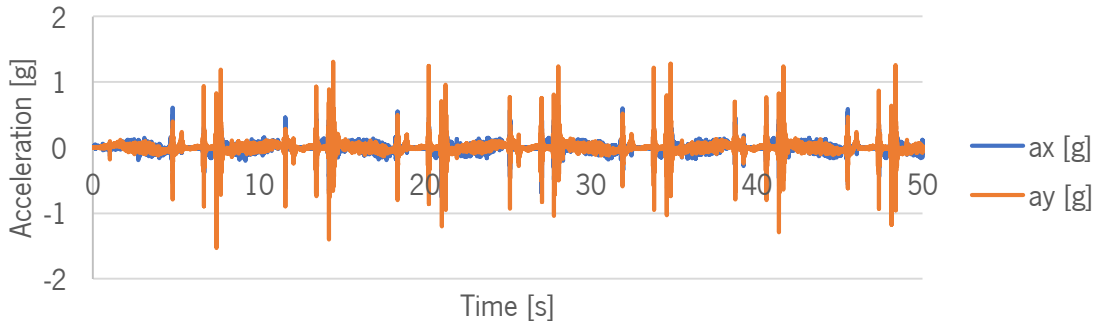

Figure 30 Acceleration data of the weft insertion system in respect to the x-axis and y-axis

In order to exploit these values, the acceleration is converted from [g] to [m.s^{-2}]:

$$a_x[m.s^{-2}] = 9{,}81 \times a_x[g]$$

$$a_x[m.s^{-2}] = 9{,}81 \times a_x[g]$$

To obtain the speed, the acceleration is integrated using a numerical integration:

$$v_n = \frac{a_{n-1} + (a_n - a_{n-1})}{2} \times (t_n - t_{n-1}) + v_{n-1} \qquad (1)$$

The resulting velocity is represented in Figure 31.

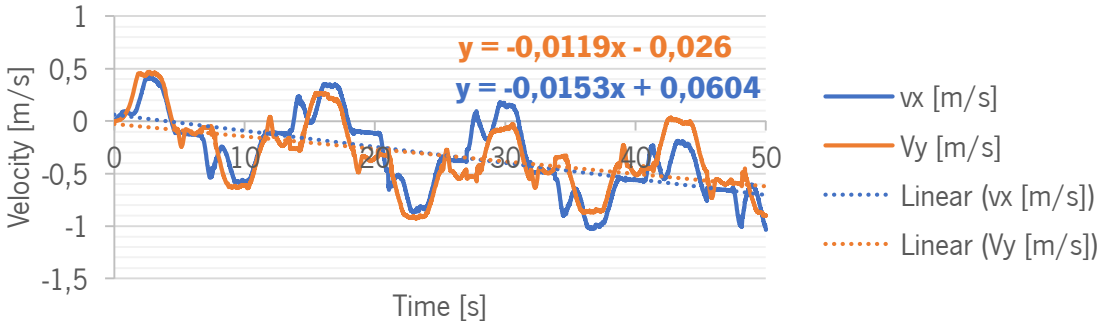

Figure 31 Velocity of the weft insertion system in respect to the x-axis and y-axis

When the weft carriage moves from one side of the transport system to the other, the velocity of the carriage system during the filling of the weft-threads to the lay-in unit is for each of the movement, zero. The velocity should vary around the 0 axis, which is not the case here. This is due to the imprecision of the values from the phone application. To resolve this problem, the trend of the velocity graphic is determined:

$$v_x\colon\ y = -0{,}0119x - 0{,}026$$
$$v_y\colon y = \ -0{,}0153x + 0{,}0604$$

And to level up the velocity around the 0 axis, the equation is added to the velocities and the following graphic is obtained (Figure 32):

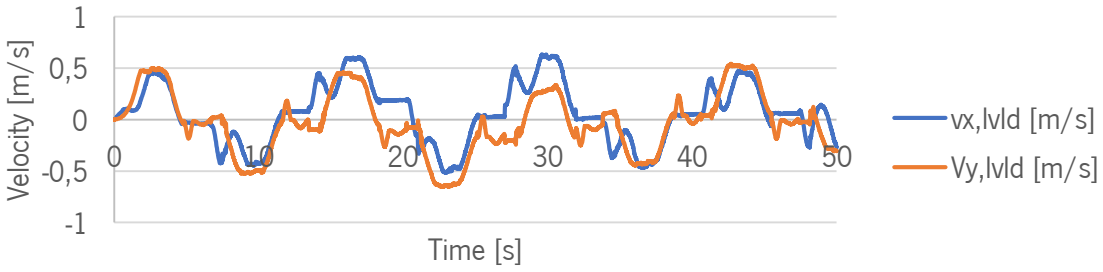

Figure 32 Levelled velocity of the weft insertion system in respect to the x-axis and y-axis

And finally, to obtain the position of each point during the time, the velocity is integrated:

$$x_n = \frac{v_{n-1} + (v_n - v_{n-1})}{2} \times (t_n - t_{n-1}) + x_{n-1} \qquad (2)$$

The resulting path is represented in Figure 33:

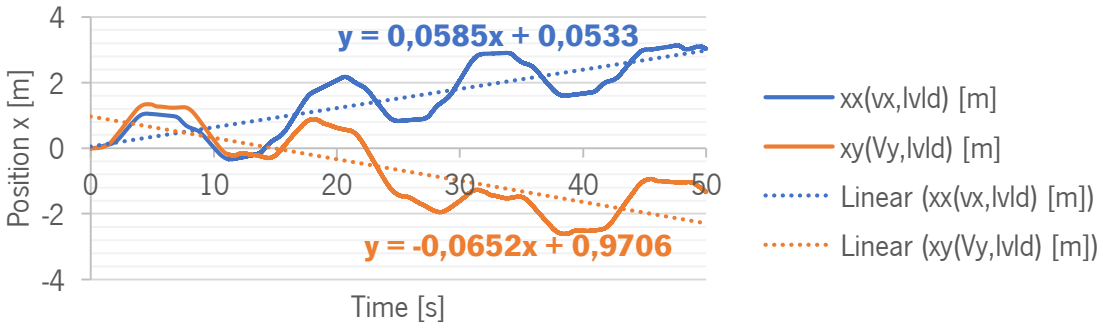

Figure 33 Path of the weft-insertion system in respect to the x-axis and y-axis

When the weft carriage moves from one side of the transport system to the other, the position of the carriage, during the filling of the weft-threads to the lay-in unit, is zero, which is not the case here. This can be due to the imprecision of the values from the phone application or because of the undetermined constants of the integration. To resolve this problem, the trend for the position is determined:

$$xx:\ y = -0{,}0585x - 0{,}0533$$

$$xy: y = -0{,}0652x + 0{,}9706$$

And to level up the position around the 0 axis, the equation is added to the position values and the following graphic is obtained (Figure 34):

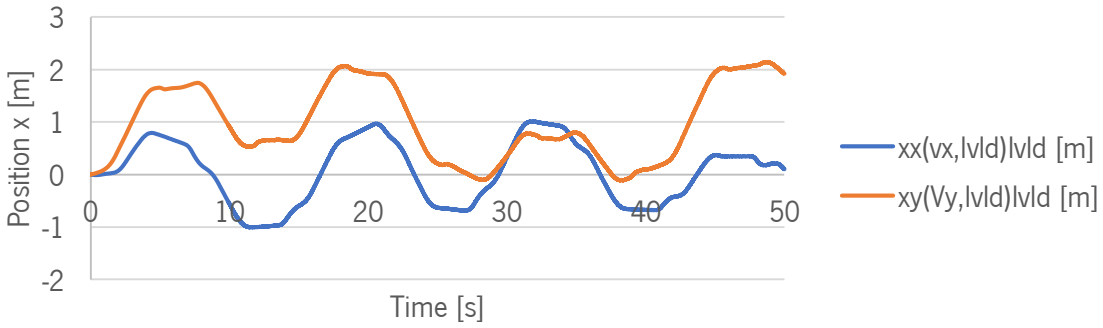

Figure 34 Levelled path of the weft-insertion system in respect to the x-axis and y-axis

5.1.4.2 Kinematics of the 45° movement

The movement of the weft insertion system during the second phase is of a 45° angle, it is the part of the process where the highest accelerations and velocities are met. Since the values collected so far are in relation to the x-axis and y-axis, a transformation is needed to have the relative velocity of the fibers and determine the maximum acceleration and velocity of the system. To represent the velocity along the 45° angle movement, the values of the velocity are transformed, thanks to the Pythagorean formula:

$$v_{45°,lvld} = \sqrt{v_x^2 + v_y^2} \qquad (3)$$

The resulting velocity is represented in Figure 35:

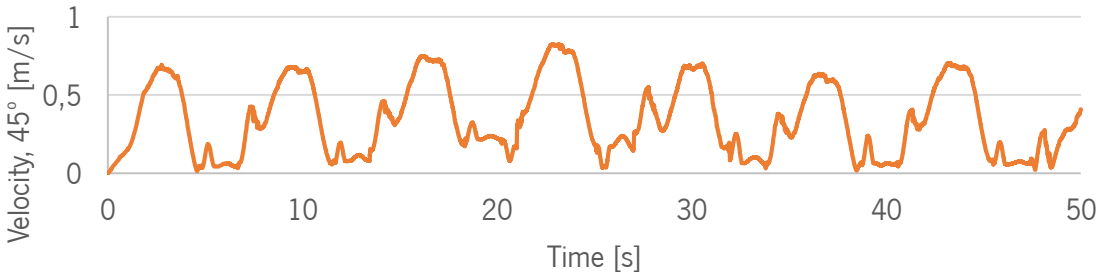

Figure 35 Velocity of the weft insertion system (45°)

When observing the velocity variations, two main steps can be recognized, underlined in Figure 36. The green part represents the moment where the system fills the needles with the slivers, the velocity is low (First phase). The yellow part represents the moment when the system moves from one side to the other,

the velocity is higher (Second phase). In red, the values are not representative, as they represent the beginning and ending of the testing.

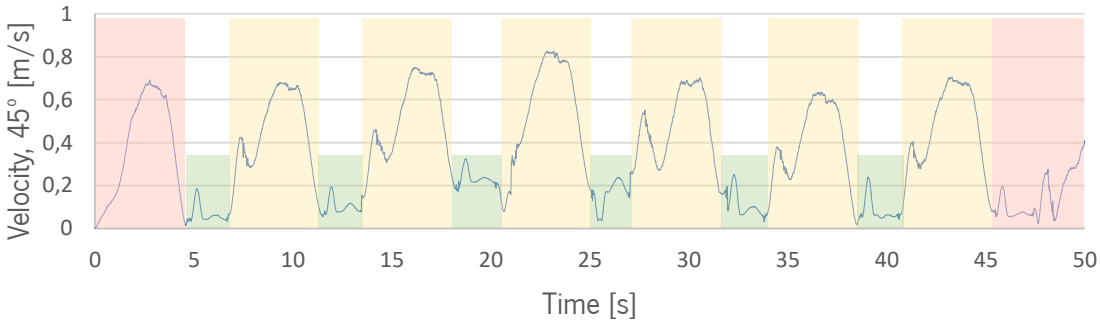

Figure 36 Separation of the different velocity phases of the weft insertion system

5.1.4.3 First phase kinematics

To determine a general function of velocity, the values of each step are isolated and processed. For the first phase, filling the hooks, the absolute values of the velocity are isolated (Figure 37):

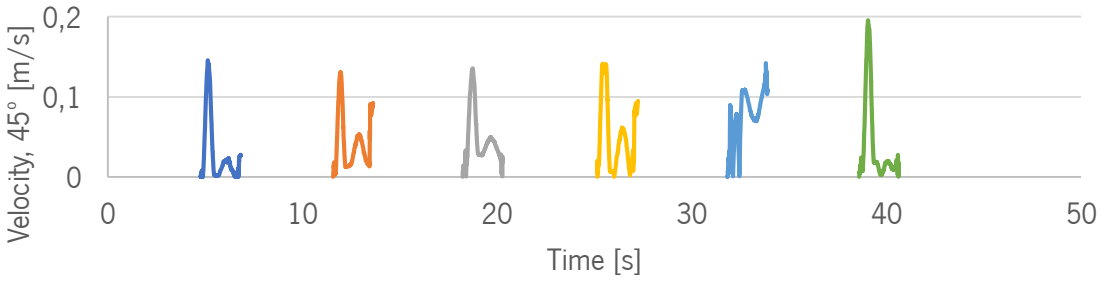

Figure 37 First phase weft insertion system velocity

The average velocity of those values is represented in the following Figure 38. The closest linear trend is a polynomic function of factor 6:

$$y = 0{,}2286x^6 - 1{,}1961x^5 + 2{,}0342x^4 - 0{,}8554x^3 - 0{,}8332x^2 + 0{,}6773x - 0{,}0287$$

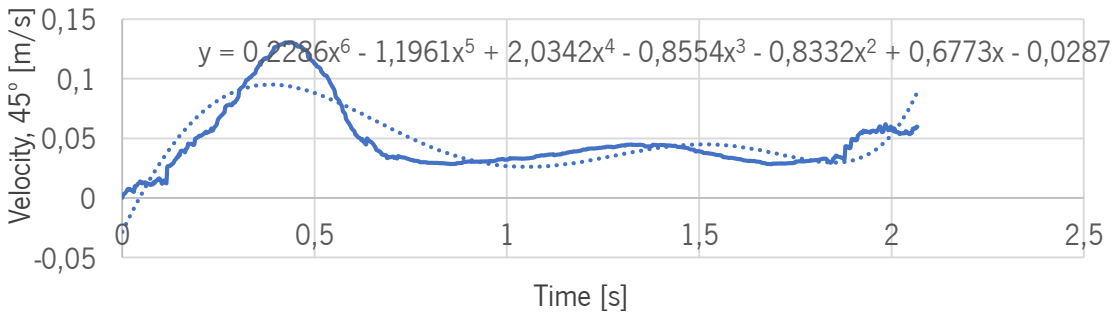

Figure 38 General velocity of the weft insertion system in the first phase

5.1.4.4 Second phase dynamics

The same steps are made for the second phase, the motion of the weft insertion device from one side to the other. The absolute velocities are isolated (Figure 39):

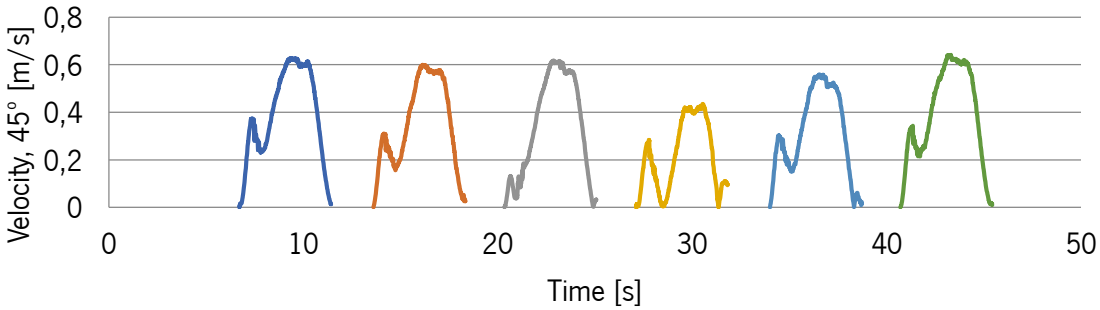

Figure 39 Second phase weft insertion system velocity

The average motion of those values was represented in the following Figure 40.

The closest linear trend is a polynomic function of factor 6:

$$y = -0{,}0045x^6 + 0{,}0797x^5 - 0{,}5258x^4 + 1{,}578x^3 - 2{,}1419x^2 + 1{,}2806x - 0{,}0539$$

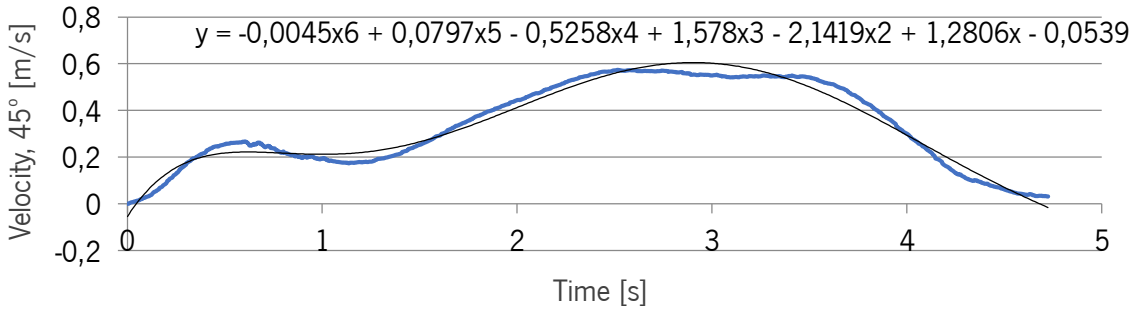

Figure 40 General velocity of the weft insertion system in the second phase

This function gives the general velocity of the weft insertion system, for the second phase movement. With this function, it is possible to give the average acceleration and the average position of the weft insertion system.

By deriving the velocity function, the acceleration function is:

$$a(t) = 3{,}189x^5 - 14{,}9245x^4 + 22{,}924x^3 - 11{,}1561x^2 - 1{,}3648x$$

The general acceleration path is represented in Figure 41:

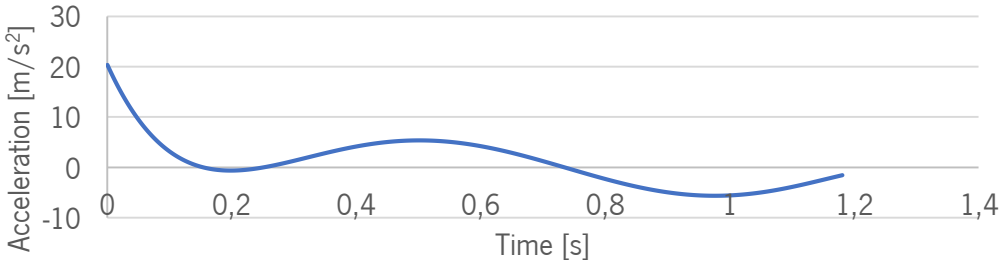

Figure 41 General acceleration of the weft insertion system in the second phase

For the position function of the weft insertion system, the velocity function is integrated:

$$x(t) = 0{,}075928571x^7 - 0{,}497483333x^6 + 1{,}1462x^5 - 0{,}929675x^4 - 0{,}227466667x^3 + 0{,}5977x^2 - 0{,}0399x$$

The general path is represented in Figure 42:

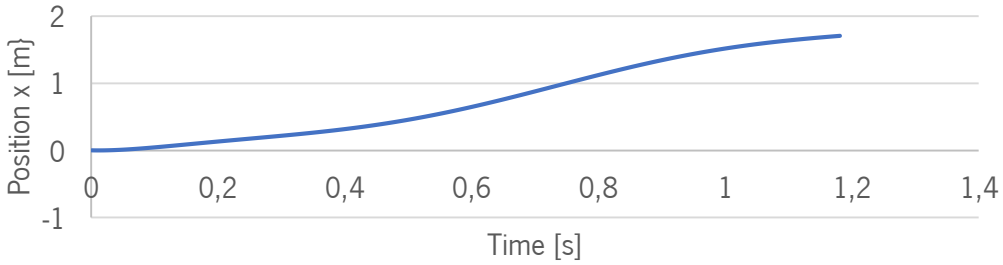

Figure 42 General path of the weft insertion system

5.1.4.5 Kinematics conclusions

For the production speed of 25 m/h:

- The maximum acceleration of the weft insertion system is 1,8 m/s².
- The maximum velocity of the weft insertion system is 1,61 m/s.

In order to determine the maximum acceleration and speed of the weft insertion system for a production speed of 100 m/h, the same method was used. The following results were obtained:

- The maximum acceleration of the weft insertion system is 8 m/s².
- The maximum velocity of the weft insertion system is 3 m/s.

5.1.5 Requirements list

All the requirements for the weft-insertion system are assembled in Table 11.

Table 11 Requirements list

Requirements list *Tricot Machine with Multiaxial Weft Insertion (LIBA Copcentra Max 3 CNC): Development of a new weft-insertion system.*	
Demand (D) Wish (W)	**Requirements**
	Geometry
D	Size of the weft insertion device: • Length ≤ 320 mm • Breadth ≤ 280 mm • Height ≤ 355 mm
D	Weft insertion Entrance: • Length ≤ 240 mm • Width ≤ 50 mm
D	Weft insertion Exit: • Length ≤ 240 mm • Width ≤ 75 mm
D	Lay-in unit: • Needles gauge E12 • Clamps gauge E9
D	Working width: 1270 mm
	Kinematics
D	Speed of the transport chain: 25 m/h
D	Max. speed of the weft carriage system: 6 $m.s^{-1}$
D	Max. acceleration of the weft carriage system: 15 $m.s^{-2}$
D	Max. path acceleration: $a_{b,x} = a_{b,z} = 8\ m.s^{-2}$

	Forces
D	Friction force on the sliver during the lay-up process: approx. 350 cN
D	Clamps fix the weft threads with optimum tension and in their exact position.
D	The weft threads are drawn parallel and at a fixed tension.
	Material
D	Number of layers: 2
D	Fiber Orientation of the layers: ± 45°
D	Weight per area for each layer: 150 g/m²
D	Laying width of the sliver: • For 90° insertion: 3,33 cm; • For 45° insertion: 4,71 cm.
	Production
D	Tolerance for the fiber orientation: ± 5%
D	Tolerance for the weight per area: ± 10%
D	Manufacturing processes with ITA's available equipment and tools
	Ergonomics
W	Easy transportation from the creel to the weft insertion system
W	Good accessibility
	Operation
D	Assemblage not to complex and easy to implement
	Maintenance
W	Long maintenance intervals
W	Worn parts easily exchangeable
	Safety
W	Operational and environmental safety in regards of the possible carbon fibers presence in the laboratory

*N.B: "**Demands** are requirements that must be met under all circumstances, if those requirements are not fulfilled the solution is unacceptable. **Wishes** are requirements that should be taken into consideration whenever possible"*

5.2 Function structure

Thanks to the requirements list, the task is better clarified and the main problem, which is the lay-up of a natural fiber sliver, can be subdivided into sub functions, as shown in Figure 43, thus facilitating the future research of solutions.

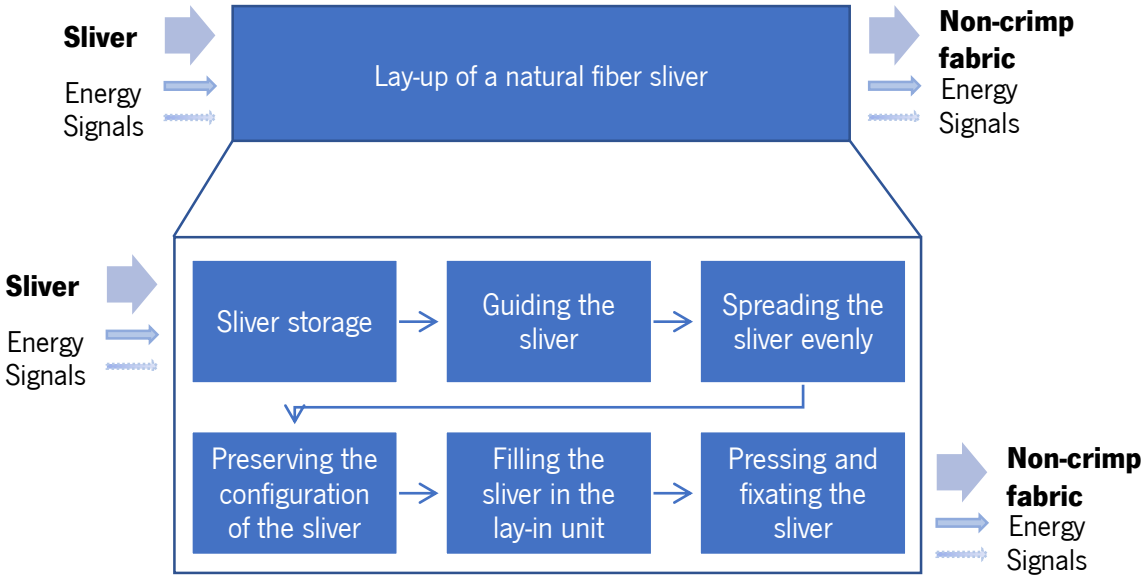

Figure 43 Function Structure

In order to lay-in the sliver, it's first **transported** from the creel to the weft insertion device, it is **guided** through the weft-insertion device and tensioned, the sliver is **spreading evenly,** to control the mass surface of the layer, **without changing the sliver configuration**. The sliver is finally **filled in the hook chain of the lay-in unit** and fixated by being pressed.

5.3 Determination of partial solutions

The processability of the untwisted flax sliver is investigated with regard to the existing process frame conditions on the COP-CENTRA MAX 3 CNC machine from Karl Mayer. An analysis of each sub-function of the process is made with the determination of possible solutions. The transportation of the sliver has been undertaken by another group project, it will be overviewed in the following work, and the filling and pressing of the slivers in the lay-in unit will be part of another project, but also slightly overviewed.

5.3.1 Feeding of the weft insertion system

5.3.1.1 Transportation

When transporting the untwisted flax slivers to the weft insertion system, the fibers of the sliver slip and the sliver ends up breaking. This is due to the withdrawal force of the system, which is higher than the supported force of the flax untwisted slivers. The adhesive friction force for the withdrawal system for glass fibers if of approx. 350 cN and increases during the accelerations of the lay-up process.

Thus, the processing of untwisted flax slivers into fabrics is not possible without a new strategy of transportation from the creel to the weft insertion system. For responding to this problem, the sliver is temporary twisted. A false twist (Figure 44) is the application of a temporary twist which returns after transportation. It can strengthen the flax slivers, which would allow to conduct the transportation of the material to the weft-insertion system (Koenig, 2014).

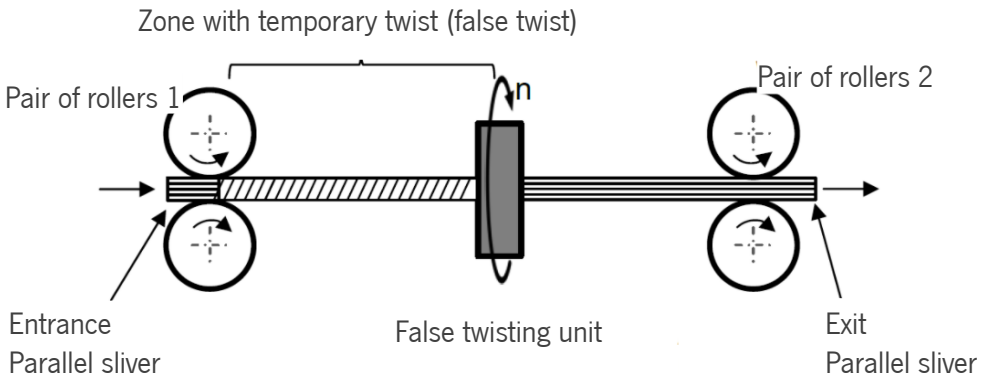

Figure 44 Principle of the false twist (Klein and Rieter Machine Works, 2008)

5.3.1.2 Entrance

The entrance of the weft-insertion system (Figure 45) is adapted for the processing of glass fibers. In order to process flax slivers, the entrance has to be adapted.

Figure 45 Entrance of the weft insertion system

The multiple entries system (a) has multiple ceramic eyelets that allow material to slide in. The more eyelets there are, the more there is friction (Kyosev, 2016). This entry system can easily be changed by a single entrance unit (b) (see Figure 46). With less friction, the flax sliver can, without difficulty, enter the system.

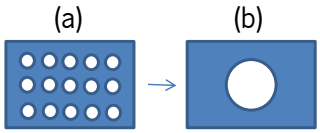

Figure 46 Entrance solution

5.3.2 Guiding of the sliver

The weft-insertion system guides the glass fibers and maintains an adapted tension for the laying of the glass fibers (Figure 47).

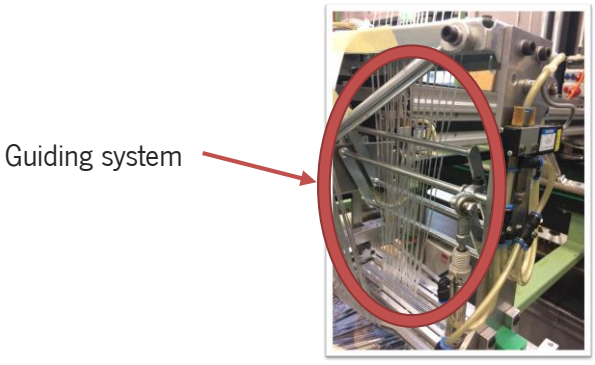

Figure 47 Weft-insertion guiding system

However, this system is not adapted for the processing of untwisted flax slivers, as they tend to break with the actual unit, and when processing the flax slivers without any guidance and tension, the sliver is loose and hard to lay-in. To respond to this problem, a new guiding system must be conceptualized. Various guiding systems exist:

5.3.2.1 Belt conveyor

Belts can be used as short transport systems within a machine, to carry the sliver (Lord, 2003). They are endless circulating belts. The belts are driven by shafts that simultaneously serve for the belt tensioning. They allow to work at high speeds but the belt causes friction and the material can to stick to the belt (Klein, 2016a).

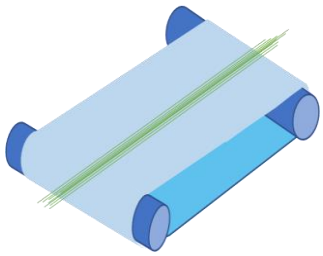

Figure 48 Belt conveyor transportation (Klein, 2016a)

The advantages and disadvantages of the belt conveyor are presented in Table 12:

Table 12 The advantages and disadvantages of the belt conveyor

Advantages	Disadvantages
• Simple implementation; • High speed process;	• Material can stick to the belt;

5.3.2.2 Roller pairs

Guiding systems can be found the production chain for sliver production. During the drafting of the sliver, explained in 3.2.1, the nip pair roller system (Figure 49) presents good guiding characteristics.

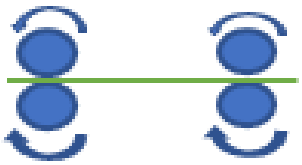

Figure 49 Roller pairs transportation

The break-draft part of the drafting system has the function of pre-tensioning and transporting the sliver. Here, the sliver configuration should be preserved. Drafting only occurs when the speed of the rollers increases from pair roller to the next. To avoid drafting, the speed of the rollers has to be equal.

The distance between the rollers is important for good guidance of the fibers (Klein, 2016a):

- If the distance is to wide, it will increase the number of floating fibers and result in higher unevenness of the sliver.
- If the distance is too narrow, it will cause fiber damage;

However, for the guiding systems, as the fibers are not drawn, the parameter that counts the most is that the distance is not to wide and covers most of the fiber lengths.

The material of the rollers is an important parameter to consider enhancing the guiding properties. In fact, the top rollers should be coated with a thick synthetic rubber coat. The rubber is used to improve the grip on the fibers, the more the coats are soft the better they will surround the fiber and guide it. Hard coats will enhance drafting, which is not wanted here (Klein, 2016a):

- **Soft: 65° - 75° Shore**
- Medium: 75° - 80° Shore
- Hard: Above 80° Shore

Coats can be made out of urethane or silicone. Silicone coats are more expensive than urethane coats and have higher coefficient of friction, so better drafting properties. Here a urethane coat responds better to the requirements as it is cheaper and has good durability and lower coefficient friction (Schaefer, 2018).

For the bottom rollers, the material most generally used is steel, with a hardness of 150 HB.

The advantages and disadvantages of the roller pairs are presented in Table 13:

Table 13 The advantages and disadvantages of the roller pairs

Advantages	Disadvantages

• Simple implementation; • Good transportation; • Adjustable tension. • Simple combination with other processes.	• Fibers with high quality or medium fiber length required; • No data on fiber damage;

5.3.2.3 Trumpet-Take-up rolls:

In 3.2.1, the transportation system from the sliver condenser to the can be used as a solution for the guiding system (Figure 50).

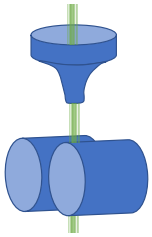

Figure 50 Trumpet - Take-up rolls transportation (Lord, 2003)

When exiting the sliver condenser, the sliver passes through a trumpet, which condenses it and is discharged by a take-up rolls system into the can.

However, the trumpet size has to be changed according to the sliver weights (Lord, 2003). If included in the feeding system of the weft-insertion device, the trumpet would have to be changed for differing sliver weights. The throat diameter of the trumpet should be between $1{,}6\sqrt{n}$ and $1{,}9\sqrt{n}$, with n, the linear density of the sliver in ktex and the diameter expressed in mm.

The advantages and disadvantages of the "trumpet – take-up rolls" are presented in Table 14:

Table 14 The advantages and disadvantages of the trumpet-take-up rolls

Advantages	Disadvantages
• Good guiding.	• Difficult implementation.

5.3.2.4 Loop tensioner

The loop tensioner can transport a thread and keep it under tension (Figure 51). This system is used in braiding systems for rewinding, with synthetic fibers (Ebel, Brand and Drechsler, 2013). There is no existing data in the efficiency of the process for natural fibers.

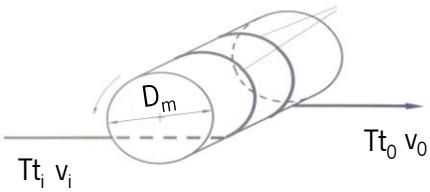

Figure 51 Loop tensioner dynamic

In Figure 51, the thread has an initial velocity v_i and a fineness Tt_i. It comes out from the system with the velocity v_0 and the fineness Tt_0. For our case scenario, the thread fineness must remain the same, as we only aim to guide and give appropriate tension to the sliver. This is possible under the condition that (Brünig and Beyreuther, 2006):

- $v_0 = v_i$

The resulting transportation system is represented in Figure 52.

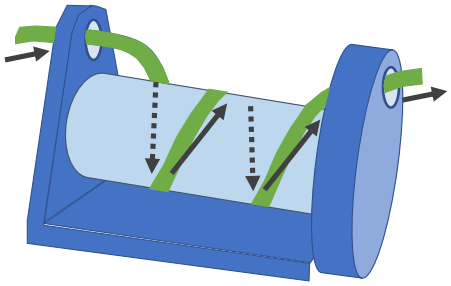

Figure 52 Loop tensioner transportation (Ebel, Brand and Drechsler, 2013)

The advantages and disadvantages of the loop tensioner are presented in Table 15:

Table 15 The advantages and disadvantages of the loop tensioner

Advantages	Disadvantages
• Good guiding;	• High fiber damage; • High tensions.

5.3.2.1 Final evaluation of the guiding system

The presented guiding methods are evaluated on the basis of three different evaluation criteria in order to determine a suitable method for the processing of natural fiber slivers. The evaluation criteria are defined on the basis of the task and weighted according to their priority. This includes implementability, costs and required installation space. In Table 16 the weighting factors are presented. The implementability is the highest priority, the costs are second and the required installation space is the last priority.

Table 16 Determination of the weighting factors of the evaluation criteria (Jänsch, 2006)

Evaluation criteria	Priorities (p_i)
Implementability	3
Costs	2
Required installation space	1

$$g_i = \frac{p_i}{\sum p_i}$$

Weighting factors (g_i)
0,5
0,33
0,17

[3: highest priority, 1: lowest priority]

The individual spreading methods are quantitatively evaluated on a scale of 0 to 4 with regard to the three evaluation criteria. A rating of 4 points is a very high suitability with regard to the respective evaluation criterion, a rating of 2 points, however, represents the minimum necessary degree of fulfilment of the requirement (see Table 17). A score of 1 or 0 points means that the requirements cannot be met.

Table 17 Scale of points for quantitative evaluation of the spreading principles

	Evaluation criteria		
Points	**Implementability**	**Costs**	**Installation space**
4	Extremely high	Extremely low	Extremely low
3	High	Low	Low
2	Moderate	Moderate	Moderate
1	Low	High	High
0	Extremely low	Extremely high	Extremely high

The evaluation is based on the theoretical considerations from the previous parts and with the evaluation. The results are regrouped in the following Table 18:

Table 18 Evaluation and evaluation of the guiding methods considering the respective weighting factors (Jänsch, 2006)

	Implementability	Costs	Installation space	Sum
Weighting factors	**0,5**	**0,33**	**0,17**	**Σ gi * wi**
Belt conveyor	4	3	4	3,67
Roller pairs	4	3	4	3,67
Trumpet-Take-up rolls	1	3	3	2
Loop tensioner	1	2	3	1,67

The evaluation shows that the belt conveyor and the roller pairs should be the best suited solutions for guiding the slivers. The minimum requirements were exceeded for all the criteria.

5.3.3 Spreading the sliver evenly

The slivers need to be spread-out to obtain a defined width. To do so, various spreading methods exist: electrostatic, mechanical (with spreader bars, spreader rollers, spreader combs or knives), pneumatical (with jets operated by pressurized air) and also jet-liquid spreading or acoustic spreading. Some of those methods are detailed in the following part (Cherif, 2015).

5.3.3.1 Spreader bars

Spreading by means of spreader bars is currently the most frequently used method. It is based on the principle of pulling fibers over spreader bars using high tension (Composites World and Gardinier, 2018).

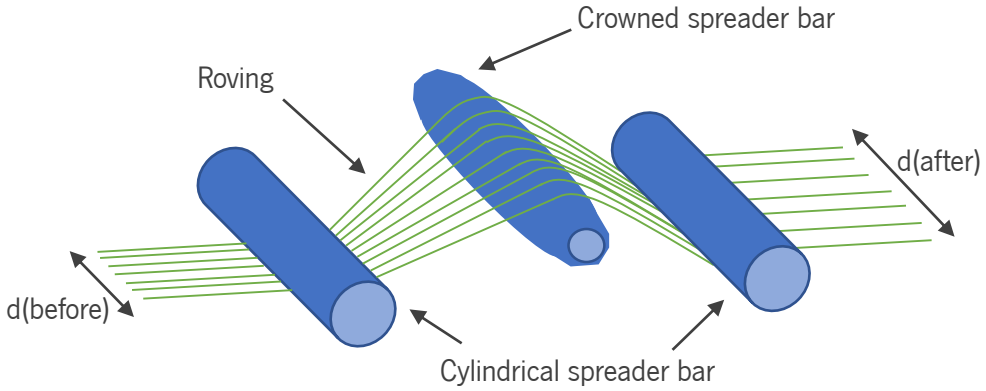

Figure 53 Spreading by spreader bars

The filaments which are further away from the central axis of the bar cover a longer distance than the filaments which go through the central axis. As a result, the stress of the filaments increases the higher the distance with the central axis. These stresses cause forces in the direction of the central axis and leads to splitting up the strips in the axial direction of the bar (Irfan *et al.*, 2012). The sliver thickness and basis weight are reduced. In order to reduce filament damage, the friction between the bar surface and the filaments should be as low as possible. A smooth bar surface is therefore desired for fixed bars (Yamamoto, Yamatsuta and Abe, 1988).

The spreading can be influenced by the spreader bar geometry. Spherical bars, for example, reinforce the spreading but can lead to the formation of gas if the yarn guide is not exact. Cylindrical bars homogenize the belt and requires less yarn guidance precision.

When processing untwisted natural fiber slivers, even small tensions can cause the sliver to tear apart, as the individual fibers slide from each other. For working with natural fibers, to avoid the slivers from breaking, the distance between the bars should be smaller than the average fiber length. It is therefore useful to work with high fiber length, but high fiber length, for slivers, implies that the quality of material is higher and so is the resulting cost of the material. Therefore, the process becomes expensive.

The other disadvantages of this method are that the production speed is limited to 25m/min. At higher speeds, the friction is too high and damages the fibers. Also, spreading is limited to 3 times the initial width (Composites World and Gardinier, 2018).

The advantages and disadvantages of fluid flow are presented in Table 19.

Table 19 Advantages and disadvantages of spreading with spreader bars

Advantages	Disadvantages
• Simple implementation; • Variety of variations; • Simple combination with other processes.	• High fiber damage; • High yarn tensions; • Fibers with high quality or medium fiber length required; • Low speed process.

5.3.3.2 Fluid flow spreading

Spreading processes with fluid flows represent an alternative to the mechanical spreading processes, which usually lead to a certain damage of the filaments. Thanks to gas or liquid flows, the filaments can be spread to 6-7 times the initial width (Composites World and Gardinier, 2018). The flow hits the filaments perpendicularly to the process direction (Figure 54).

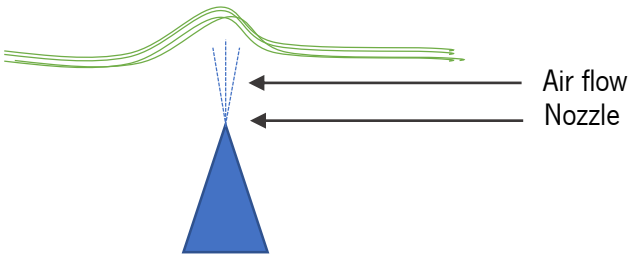

Figure 54 Spreading by air flow

The simplest method is spreading by means of gas flow. The air flow is generated by overpressure (or under pressure) and directed from the nozzles onto the filaments.

With this contactless spreading method, the fibers are spread very gently. Natural fiber slivers can be processed without fiber damage.

Spreading by liquid flow is however not adapted for the processing of natural fibers as they have high liquid absorption capacity and if spread by liquid flow, an additional drying step would be needed.

The advantages and disadvantages of fluid flow are presented in Table 20:

Table 20 Advantages and disadvantages of fluid flow spreading

Advantages	Disadvantages
• High degree of expansion; • Constant degree of expansion; • Low yarn tensions; • Low filament damage; • Good adjustability; • Homogenizing effect (self-regulation).	• High complexity; • Low process speeds; • High costs due to drying processes (when using liquids).

5.3.3.3 Air vibration spreading

An alternative to the continuous air flow spreading, is spreading using airborne sound. The filaments are guided via a loudspeaker as shown in Figure 55. The membrane of the loudspeaker generates sound waves, which stimulate the fibers to vibrate. The vibrations of the fibers lead to the filaments to repel each other and result in the fragmentation of the sliver (Composites World and Gardinier, 2018).

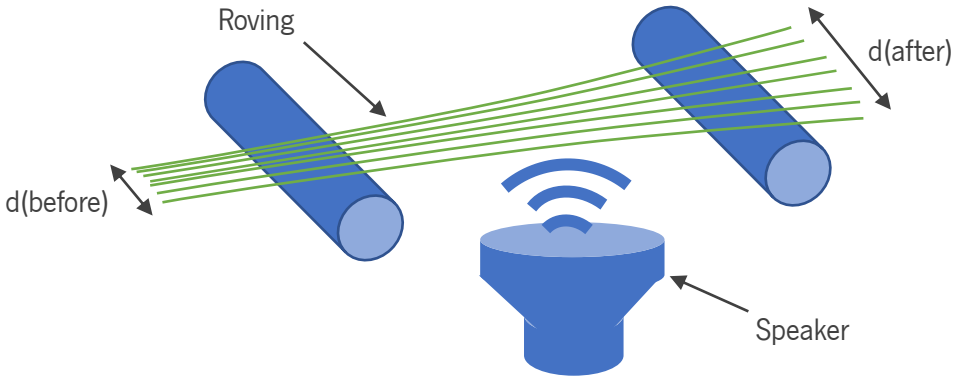

Figure 55 Spreading by air vibration

In order to achieve high spreading degrees, it must be ensured that the frequency range is adapted to the filaments. The higher is the energy absorption of the filaments – and thus the vibration - the higher is the degree of spreading. The problem with processing natural fibers could be that the vibrations are not as well transmitted for staple fibers as they are for filaments and therefore the energy absorption capacity is too low. Vibrations could also loosen the sliver so much that the cohesion is no longer guaranteed, and the sliver would break. Further advantages and disadvantages of this method are shown in the following Table 21.

Table 21 Advantages and disadvantages of spreading by air vibration

Advantages	Disadvantages
• Very high degree of spreading; • Low yarn tensions; • High process speeds.	• Noise protection necessary due to high sound pressures; • No information regarding the filament damage.

5.3.3.4 Electrostatic spreading

Another spreading method is the electrostatic repulsion. The roving needs to be electrically conductive, if it is not naturally conductive, the rovings can be wet with a conductive liquid. The roving is then passed through a charging electrode which generates an electric field (Figure 56). This saturates the ambient air with Ions of one polarity. As a result of the excess charge of one polarity, the filaments repulse each other.

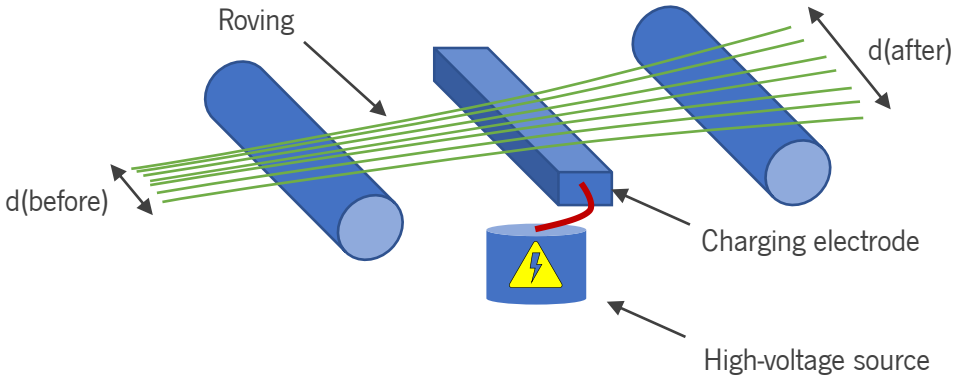

Figure 56 Spreading by electrostatic repulsion

For processing natural fibers, a conductive liquid must be applied to the fibers and therefore, has to be removed in an additional step after the spreading. This increases the complexity and costs of the procedure. Further advantages and disadvantages of the spreading method are clearly presented in the following Table 22:

Table 22 Advantages and disadvantages of spreading by electrostatic repulsion

Advantages	Disadvantages
• Very good spreading degrees; • Low filament damage; • Very low yarn tensions; • High process speeds.	• High complexity; • Danger to the user by high-voltage operation; • High energy costs.

5.3.3.5 Final evaluation of the spreading system

The evaluation is based on the theoretical considerations from the previous parts and with the evaluation criteria from 5.3.2.1. The results are shown in the following Table 23.

Table 23 Evaluation of the spreading methods considering the respective weighting factors

	Implementability	Costs	Installation space	Sum
Weighting factors	**0,5**	**0,33**	**0,17**	**Σ gi * wi**
Spreader bars	1	4	3	2,33
Fluid flow (liquid)	1	1	1	1
Fluid flow (gas)	4	3	4	3,67
Air vibration	2	3	4	2,67
Electrostatic	1	1	2	1,17

The evaluation shows that the fluid flow method with gas is best suited for an application on flax slivers in regard to the evaluation criteria of implementability, cost and installation space. The minimum requirements were exceeded for all the criteria.

5.3.4 Laying the sliver in the lay-in unit

When filling the flax sliver to the laying unit of the Copcentra Max 3 CNC (Figure 57), the sliver overloaded the needles, there is a damage of the sliver and material loss along the process.

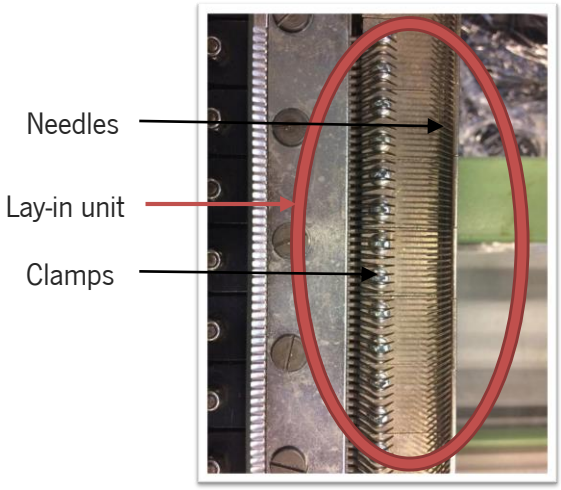

Figure 57 Laying unit

The laying unit for the COPCENTRA Max 3 CNC is the hook system, explained in 4.2.2.2. The clamping system would probably be more adapted for the processing of natural slivers, as the slivers would be cut and clamps to the lay-in unit and no material overpacking would occur. However, the machine is yet too expensive, further research should be made for the optimization of the hook system.

5.4 Development of concepts

5.4.1 Morphological box and concepts developments

To generate the solutions for the weft-insertion system, the partial solutions are regrouped in a morphological box (

Table 24). The partial solutions that were evaluated best fitted for responding to the problem are combined to form solutions.

Table 24 Morphological box and concepts developments

Solutions / Functions	1	2	3	4
F1: Sliver entrance	 Multiple entrance	 Single entrance		
F2: Guiding the sliver	 Roller pairs	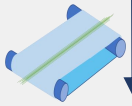 Belt conveyor	 Trumpet/ Take-up rolls	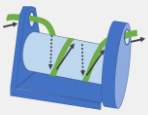 Loop tensioner
F3: Spacing sliver evenly	 Air flow	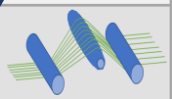 Spreader bars	 Air vibration	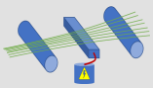 Electrostatic
F4: Controlling width of the sliver	 Bar width			

A		B	
F1	2	F1	2
F2	1	F2	2
F3	1	F3	1
F4	1	F4	1

There are two combined solutions:

- Solution A: Combines the single entrance with the roller pairs, the air flow system and in order to control the width a bar system should be installed.
- Solution B: Combines the single entrance was combined with the belt conveyor and air flow system. The width is also controlled with two bars.

5.4.2 Solution A

In solution A (Figure 58), the sliver is guided and tensioned by a pair of guiding rollers, an air flow system, with a determined air pressure, spreads the slivers. In order to control the width variation, the air pressure must be controlled, and adjustable bars should be installed to avoid slippage from the fibers at the extremities.

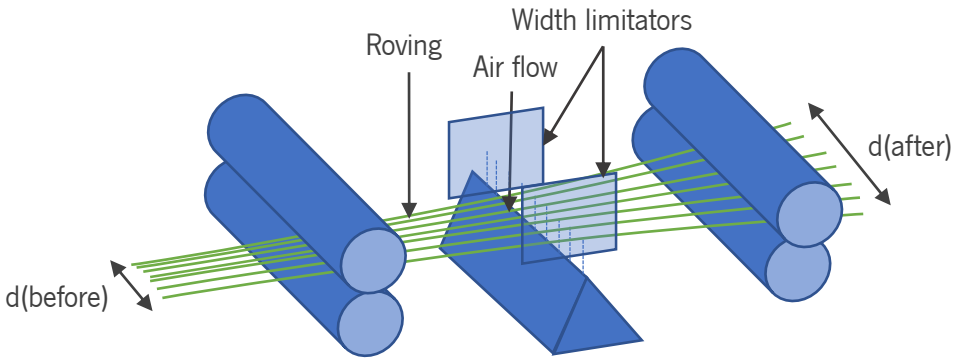

Figure 58 Solution A

5.4.3 Solution B

In solution A (Figure 59), the sliver is guided by a belt conveyor, an air flow system, with a determined air pressure, spreads the slivers. In order to control the width variation, the air pressure must be controlled, and the belt should have a width limitation. The problem with that solution is that the width limitation system is not adjustable according to the needed width, the belt should therefore be changed for each width which is costly and not practical.

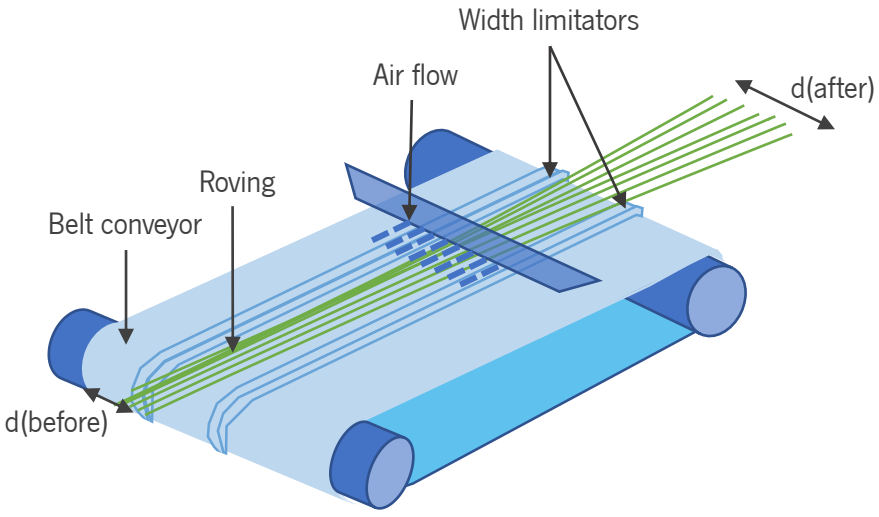

Figure 59 Solution B

5.4.4 Evaluations of the solutions

When evaluating the solutions, with the same method explained in 5.3.2.1, Table 25 regroups the evaluation criteria for each solution:

Table 25 Solutions evaluation

	Feasibility	Costs	Installation space	Sum
Weighting factors	**0,5**	**0,33**	**0,17**	**Σ gi * wi**
A	4	3	4	3,67
B	1	1	4	1,51

The evaluation shows that the solution A is the best suited solution for replacing the actual weft-insertion system. The minimum requirements were exceeded for all the criteria.

5.5 Validation of the concept

In order to validate the solution A, a test stand is constructed with the available material at ITA. An experiment design is conducted to determine the influencing factors and setting ranges of the solution and the results are finally evaluated for the effectiveness of spreading the flax sliver.

5.5.1 Preliminary testing

The test stand (see Figure 60) helps to evaluate the suitability of the solution A for spreading the flax slivers and allows to determine the influencing parameters and their limits. The guiding rollers system could not be implemented, as the system was built with the available components at ITA.

The distance between the individual units are reduced as much as possible in order to reduce the risk of sliver damage (the distance between the force introduction points must be smaller than the average fiber length). Also, as the sliver is conveyed directly from the container to the conveyor, and additional ring, through which the sliver is guided, ensures centering the sliver.

In order to have control on the degree of spreading more precisely, the sliver above the air nozzle is limited laterally by adjustable plates. Camera systems are installed in front and behind the spreading unit to measure the fiber sliver width. A VGA camera with a resolution of 640x480 pixels records the width before the spread, a line camera with a resolution of 2000 pixels records the width after the spread. LED panels are placed under the fibers to create contrast.

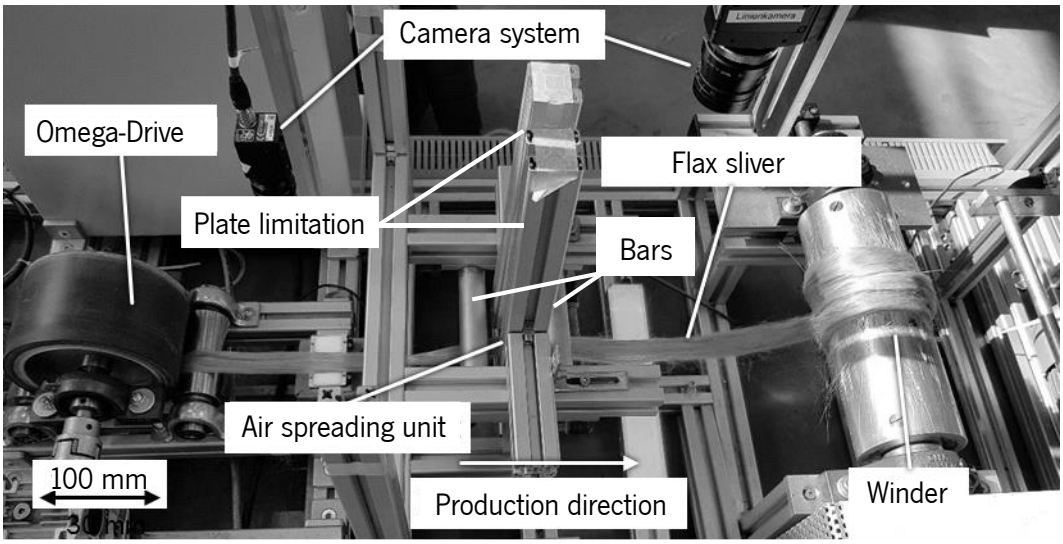

Figure 60 Test stand of solution A

In Figure 61 a schematic illustration of the spreading unit is represented and in Figure 62 a schematic lateral view of the test stand is illustrated.

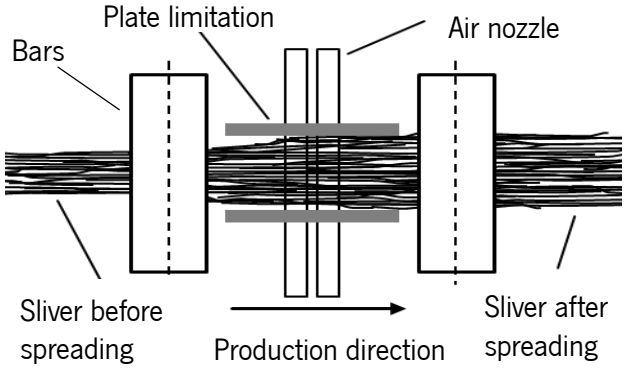

Figure 61 Air spreading in the test stand

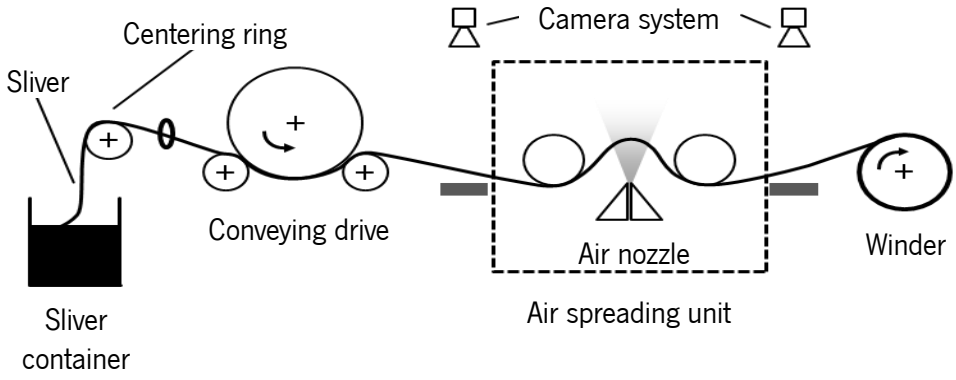

Figure 62 Schematic structure of the test stand in lateral view

Five influential parameters for the spreading unit can be highlighted:

- **Process speed**: The process speed is determined by the speed of the Omega drive. A higher speed results in shorter spreading time of the sliver over the air nozzle, thus lower spreading of the sliver. For the following tests the sliver speed is kept constant at 3,12 m/min.
- **Height of the sliver in the spreading unit:** The speed of the winder is adapted to the speed of the Omega drive and varies slightly to keep the tension within the sliver constant. A constant tension of the sliver is essential for a good spreading process, as this has an effect on the height of the sliver in the spreading unit. Higher tensions cause a higher height, lower tensions cause a low height and floating sliver. When the sliver has a low height and floats above the air nozzle system, the sliver oscillates due to turbulent flows. The sliver is then subjected to uneven stress and the air flow cannot be directed correctly through the sliver. For the following tests, a height of approx. 5 cm has been chosen.
- **Air pressure:** The air pressure also has a direct effect on the result of the spread. A low air pressure has hardly noticeable effects on the sliver, a high air flow induces greater forces in the sliver and thus causes higher spreading degrees. However, if the pressure is too high, individual fibers can get loose, especially in the edges of the sliver and damage can occur. For the following tests, the minimum air pressure is set to 1 bar and the maximum air pressure to 2 bar.
- **Distance between bars in the spreading unit:** The distance between the bars of the spreading unit have also an effect on the spreading of the sliver. A larger distance leads to a larger radius of the arc, smaller distances cause an arc with a smaller radius. Due to the design of the spreading unit, the minimum distance between the bars is limited to 9.5 cm, the maximum distance is set to 12 cm.
- **Width of the lateral plate limitation:** The lateral limitation of the sliver regulates the maximum width of the sliver above the nozzle of the air spreading unit. This limitation limits the maximum achievable spreading degree of the sliver, but at the same time leads to a smoothing of the sliver after spreading. The unprocessed width of the sliver varies around 3 cm, in the preliminary tests, it turned out that a width of less than 3 cm for the plates does not lead to any meaningful spreading results, since it is lower than the unprocessed sliver width. Instead of spreading the sliver, the sliver is folded, and the width reduced. At widths over 5 cm, the limitation has almost no effect, since the sliver doesn't touch the plates.

5.5.2 Experiment design

In order to investigate the effect of the influential parameters, determined above, on the sliver, an experimental design is made. The individual parameters (the process speed, the air pressure, the distance between the bars of the spreading unit, the width of the lateral plate limitation of the spreading unit and the height of the sliver in the spreading unit) are evaluated in two levels, a low (-) level and a high (+) level (see Table 26). The levels were previously determined in the preliminary tests and must not exceed machine or material limits.

The process speed is kept constant at 0.05 m/s during the tests. The height of the sliver is kept at approx. 5 cm by manually adjusting the take-off speed. Thus, three parameters remain, which are varied within the parameter ranges determined in the preliminary tests. The air pressure (A) can be adjusted between 1 bar and 2 bar, the lateral plate limitation of the spreading unit (B) between 3 and 5 cm and the distance between the bars (C) between 9,5 and a maximum of 12 cm.

Table 26 Factor limitations

A [bar]		B [cm]		C [cm]	
-	+	-	+	-	+
1	2	3	5	9,5	12

In order to determine the influence of the factors, a combination of 8 tests is made (see Table 27).

Table 27 Factor experimental design

Combination	A	B	C
(1)	-	-	-
a	+	-	-
b	-	+	-
c	-	-	+
ab	+	+	-
ac	+	-	+
bc	-	+	+
abc	+	+	+

5.5.3 Test evaluation

For the test evaluation, the values recorded by the cameras in front of and behind the spreading unit for the width of the sliver were evaluated. In the unprocessed state, the width of the strip varies greatly. In order to determine the spreading effect of the air spreading unit, the width of the same specific sliver section must be compared before and after the spreading. For this reason, the measured value curves must be corrected in time by the amount of time the sliver section needs from the first to the second measuring point. The length of the sliver between the first and second measuring point is approx. 39,7 cm. For a sliver speed of 52 mm.s^{-1} the time difference is of 7,6 s. In addition to the time shift, incorrect values may have to be corrected or excluded from the evaluation. Incorrect values occur when the edges of the sliver cannot be correctly determined, for example when single fibers are loose around the sliver. These lead to contrasts in the recorded image, which are recognized by the edge detection algorithms. These defective measuring points are excluded for the test evaluation. All the values gathered per factor of combination before and after the spread are evaluated below. In Figure 63, the sliver width before and after the spread for different factors combination is represented.

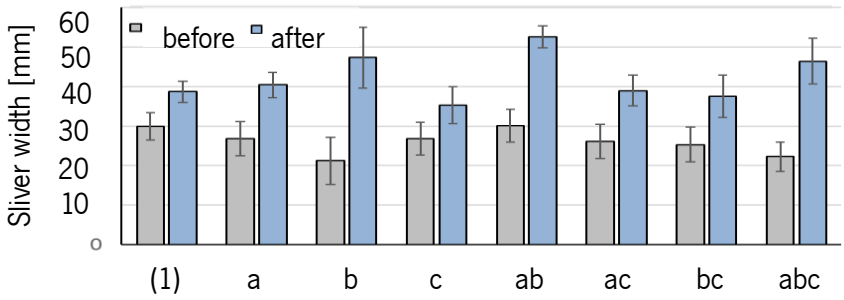

Figure 63 Mean sliver width before and after the spread for different factor combinations

An increase in sliver width can be achieved for each combination of factors. The highest average width of 52,54 mm can be achieved with the factor combination "ab", however, it must be taken into account that the entrance width of 30,11 mm was also the highest. Even before spreading, the sliver shows strong variations in its width. It should be investigated whether these fluctuations can be reduced by air spreading and whether the sliver is more uniform. To assess the actual spreading effect, the degree of spreading can be considered. This results from the ratio of the width after and before the spread:

$$SD = b(after)/b(before)$$

SD: Spreading degree

b(after): Width of the sliver after the spread[mm].

b(before): Width of the sliver before the spread[mm]

In Figure 64, it is possible to observe that the factor combination "ab", which reaches the highest average width after spreading, does not achieve the highest spreading effect. Instead, the highest spreading effect is achieved by increasing the distance between the lateral areas with the factor combination "b".

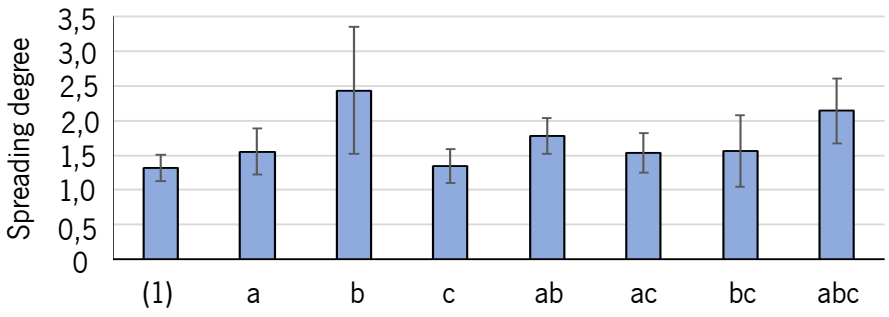

Figure 64 Spreading degree for different factor combinations

To evaluate the suitability of the spreading unit for the uniformity of the sliver width, the coefficients of variation can be considered:

$$v = \frac{\sigma}{x} * 100$$

v: Coefficient of variation [%]

σ Standard deviation

x: Mean value

In Figure 65, the variation coefficients of the mean sliver width for each of the factor combinations is represented before and after spread. For each factor combination, the coefficient of variation is reduced and thus a homogenization of the fiber is achieved. For the factor combination "ab" the coefficient of variation could be reduced from approx. 14 % to 5 %.

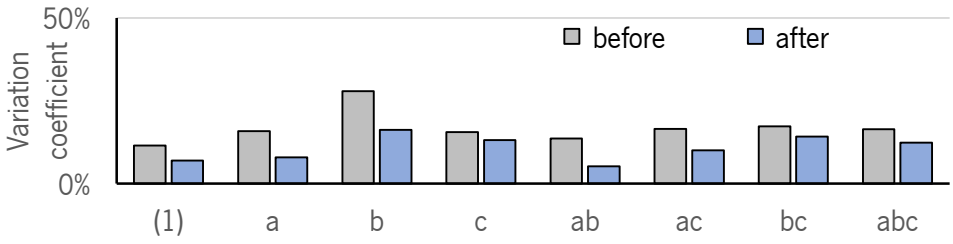

Figure 65 Variation coefficient of the mean sliver width for different factor combinations

In Figure 66, the effect of air pressure on the sliver width after spreading is represented. This results in a linear influence, since only two factor levels were investigated. The width of the sliver increases by 4,86 mm from an air pressure of 1 to 2 bar.

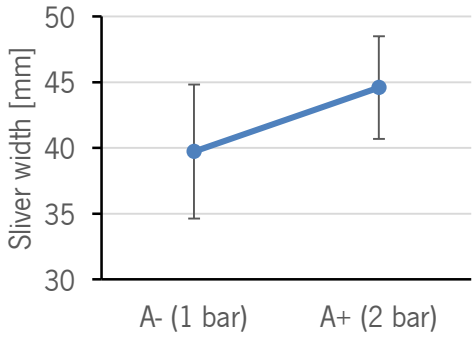

Figure 66 Effect of air pressure (A) on the width of the sliver after spreading

The plate width limitation is the most influential parameter for the width of the sliver after spreading. The width of the sliver increases by 7,61 mm from a plate distance of 3 to 5 cm.

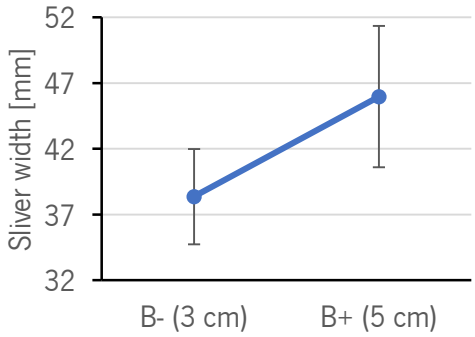

Figure 67 Effect of the plate width limitation (B) of the sliver after spreading

The effect of the bar spacing on the width of the sliver after spreading is less influential than the other effects. Nevertheless, its effect is not to be neglected, as an increase in the bar spacing in the spreading unit leads to a reduction in the mean sliver width after spreading.

The greater the distance between the bars, the less the sliver will be fixated and the more it will be flexible. The air flow will no longer be orthogonal to the sliver and the distribution of the fiber will be irregular.

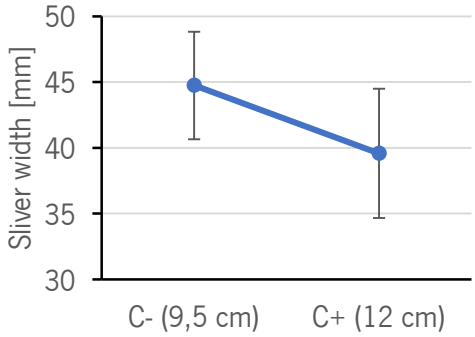

Figure 68 Effect of the bar spacing on the width of the sliver after spreading

6 Construction of the new weft insertion system prototype

6.1 Requirements list for the new weft insertion system prototype

6.1.1 Roller pairs parameters

As described in 5.3.2.2, the distance between the rollers should cover most of the fiber length (Klein, 2016a). The average fiber length here being of 200mm, it was decided that the distance between the rollers should be smaller than 150mm.

Also, the top rollers should be coated with a soft (65° - 75° Shore) synthetic rubber coat, for a good guidance of the sliver. For the bottom rollers, the material most generally used is steel, with a hardness of 150 HB. The diameter of the rollers normally varies between 40 to 60 mm (Klein, 2016a) and the length of the rollers should obliged by the following equation (Whiteside, 2007):

$$\frac{Length}{Diameter} = 16 \; or \; less$$

6.1.2 Motor parameters

In order to choose the motor for the weft insertion system, it is necessary to determine the torque and speed needed.

The **speed** of the weft insertion system was described in 0. However, the speed to analyze here is the rotation speed needed for the roller pairs.

The speed rotation is determined thanks to the following equation:

$$v_{rot}(t) = \frac{v(t)}{D_{roller} \times \pi} \qquad (4)$$

With,

$D_{roller} = diamater \; of \; the \; roller = 65mm.$

And with the obtained values, the torque and the pulse per second (PPS) could be determined. For the determination of the PPS, the following equation was used:

$$PPS = v_{rot} \times (steps \; per \; revolution) \times (gear \; ratio)$$

With,

$steps\ per\ revolution = number\ of\ steps\ the\ motor\ has\ for\ one\ rotation = 200$

$gear\ ratio = \frac{number\ of\ teeth\ for\ the\ disc\ shaft}{number\ of\ teeth\ disk\ motor} = \frac{36}{72} = 0{,}5$

The **torque** is determined with the following equations:

$$M = \frac{ABS((v_{rot} \times (M_{rollers} + M_{belts} + M_{motor} + M_{roll}))}{gear\ ratio}$$

With,

$M_{rollers} = 0{,}001230902\ Nm$ (determined by AutoInventor)

$M_{belts} = 0{,}000062812\ Nm$ (determined by AutoInventor)

$M_{motor} = 0{,}00022\ Nm$ (estimated)

$M_{roll} = 0{,}033673806\ Nm$ (estimated)

The resulting torque and speed needed for the system for the first phase (filling the hooks) is represented in Figure 69. The second phase, weft carriage moving from one side to the other, is represented in Figure 70.

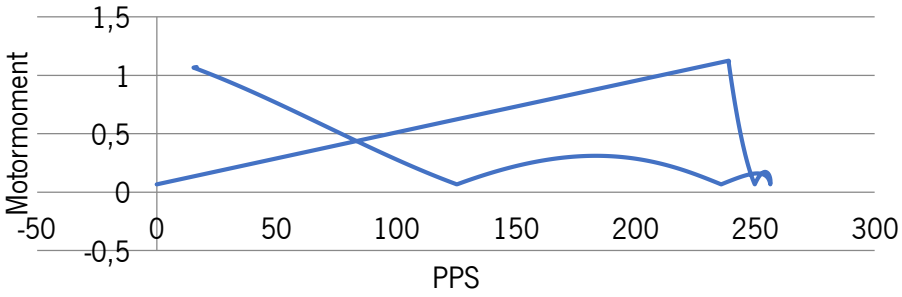

Figure 69 First phase motor characteristics

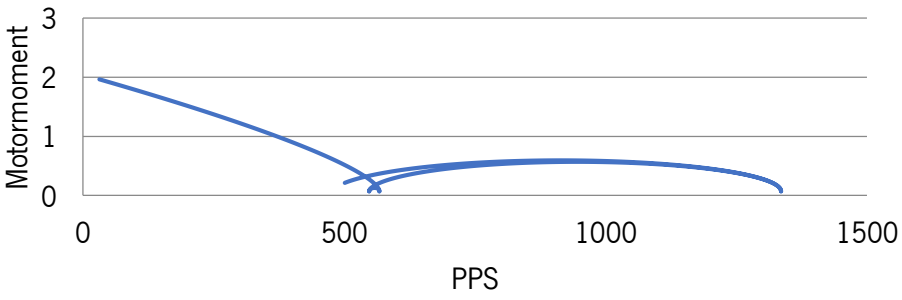

Figure 70 Second phase motor characteristics

For choosing the motor, the torque and the PPS must be fulfilled. The motor that fitted best the characteristics and was at a reasonable price was a motor from Oriental Motor Co. Ltd., PKP299D63A. The characteristics of the motors are represented in Figure 71:

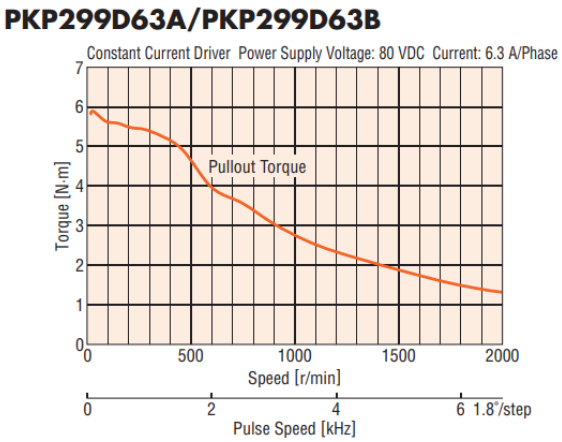

Figure 71 Selected motor characteristics

6.1.3 Requirements list

Requirements list *Tricot Machine with Multiaxial Weft Insertion (LIBA Copcentra Max 3 CNC): Development of a new weft insertion device.*	
Demand (D) Wish (W)	**Requirements**
	Geometry
D	Nip to nip distance between the rollers: • Max. 150 mm; • Must be adjustable.
D	Diameter of rollers: • 40 to 60 mm.
D	Length of rollers (Whiteside, 2007): • $\frac{Length}{Diameter} = 16\ or\ less$
D	Width limitation: • 10 to 100 mm; • Must be hand adjustable.
	Kinematics
D	Max. speed of the weft carriage system: 6 $m.s^{-1}$
D	Max. acceleration of the weft carriage system: 15 $m.s^{-2}$
D	Pairs of rollers independently driven
D	Conveyor speeds of the roller pairs can be synchronized
	Forces
D	Air pressure: • 1 to 10 bars; • Must be controllable; • Proportional to the speed of the weft insertion device.

D	Pressure on rollers: • Top rollers must be pressured towards the bottom rollers (by spring weighting or pneumatic weighting); • Must be adjustable.
D	Friction force on the flax fiber during the lay-up process: approx. 350 cN
D	Friction force on the glass fiber during the lay-up process: approx. 50 N
D	The weft threads are drawn parallel. No thread tension difference can occur.
	Material
D	Top rollers: • Coating material: Thick coating made of synthetic rubber; • Soft Coat: 65° to 75° Shore.
D	Bottom rollers: • Minimum hardness: 150 HB
	Ergonomics
W	Good accessibility.
	Operation
D	Assemblage not to complex and easy to implement.
	Maintenance
W	Long maintenance intervals.
W	Worn parts easily exchangeable.
	Safety
W	Operational and environmental safety in regards of the possible carbon fibers presence in the laboratory. Electrical components suitable for use in environments with CF fiber dust exposure (protection class: IP-6X)

6.2 Drawing of the new weft insertion system prototype

With the help of a mechanical engineer student at ITA, the new weft insertion system was modelized with AutoInventor (Figure 72):

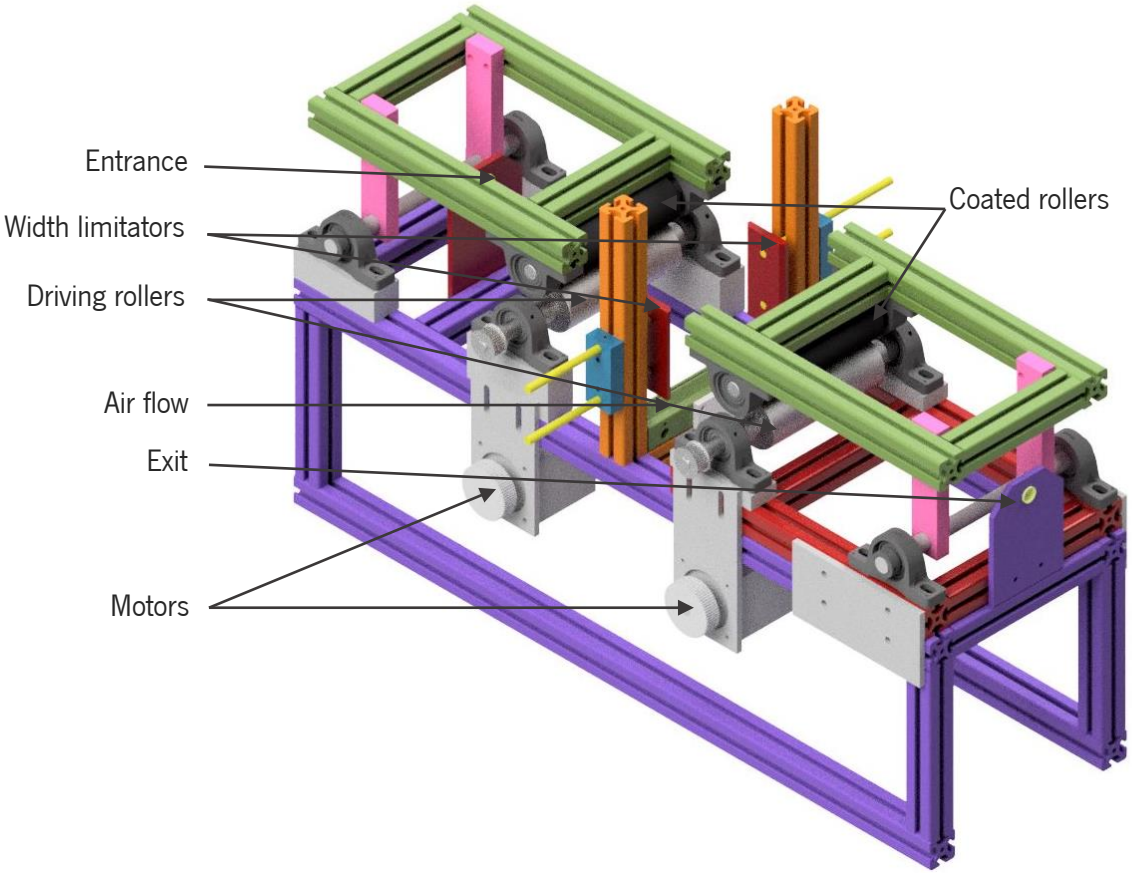

Figure 72 Weft insertion system prototype model

6.3 Constructing of the test stand

Each part of the machine was drawn as in industrial drawing to be sent to the construction site of ITA. The drawings can be found in ANNEX 4. The construction of all the elements has exceeded the time intended and it was not possible to build the construction stand on the time of the project.

7 Conclusion and Outlook

The most common fibers in fiber reinforced plastics are glass fibers and carbon fibers. However, these materials have a high ecological footprint, they are made from non-renewable resources and their production results in high energy consumption and high CO2 emission. In this project, natural fibers where studied as a potential alternative, it was found that flax fibers have comparable mechanical properties to glass fibers and have a low ecological footprint. Yet, natural fibers are rare in the composite industry and are mainly found today in components with low mechanical loads. This is due to the fact that their properties are not fully exploited. Flax fibers are currently used as yarn, but the spinning process of flax fiber is costly, it has an important environmental impact and lowers the mechanical properties of the fiber because of the negative effect of twist. Untwisted flax slivers however allow to skip the spinning process. In order to produce a fabric out of untwisted flax sliver, the multiaxial fabric is the most adapted. But the multiaxial warp-knitting machine is only adapted for the processing of synthetic fiber, and since untwisted flax slivers have low cohesion, the sliver tends to slip apart during the process. This project aim was to create a new weft-insertion system adapted for the processing of untwisted flax slivers. To design this new system, the design guideline VDI 2221 was followed. A requirements list was firstly made, setting up the limitations and objectives for the new-weft insertion system. Five central functions were deducted from the system, the transportation from the creel to the weft insertion system, the guidance of the sliver, the spreading of the sliver, the laying and fixation of the sliver to the lay-in unit. Partial solutions were designed for guiding the sliver and spreading it. The solutions were evaluated, and a roller guiding system with an air spreading device was selected. A preliminary test was made on a test stand, the sliver width could be controlled, and the coefficient of variation reduced. The solution was validated, and influential parameters were found, such as the process speed, the height of the sliver over the air spreading device, the air pressure, the distance between the bars fixating the sliver over the air spreading device and the width of the lateral plate limitation. The concept was modelized in order to build it and a kinematic study took place for the determination of the maximum accelerations and maximum velocities of the machine so to find the most adapted motor to drive the shafts that guide the slivers. Industrial drawings were made in order to produce the components of the new device, but the construction time exceeded the premeditated time and so the system could not be built. In continuation of this project, a characterization of the sliver after being processed through the new insertion system should be proceeded, in order to identify the effects on the sliver and to adjust the settings of the system accordingly. A qualitative examination of the processed sliver must be carried out, as the width and variation coefficient of the sliver

after spreading was evaluated only quantitatively in the course of this work. Also, an important project that should be carried on, once the new weft insertion is tested is the development of a new lay-in unit, by optimizing the hook chain system.

Bibliography

Ahmad, F., Choi, H. S. and Park, M. K. (2015) 'A review: Natural fiber composites selection in view of mechanical, light weight, and economic properties', *Macromolecular Materials and Engineering*, 300(1), pp. 10–24. doi: 10.1002/mame.201400089.

Antop Global Technology Co. (2017) *The application advantage of GFRP*. Available at: http://www.antopgfrp.com/info/the-application-advantage-of-gfrp-20195847.html.

Autar K. Kaw (2006) *Mechanics of Composite Materials*, *Taylor & Francis Group, LLC*. doi: 10.1016/j.fsigen.2011.07.001.

Barnes, F. and Composites World (2016) 'Recycled carbon fiber: Its time has come'. Available at: https://www.compositesworld.com/columns/recycled-carbon-fiber-its-time-has-come-.

Bledzki, A. K. and Gassan, J. (1999) 'Composites reinforced with cellulose based fibres', in *Progress in Polymer Science*, pp. 221–274.

Bogetti TA, Gillespie JW, L. M. (1992) 'Influence of ply waviness on the stiffness and strength reduction on composite laminates', *Journal of Thermoplastic Composite Materials*.

Brünig, H. and Beyreuther, R. (2006) *Dynamics of fibre formation and processing: Modelling and application in Fibre and Textile Industry*.

Cherif, C. (2015) *Textile Materials for Lightweight Constructions: Technologies - Methods - Materials - Properties*.

Cnc, C. M. A. X. (2003) 'Tricot Machine with Multiaxial Weft Insertion', pp. 1–8.

Composites World (2009) *The making of glass fiber: The old art behind this industry's first fiber reinforcement is explained, with insights into new fiber science and future developments.* Available at: https://www.compositesworld.com/articles/the-making-of-glass-fiber.

Composites World and Gardinier, G. (2018) *How is tow spread?* Available at: https://www.compositesworld.com/articles/how-is-tow-spread.

Dai, Q. *et al.* (2015) 'Life-Cycle Analysis Update of Glass and Glass Fiber for the GREET Model', (September), p. 25.

Das, S. *et al.* (2016) 'Global Carbon Fiber Composites Supply Chain Competitiveness Analysis', (May). doi: 10.2172/1333049.

Das, S. and Warren, J. (2014) *Energy Analysis of Polyolefin-Based Carbon Fiber – Case Study for Lighten-Up Tool*.

Delft University (2001) *Natural Fibre Composites in Structural Components: Alternative Applications for Sisal?* Available at: http://www.fao.org/docrep/004/Y1873E/y1873e0a.htm.

Deng, Y. and Tian, Y. (2015) 'Assessing the environmental impact of flax fibre reinforced polymer composite from

a consequential life cycle assessment perspective', *Sustainability (Switzerland)*, 7(9), pp. 11462–11483. doi: 10.3390/su70911462.

Diener, J. and Siehler, U. (1999) *Ökologischer Vergleich von NMT- und GMT-Bauteilen*.

Dissanayake, N. P. J. *et al.* (2009) 'Energy use in the production of flax fiber for the reinforcement of composites', *Journal of Natural Fibers*, 6(4), pp. 331–346. doi: 10.1080/15440470903345784.

Dissanayake NPJ, et al. (2009) 'Life cycle impact assessment of flax fibre for the reinforcement of composites', in *Biobased Mater Bioenergy*.

DOE (2002) *Energy and environmental profile of the U.S. glass industry.* Available at: http://www.nrel.gov/docs/fy02osti/32135.pdf.

Dr Elmar Witten, T. K. (2014) 'Composites Market Report 2014', (September), pp. 1–44.

Ebel, C., Brand, M. and Drechsler, K. (2013) 'Effects of Fiber Damage on the Efficiency of the Braiding Process', *TexComp-11*, (September 2013). doi: 10.13140/2.1.2473.9840.

EC (European Commission) (2009) 'Regulation (EC) No 443/2009 Of The European Parliament And Of The Council (Amended by EU No 397/2013 and EU No 333/2014)', *Official Journal of the European Communities*, 2009(443), pp. 1–27. doi: 2004R0726 - v.7 of 05.06.2013.

ELG Carbon Fibre Ltd (2018) *Why recycle?*

Energetics Incorporated (2016) 'Bandwidth Study on Energy Use and Potential Energy Saving Opportunities in the Manufacturing of Lightweight Materials: Carbon Fiber Reinforced Polymer Composites''.

Faurecia (2016) *Composite materials: leading the way to lightweight vehicles*. Available at: http://www.faurecia.com/en/decryptage-french/allegement.

FlexForm Technologies (2013) *Some History on Natural Fiber*. Available at: http://www.naturalfibersforautomotive.com/?p=62.

Food and Agriculture Organization of the United Nations (2016) *Crops Database*. Available at: http://faostat.fao.org/site/567/default.aspx#ancor.

Goutianos, S. *et al.* (2006) 'Development of flax fibre based textile reinforcements for composite applications', *Applied Composite Materials*, 13(4), pp. 199–215. doi: 10.1007/s10443-006-9010-2.

Grand View Research (2016) *Natural Fiber Composites Market Analysis By Raw Material, By Matrix, By Technology, By Application And Segment Forecasts to 2024*.

Groupement National Interprofessionnel des Semences (GNIS) (2006) 'Lin textile et societé', pp. 10–11.

'Heckle' (1989) *The Oxford English Dictionary*. Available at: https://en.wikipedia.org/wiki/Heckling_(flax).

HENRY, Todd C., RIDDICK, Jaret C., EMERSON, Ryan P., et al. (2015) *Characterization of the Effect of Fiber Undulation on Strength and Stiffness of Composite Laminates*.

Henry TC, Bakis CE, S. E. (2015) 'Determination of effective ply-level properties of filament wound composite tubes loaded in compression', *Journal of Testing and Evaluation*.

Hipp P, J. D. (1992) 'Design and analysis of filament-wound cylinders in compression', in *33rd AIAA/ASME/ASCE/AHS/ASC Structures, Structural Dynamics, and Material Conference*. Dallas, TX.

ICICI (2015) *Lightweight composites: Vital cog in the CO2 emission reduction blueprint*. Available at: http://content.icicidirect.com/mailimages/composites.htm.

International Textile Manufacturers Federation (Hrsg.) (2012) *International Production Cost Comparison*. Zürich.

Irfan, M. S. *et al.* (2012) 'Lateral spreading of a fiber bundle via mechanical means', *Journal of Composite Materials*, 46(3), pp. 311–330. doi: 10.1177/0021998311424624.

Jänsch, J. (2006) *The development of the guideline VDI 2221*, *The Association of German Engineers*.

JEC (2012) *Flax and Hemp fibres: a natural solution for the composite industry*.

JEC (2014) 'Flax and hemp composites'.

Jensen D, P. S. (1993) 'Influence of local fiber undulation on the global buckling of filament-wound cylinders', *Journal of Reinforced Plastics and Composites*.

Klein, W. (2016a) *The Rieter Manual of Spinning – Volume 3: Spinning Preparation*.

Klein, W. (2016b) *The Rieter Manual Spinning - Volume 1: Technology of short-staple spinning*.

Klein, W. and Rieter Machine Works (2008) *Technology of Short-Staple Spinning: Winterthur*.

Koenig, R. (2014) 'Das "Spinn-Strick-Verfahren" – eine bahnbrechende Innovation auf dem Gebiet der Maschenwarenherstellung', in *Vortrag auf dem Maschenkolloquium*. Institut für Textil- und Verfahrens-technik, Denkendorf.

Kozlowski, R. (2012) *Handbook of natural fibers, volume 2: Processing and applications*.

Kühnel, M. and Kraus, T. (2015) 'The global CFRP market 2015', *1st International Composite Congress (ICC)*.

Kyosev, Y. (2016) *Braiding Technology for Textiles: Principles, Design and Processes*.

Laboratory, M. S. (2012) 'Composite / Steel Cost Comparison Lecture Notes'.

Leong, Y. W. *et al.* (2014) *Compression and injection molding techniques for natural fiber composites*, *Natural Fibre Composites*. Woodhead Publishing Limited. doi: 10.1533/9780857099228.2.216.

Lewin M. (2007) *Handbook of fiber chemistry, 3rd edn*. Taylor & F.

LIBA Maschinenfabrik Gmbh (1983) 'US 4677831: Apparatus for laying transverse weft threads for a warp knitting machine'.

Lomov, S. V.; Baets, J. (2012) *Architecture of textile reinforcements and prop-erties of composites; in Flax and Hemp fibres: a natural solution for the composite industry*.

Lord, P. (2003) *Handbook of yarn production: technology, science and economics*.

Mazumdar, S. *et al.* (no date) *State of the Composites Industry Report for 2017*.

McConnell, V. (2008) 'The making of carbon fiber', *Composites World*.

Mosiniak, M. and Prat, R. (2005) *La culture du lin*. Available at: http://www.snv.jussieu.fr/bmedia/textiles/07-lin-culture.html.

Nad, L., Kolleger, J. and Horvatits, J. (2007) *GFRP and CFRP for civil applications*.

NF EN 13473: Spécifications pour les tissus multi-axiaux multicouches (2001).

NPTEL (2012) *EVENNESS*. Available at: http://nptel.ac.in/courses/116102029/33.

NPTEL (2013a) 'Glass fibre'. Available at: http://nptel.ac.in/courses/116102006/9.

NPTEL (2013b) *Manufacturing of carbon fibers*. Available at: http://nptel.ac.in/courses/116102006/5.

Pai SP, J. D. (2001) 'Influence of fiber undulations on buckling of thin filament-wound cylinders in axial compression', *Journal of Aerospace Engineering*.

Pico, D.; Wilms, C.; Seide, G.; Gries, T.; Tiesler, H.; Kleinholz, R. (2016) 'Glass Fibers', in *Ullmann's Encyclopedia of Industrial Chemistry*.

Ramaswamy, R.; Aslan, B.; Raina, M.; Gries, T. (2012) 'Biocomposites: Processing of blends of thermoplastic biopolymer fiber and industrial natural fibres', in *12th World Textile Conference AUTEX, Zadar, Croatia*.

'Retting' (2009) *Encyclopedia Britannica*.

Rinberg, R. (2012) *Technologieentwicklung zur Herstellung von naturfaserver-stärkten Bauteilen in Leichtbauweise unter Einsatz von Ganzpflanzen-rohstoffen*.

Robert Crow, J. L. R. (2015) 'Carbon fibre applications in mass-produced automotive structures', in *Franco-British Symposium on Composite Materials*.

Rue, D. *et al.* (2007) 'Industrial glass bandwidth analysis', *Gas Technology Institute, ...*, (August), p. 51. Available at: http://www.gmic.org/Final Industrial Glass Bandwidth Analysis 2007.pdf.

Ruth Heuss *et al.* (2012) 'Lightweight, heavy impact - How carbon fiber and other lightweight materials will develop across industries and specifically in automotive', pp. 1–24.

Ruth, M. (1997) *An industrial ecology of the US glass industry*.

Saint-Gobain (2018) *Glass fiber production: Energy consumption*. Available at: https://www.vetrotextextiles.com/technologies/fiberglass-manufacturing.

Sanjay, M. R. *et al.* (2016) 'Applications of Natural Fibers and Its Composites: An Overview', *Natural Resources*, 07(03), pp. 108–114. doi: 10.4236/nr.2016.73011.

Schaefer (2018) *Selecting a Nip Roll Machine*. Available at: http://www.niprolls.com/selecting.html.

Schnabel, A. and Gries, T. (2011a) 'Production of non-crimp fabrics for composites', in *Non-Crimp Fabric Composites*.

Schnabel, A. and Gries, T. (2011b) *Production of non-crimp fabrics for composites*, *Non-Crimp Fabric Composites: Manufacturing, Properties and Applications*. Woodhead Publishing Limited. doi: 10.1016/B978-1-84569-762-4.50001-1.

'Scutch' (1989) *The Oxford English Dictionary*.

Seu, M. R. (2014) 'Production Process of Non Crimp Fabrics [NCF] for aviation applications'.

Shah, D. U., Schubel, P. J. and Clifford, M. J. (2013) 'Can flax replace E-glass in structural composites? A small wind turbine blade case study', *Composites Part B: Engineering*. Elsevier Ltd, 52, pp. 172–181. doi: 10.1016/j.compositesb.2013.04.027.

Shah DU, Schubel PJ, Clifford MJ, et al. (2011) 'Mechanical characterization of vacuum infused thermoset matrix composites reinforced with aligned hydroxyethylcellulose sized plant bast fibre yarns', in *4th International Conference on Sustainable Materials, Polymers and Composites*. Birmingham, UK.

Song, Y. S., Youn, J. R. and Gutowski, T. G. (2009) 'Life cycle energy analysis of fiber-reinforced composites', *Composites Part A: Applied Science and Manufacturing*. Elsevier Ltd, 40(8), pp. 1257–1265. doi: 10.1016/j.compositesa.2009.05.020.

Soulat (2015) 'Composite class'. Roubaix.

Sparnins, E. (2006) *Mechanical properties of flax fibers and their composites*, *Campuscorner.Fibre2Fashion.Com*. Available at: http://campuscorner.fibre2fashion.com/publications/1/25/mechanical-properties-of-flax-fibers-and-their-composites6.asp.

Statista (2018) *Global glass fiber demand and capacity 2011 and 2016*. Available at: https://www.statista.com/statistics/759404/worldwide-glass-fiber-demand-and-capacity/.

Steuernagel, L. (2014) *Natural Fiber Reinforced Plastics – Effect of Injection Moulding and Primer on Mechanical Properties*.

Stromberg (2012) *GFRP - Glass Fiber Reinforced Polymer*. Available at: https://www.strombergarchitectural.com/materials/gfrp.

Summerscales, J. and Grove, S. (2014) *Manufacturing methods for natural fibre composites*, *Natural Fibre Composites*. Woodhead Publishing Limited. doi: 10.1533/9780857099228.2.176.

Sunter, D. A. *et al.* (2015) 'the Manufacturing Energy Intensity of Carbon Fiber Reinforced Polymer Composites and Its Effect on Life Cycle Energy Use for Vehicle Door Lightweigting', (July), pp. 19–24.

Suzuki, T. and Takahashi, J. (2005) 'Prediction of Energy Intensity of Carbon, Fiber Reinforced Plastics for Mass-Produced Passenger Cars', in *9th Japan, International SAMPE Symposium*.

Ticoalu, A., Aravinthan, T. and Cardona, F. (2010) 'A Review of Current Development in Natural Fiber Composites for Structural and Infrastructure Applications', in *Southern Region Engineering Conference*. Towoomba.

Tuf-Bar (2018a) *Advantages of using Glass Fiber Reinforced Polymer (GFRP) rebar*. Available at: https://www.tuf-bar.com/advantages-of-using-glass-fiber-reinforced-polymer-gfrp-rebar/.

Tuf-Bar (2018b) *Civil engeneering applications of GFRP bars*. Available at: https://www.tuf-bar.com/civil-engineering-applications-of-gfrp-bars/.

Turunen, L. and Van der Werf, H. M. G. (2008) *The environmental impacts of the production of hemp and flax textile yarn. Industrial Crops and Products*.

University of Arkansas (2016) *Advantages and Disadvantages of Carbon Fiber Reinforcement Polymer*. Available at: https://studymoose.com/advantages-and-disadvantages-of-carbon-fibre-reinforcement-polymer-essay.

USTER (2016) 'Uster Technologies AG , Textile Laboratory Testing Services', pp. 1–7.

Verpoest, I. (2012) *A general introduction to composites, highlighting the ad-vantages of flax & hemp composites; in Flax and Hemp fibres: a natural solution for the composite industry*.

Wallenberger, F. T., Watson, J. C. and Hong, L. (2001) 'Glass Fibers', *ASM Hanbook*, 21(Ref 19), pp. 27–34. doi: 10.1361/asmhba0003353.

Whiteside, D. (2007) 'Basics of web tension control summary', *Polymers, Laminations, Adhesives, Coatings, Extrusions*, 1, pp. 292–314. Available at: http://www.scopus.com/inward/record.url?eid=2-s2.0-51849093009&partnerID=tZOtx3y1.

Worrell, E. *et al.* (2008) *Energy efficiency improvement and cost saving opportunities for the glass industry.* Available at: http://www.energystar.gov/ia/business/industry/Glass-Guide.pdf.

Yamamoto, K., Yamatsuta, K. and Abe, Y. (1988) 'EP0292266 A2: Spreading fibre bundle'.

ZOLTEK (2018) *How is Carbon Fiber Made?* Available at: http://zoltek.com/carbon-fiber/how-is-carbon-fiber-made/.

ANNEX 1: Unevenness F-Flax and G-Flax

USTER® TESTER 5 - S800 R 5.7 Seite 1
Fr 16.03.18 10:09

TU	UT5-1	Katalog	U1	Garnart	Flachsband
Laborant	J. Hass	Proben ID	03215	Nom. Feinheit	5.1 ktex
Forschungsprojekt	AiF HyperNFK	Tests	1 / 1	Nom. Drehung	0 T/m
Artikel	Flachs	Langstapel		Messschlitz	1
Kommentar	A2018_127			v= 25 m/min	
				t= 5 min	

Einzelwerte und Diagramme

Total Prüfungen : 1 / 1 Einzeltest(s)

Nr	U% %	CVm %	CVm 1m %	CVm 3m %	CVm 10m %	Dünn -30% /km	Dünn -40% /km	Dünn -50% /km	Dick +35% /km	Dick +50% /km	Niss +140% /km	Niss +200% /km	Niss +400% /km	Feinh. Rel. ± %
Band A	14.31	17.78	4.75	3.09										0.0
Mw	14.31	17.78	4.75	3.09										0.0
CV														
Q95														

Nr	Index	H	sh	sh 1m	sh 3m	2DØ	CV2D 8mm %	s2D 8mm	CV2D 0.3mm	CV FS %	CV1D 0.3mm	Shape	D (nom) g/cm3
Band A	40.15												
Mw	40.15												
CV													
Q95													

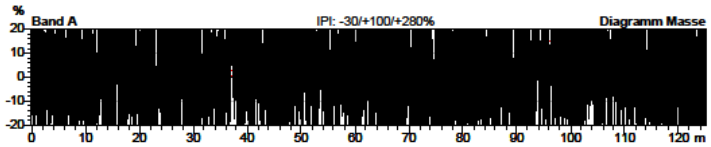

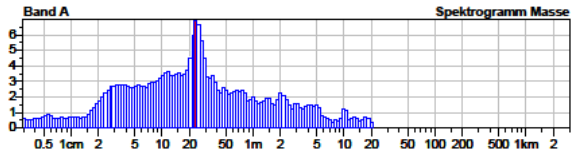

USTER® TESTER 5 - S800 R 5.7 Seite 1

TU	UT5-1	Katalog	U1	Garnart	Flachsband
		Proben ID	03252	Nom. Feinheit	8.93 ktex
		Tests	1 / 1	Nom. Drehung	0 T/m
Artikel	Flachs	Langstapel		Messschlitz	1
Kommentar	A 2018_236_C			v= 25 m/min	
				t= 5 min	

Einzelwerte und Diagramme

Total Prüfungen : 1 / 1 Einzeltest(s)

Nr	U% %	CVm %	CVm 1m %	CVm 3m %	CVm 10m %	Dünn -30% /km	Dünn -40% /km	Dünn -50% /km	Dick +35% /km	Dick +50% /km	Niss +140% /km	Niss +200% /km	Niss +400% /km	Feinh. Rel. ± %
Flachs	13.23	16.92	6.60	3.17										0.0
Mw	13.23	16.92	6.60	3.17										0.0
CV														
Q95														

Nr	Index	H	sh	sh 1m	sh 3m	2DØ	CV2D 8mm %	s2D 8mm	CV2D 0.3mm	CV FS %	CV1D 0.3mm	Shape	D (nom) g/cm3
Flachs	50.57												
Mw	50.57												
CV													
Q95													

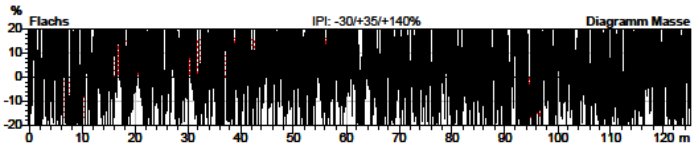

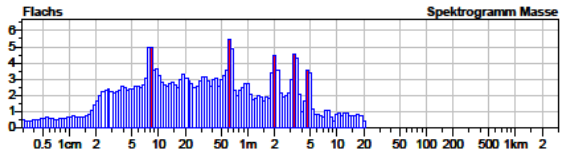

ANNEX 2: Mechanical characterization Sliver F-Flax and G-Flax

Textechno 20.03.2018/3307 Seite 1

TEXTECHNO H. STEIN
41066 Mönchengladbach
STATIMAT 4U
Haft/Gleit-Prüfung

ITA | RWTH AACHEN UNIVERSITY

Datum/Prüfnummer	20.03.2018/3307	Material	Flachs Faserband
Auftraggeber	C. Uthemann	Prüfauftrag	2018_127
Prüfer	M. Steffens	Klima	klimatisiert
Projekt	AiF Hyper NFK	Klemmenbelag	Haft-Gleit-Klemme
Bemerkung	Stapellänge:unknown	Bemerkung	Lo = 3fache Stapellänge

Gruppe: Gruppe8 (Haft-Gleit-Prüfung)

Haft/Gleit-Prüfung

Gerät	STATIMAT 4U			Seriennummer	38141
	Messkopf	100	N	Seriennummer	38498
Haft/Gleit-Prüfung	Einspannlänge	240,0	mm	Prüfgeschwindigkeit	20 mm/min
	Vorspannung	0,00	cN		

Spule **Material A** 10 Versuche 0 gelöscht 0 ausgeblendet

Versuch Nr.	E(Fmax) %	Kraft N	Zeit sec	Gewicht g	Haftlänge m
1	2,04	18,59	175,3	1,240	366,98
2	3,14	18,22	167,8	1,225	364,14
3	0,94	14,02	194,9	1,208	284,13
4	1,45	16,90	238,6	1,155	356,12
5	1,26	22,82	196,6	1,193	468,35
6	1,23	25,23	145,2	1,193	517,80
7	1,00	19,29	179,4	1,238	381,35
8	1,74	19,26	208,4	1,172	402,20
9	0,82	18,66	178,6	1,164	392,54
10	0,89	16,51	151,6	1,217	332,17

atistik Spule Material A	-N-	-X-	-S-	-CV-	-Q-	-MIN-	-MAX-
Höchstzugkraft	10	18,95 N	3,16	16,68	2,26	14,02	25,23
Zeit (Ebruch)	10	183,66 sec	27,49	14,97	19,66	145,18	238,64

Kraft/Dehnungs-Diagramm

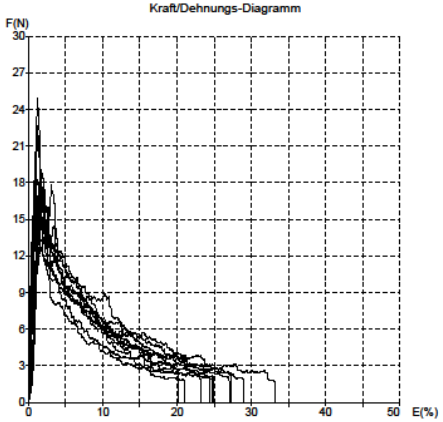

Textechno 02.07.2018/3529 Seite 1

TEXTECHNO H. STEIN
41066 Mönchengladbach
STATIMAT 4U
Haft/Gleit-Prüfung

ITA | RWTH AACHEN UNIVERSITY

Datum/Prüfnummer	02.07.2018/3529	Material	Flachs Faserband
Auftraggeber	C. Uthemann	Prüfauftrag	2018_236
Klima	klimatisiert		
Projekt	AiF Hyper NFK_A	Klemmenbelag	Haft-Gleit-Klemme
Bemerkung	Stapellänge:unknown	Bemerkung	Lo = 3fache Stapellänge

Gruppe: Gruppe8 (Haft-Gleit-Prüfung)

Haft/Gleit-Prüfung

Gerät	STATIMAT 4U			Seriennummer	38141
	Messkopf	100	N	Seriennummer	38498
Haft/Gleit-Prüfung	Einspannlänge	240,0	mm	Prüfgeschwindigkeit	20 mm/min
	Vorspannung	0,00	cN		

Spule **Flachsband 8,93 ktex** 10 Versuche 0 gelöscht 0 ausgeblendet

Versuch Nr.	E(Fmax) %	Kraft N	Zeit sec	Gewicht g	Haftlänge m
1	5,04	8,49	164,5	2,038	102,01
2	2,22	9,64	124,5	2,106	112,02
3	1,73	12,52	170,5	2,082	147,16
4	1,58	11,14	176,9	2,183	124,97
5	1,88	14,10	205,4	1,923	179,54
6	1,16	8,66	166,0	2,180	97,20
7	2,07	8,00	145,7	1,895	103,35
8	1,07	7,82	250,8	2,113	90,55
9	1,64	11,63	145,7	2,067	137,78
10	1,89	11,21	210,5	2,314	118,63

Spule Flachsband 8,93 ktex	-N-	-X-	-S-	-CV-	-Q-	-MIN-	-MAX-
Höchstzugkraft	10	10,32 N	2,12	20,57	1,52	7,82	14,10
Zeit (Ebruch)	10	176,05 sec	37,12	21,09	26,55	124,48	250,83

Kraft/Dehnungs-Diagramm

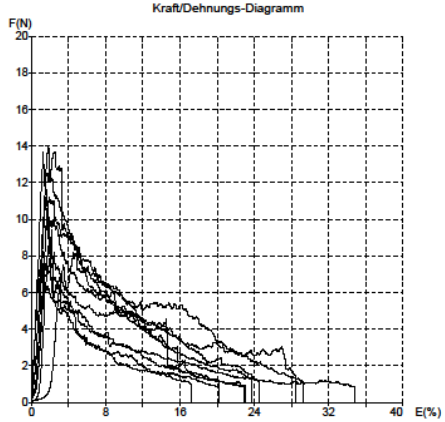

ANNEX 3: Mechanical characterization Fiber F-Flax and G-Flax

Textechno 29.03.2018/3272 Seite 1

Institut für Textiltechnik
RWTH AAchen
FAVIMAT+ FIBRE TEST
Prüfprotokoll

ITA | RWTH AACHEN UNIVERSITY

Datum/Prüfnummer	29.03.2018/3272	Prüfer:	F. Krings
Auftragsnr.:	A 2018 127	Material:	Flachs Bastfasern
Auftraggeber:	C. Uthemann	Klemmenbelag:	Plexiglas/Plexiglas
Projekt:	AiF HyperNFK	Klemmendruck:	4
ohne [g/cm³]:	1,4		
Bemerkung:	klimatisiert		

Gruppe: Carbon_25mm (Carbon_25mm)

1. Allgemeine Parameter

Gerät	Favimat+		Seriennummer	39244	
Messkopf	1200	cN	Seriennummer	27402489	
Fenster geschlossen	Ja				
Klemmen Type	Klemme (4mm)				

2. FAVIMAT+ Faserprüfung

Einspannlänge	25,0	mm			
Feinheit	10,77	dtex	Dichte	1,40	g/cm³

Zugversuch

Prüfgeschwindigkeit	2,5	mm/min	Vorspannung	0,50	cN/tex
Kraftschwelle	0,10	%	Kraftabfall	50,0	%

Probe **Material A** 50 Versuche 0 gelöscht 0 ausgeblendet 0 Versuch nicht möglich

1. FAVIMAT+ Faserprüfung

Versuch	Dehnung %	Kraft cN	Fein.Kr. cN/tex	Br.spann. GPa	R.Arbeit cN*cm	RZeit sec	Feinh. dtex	Durch. µm
							10,77	31,30
1	2,21	171,86	159,57	2,23	4,252	13,4		
EAR	2,23	85,93	79,79		4,316			
2	1,58	135,30	125,63	1,76	2,439	9,7		
EAR	1,62	67,65	62,81		2,533			
3	1,55	110,80	102,88	1,44	2,245	9,5		
EAR	1,58	55,40	51,44		2,292			
4	2,20	45,37	42,12	0,59	1,044	13,4		
EAR	2,23	22,68	21,06		1,068			
5	1,22	51,32	47,65	0,67	0,697	9,9		
EAR	1,66	25,66	23,83		1,151			
6	1,22	64,02	59,44	0,83	1,006	8,6		
EAR	1,43	32,01	29,72		1,320			
7	1,39	108,17	100,44	1,41	1,955	9,4		
EAR	1,56	54,09	50,22		2,312			
8	1,92	23,87	22,16	0,31	0,723	11,7		
EAR	1,95	11,94	11,08		0,650			
9	0,90	35,04	32,54	0,46	0,403	5,6		
EAR	0,93	17,52	16,27		0,418			
10	2,37	227,71	211,43	2,96	5,947	14,5		
EAR	2,41	113,86	105,72		6,104			
11	0,90	38,80	36,02	0,50	0,418	6,3		
EAR	1,04	19,40	18,01		0,526			
12	2,54	604,24	561,04	7,85	18,91	16,8		
EAR	2,80	302,12	280,52		22,06			
13	1,71	54,99	51,06	0,71	0,905	10,4		
EAR	1,73	27,50	25,53		0,928			
14	1,44	164,93	153,14	2,14	2,897	9,5		
EAR	1,59	82,46	76,57		3,212			
15	0,40	4,05	3,76	0,05	0,025	2,5		
EAR	0,42	2,03	1,88		0,027			
16	1,83	128,22	119,06	1,67	2,705	11,2		
EAR	1,87	64,11	59,53		2,816			
17	1,48	42,24	39,22	0,55	0,749	9,0		
EAR	1,51	21,12	19,61		0,767			
18	0,80	34,98	32,48	0,45	0,368	4,9		
EAR	0,82	17,49	16,24		0,382			
19	1,05	113,78	105,65	1,48	1,365	6,5		
EAR	1,08	56,89	52,82		1,408			
20	2,20	326,70	303,34	4,25	7,983	13,5		
EAR	2,24	163,35	151,67		8,246			
21	1,76	275,06	255,40	3,58	5,931	11,0		
EAR	1,83	137,53	127,70		6,308			
22	1,78	246,68	229,04	3,21	5,133	11,8		

Textechno 29.03.2018/3272 Seite 2

EAR	1,97	123,34	114,52		5,845	
23	1,05	65,33	60,66	0,85	0,775	6,4
EAR	1,07	32,67	30,33		0,798	
24	1,90	49,46	45,92	0,64	1,249	11,6
EAR	1,93	24,73	22,96		1,253	
25	1,14	49,45	45,92	0,64	0,884	7,0
EAR	1,17	24,73	22,96		0,706	
26	1,85	72,83	67,63	0,95	1,343	11,4
EAR	1,89	36,42	33,81		1,405	
27	1,67	116,09	107,79	1,51	3,192	10,4
EAR	1,73	58,04	53,89		3,117	
28	2,07	79,23	73,56	1,03	1,877	14,0
EAR	2,34	39,61	36,78		2,225	
29	3,47	790,07	733,58	10,27	30,31	21,1
EAR	3,51	395,03	366,79		30,97	
30	1,28	34,60	32,12	0,45	0,543	8,9
EAR	1,48	17,30	16,06		0,643	
31	1,84	234,28	217,53	3,05	5,300	11,2
EAR	1,87	117,14	108,76		5,398	
32	2,16	133,38	123,84	1,73	3,767	13,1
EAR	2,18	66,69	61,92		3,822	
33	1,38	82,61	76,70	1,07	1,478	9,4
EAR	1,56	41,31	38,35		1,779	
34	2,20	468,14	434,67	6,09	11,82	13,6
EAR	2,27	234,07	217,34		12,48	
35	1,10	51,19	47,53	0,67	0,658	6,8
EAR	1,13	25,59	23,76		0,679	
36	2,95	67,91	63,05	0,88	2,320	17,8
EAR	2,97	33,95	31,53		2,316	
37	3,49	495,73	460,29	6,44	19,07	21,1
EAR	3,52	247,86	230,14		19,37	
38	1,26	48,83	45,34	0,63	0,706	7,7
EAR	1,29	24,42	22,67		0,726	
39	1,86	259,01	240,49	3,37	5,896	11,4
EAR	1,90	129,50	120,25		6,061	
40	0,69	58,83	54,62	0,76	0,499	4,5
EAR	0,75	29,42	27,31		0,561	
41	2,51	371,97	345,37	4,84	11,00	15,2
EAR	2,54	185,98	172,69		11,18	
42	3,09	80,55	74,79	1,05	2,877	18,9
EAR	3,16	40,28	37,40		2,968	
43	1,34	63,81	59,25	0,83	1,016	8,2
EAR	1,37	31,91	29,62		1,041	
44	2,03	90,32	83,86	1,17	2,370	12,3
EAR	2,05	45,16	41,93		2,405	
45	2,07	168,45	156,41	2,19	4,287	12,6
EAR	2,10	84,23	78,20		4,357	
46	1,77	92,39	85,78	1,20	1,801	11,5
EAR	1,92	46,19	42,89		2,021	
47	1,76	26,37	24,49	0,34	0,526	10,7
EAR	1,78	13,19	12,24		0,537	
48	2,40	155,73	144,60	2,02	4,469	14,5
EAR	2,42	77,86	72,30		4,521	
49	1,54	70,62	65,57	0,92	1,439	9,4
EAR	1,57	35,31	32,78		1,465	
50	1,96	240,02	222,86	3,12	6,072	11,9
EAR	1,99	120,01	111,43		6,183	

Statistik	-N-	-X-		-S-	-CV-	-Q(95%)-	-MIN-	-MAX-
Dehnung (Fmax)	50	1,76	%	0,66	37,48	0,19	0,40	3,49
Bruchd.: 50% Fmax	50	1,84	%	0,66	35,72	0,19	0,42	3,52
Höchstzugkraft	50	150,51	cN	159,07	105,69	45,18	4,05	790,07
Kraft; 50% Fmax	50	75,25	cN	79,54	105,69	22,59	2,03	395,03
Fein.Kraft; 50% Fmax	50	69,87	cN/tex	73,85	105,69	20,98	1,88	366,79
Reissarbeit (...Emax)	50	4,11	cN*cm	5,89	143,34	1,67	0,03	30,87
Feinheitsb.Kraft	50	139,75	cN/tex	147,70	105,69	41,95	3,76	733,58
Bruchspannung	50	1,96	GPa	2,07	105,69	0,59	0,05	10,27
Feinheit	1	10,77	dtex					
Durchmesser	1	31,30	µm					
Reisszeit	50	11,04	sec	3,94	35,73	1,12	2,54	21,14

Textechno 11.07.2018/3516 Seite 1

Institut für Textiltechnik
RWTH AAchen
FAVIMAT+ FIBRE TEST
Prüfprotokoll

ITA | RWTH AACHEN UNIVERSITY

Datum/Prüfnummer	11.07.2018/3516	Dichte [g/cm³]	1,4
Auftragsnr.:	A 2018 236 C	Klemmenbelag:	Plexiglas/Plexiglas
Auftraggeber:	C. Uthemann	Klemmendruck:	6
Material:	Flachs		
Klimatisiert:	ja		
Bemerkung:	Die Feinheit 10 dtex ist ungenau.		

Gruppe: Filament_25mm (Filament_25mm)

1. Allgemeine Parameter

Gerät	Favimat+		Seriennummer	39244	
Messkopf	1200	cN	Seriennummer		
Fenster geschlossen	Nein				
Klemmen Type	Klemme (4mm)				

2. FAVIMAT+ Faserprüfung

Einspannlänge	25,0	mm			
Feinheit	10,00	dtex			

Zugversuch

Prüfgeschwindigkeit	2,5	mm/min	Vorspannung	0,50	cN/tex
Kraftschwelle	0,10	%	Kraftabfall	50,0	%

Probe **Flachs** 54 Versuche 0 gelöscht 4 ausgeblendet 0 Versuch nicht möglich

1. FAVIMAT+ Faserprüfung

Versuch	Dehnung %	Kraft cN	Fein.Kr. cN/tex	R.Arbeit cN*cm	RZeit sec	Feinh. dtex
						10
1	1,45	70,06	70,06	1,201	8,9	
EAR	1,48	35,03	35,03	1,227		
2	1,16	18,28	18,28	0,314	7,1	
EAR	1,19	9,14	9,14	0,311		
3	0,85	10,32	10,32	0,119	7,7	
EAR	1,28	5,16	5,16	0,184		
4	0,28	6,14	6,14	0,017	1,8	
EAR	0,31	3,07	3,07	0,019		
5	1,12	42,18	42,18	0,592	6,9	
EAR	1,14	21,09	21,09	0,609		
6	1,19	38,83	38,83	0,543	8,6	
EAR	1,43	19,42	19,42	0,679		
7	2,45	271,90	271,90	7,328	14,8	
EAR	2,47	135,95	135,95	7,323		
8	1,82	73,21	73,21	1,627	11,6	
EAR	1,93	36,60	36,60	1,775		
9	1,18	125,81	125,81	1,816	7,2	
EAR	1,21	62,81	62,81	1,877		
10	0,66	25,93	25,93	0,231	5,9	
EAR	0,98	12,96	12,96	0,353		
11 ausgeblendet						
12	1,37	76,00	76,00	1,381	8,4	
EAR	1,40	38,00	38,00	1,410		
13	1,23	28,91	28,91	0,444	7,5	
EAR	1,26	14,45	14,45	0,454		
14	2,04	125,89	125,89	2,376	12,4	
EAR	2,07	62,95	62,95	2,435		
15	2,41	78,71	78,71	2,212	15,6	
EAR	2,61	39,36	39,36	2,523		
16	1,80	67,55	67,55	1,490	11,0	
EAR	1,83	33,78	33,78	1,522		
17	0,51	12,40	12,40	0,094	3,2	
EAR	0,53	6,20	6,20	0,089		
18	2,98	159,95	159,95	4,554	18,0	
EAR	3,00	79,98	79,98	4,621		
19 ausgeblendet						
20	2,20	82,11	82,11	1,926	13,4	
EAR	2,23	41,05	41,05	1,966		
21	1,02	59,11	59,11	0,655	8,2	
EAR	1,36	29,56	29,56	1,024		
22	1,17	32,21	32,21	0,548	14,5	
EAR	2,42	16,11	16,11	1,217		
23	2,19	48,79	48,79	1,067	13,9	

Textechno 11.07.2018/3516 Seite 2

EAR	2,31	24,40	24,40	1,197		
24	2,89	169,91	169,91	5,148	16,3	
EAR	2,72	84,96	84,96	5,212		
25	1,80	162,77	162,77	4,051	11,0	
EAR	1,83	81,38	81,38	4,088		
26	2,96	193,00	193,00	6,807	17,9	
EAR	2,98	96,50	96,50	6,680		
27	2,75	330,74	330,74	9,612	16,7	
EAR	2,78	165,37	165,37	9,771		
28	1,27	31,77	31,77	0,615	7,8	
EAR	1,30	15,88	15,88	0,623		
29	1,91	233,66	233,66	5,882	12,0	
EAR	2,00	116,83	116,83	6,095		
30	2,16	62,33	62,33	1,596	16,4	
EAR	2,74	31,16	31,16	2,149		
31	2,53	158,18	158,18	4,309	15,3	
EAR	2,56	79,09	79,09	4,373		
32 ausgeblendet						
33	1,87	115,46	115,46	2,609	11,7	
EAR	1,94	57,73	57,73	2,778		
34 ausgeblendet						
35	0,72	10,95	10,95	0,102	4,5	
EAR	0,75	5,48	5,48	0,106		
36	1,52	63,10	63,10	1,185	9,3	
EAR	1,56	31,55	31,55	1,218		
37	1,86	34,06	34,06	0,894	10,1	
EAR	1,89	17,03	17,03	0,707		
38	1,71	58,90	58,90	1,113	11,8	
EAR	1,97	29,45	29,45	1,422		
39	2,45	260,40	260,40	6,991	14,8	
EAR	2,48	130,20	130,20	7,162		
40	1,39	92,23	92,23	1,451	8,5	
EAR	1,41	46,12	46,12	1,488		
41	2,12	143,97	143,97	3,943	13,0	
EAR	2,17	71,99	71,99	3,960		
42	1,45	18,15	18,15	0,351	13,6	
EAR	2,26	9,07	9,07	0,634		
43	2,12	183,40	183,40	4,655	13,9	
EAR	2,31	91,70	91,70	5,201		
44	3,14	236,90	236,90	7,162	19,9	
EAR	3,32	118,45	118,45	7,779		
45	1,10	120,88	120,88	1,741	7,1	
EAR	1,19	60,44	60,44	1,962		
46	0,86	11,97	11,97	0,164	5,3	
EAR	0,89	5,99	5,99	0,162		
47	1,21	44,14	44,14	0,827	7,5	
EAR	1,24	22,07	22,07	0,652		
48	1,95	103,07	103,07	2,176	11,9	
EAR	1,98	51,53	51,53	2,218		
49	2,39	204,92	204,92	4,588	14,5	
EAR	2,42	102,46	102,46	4,673		
50	1,89	116,45	116,45	2,378	12,2	
EAR	2,04	58,23	58,23	3,269		
51	1,10	32,57	32,57	0,406	7,4	
EAR	1,23	16,28	16,28	0,490		
52	2,42	118,48	118,48	3,366	14,9	
EAR	2,49	59,24	59,24	3,526		
53	0,45	15,38	15,38	0,099	4,2	
EAR	0,71	7,69	7,69	0,175		
54	1,06	20,83	20,83	0,281	6,9	
EAR	1,15	10,41	10,41	0,318		

Statistik	-N-	-X-		-S-	-CV-	-Q(95%)-	-MIN-	-MAX-
Dehnung (Fmax)	50	1,67	%	0,71	42,29	0,20	0,28	3,14
Bruchd.: 50% Fmax	50	1,81	%	0,71	38,95	0,20	0,31	3,32
Höchstzugkraft	50	96,05	cN	79,55	82,82	22,59	6,14	330,74
Kraft; 50% Fmax	50	48,03	cN	39,77	82,82	11,30	3,07	165,37
Fein.Kraft; 50% Fmax	50	48,03	cN/tex	39,77	82,82	11,30	3,07	165,37
Reissarbeit (...Emax)	50	2,43	cN*cm	2,39	98,35	0,68	0,02	9,77
Feinheitsb.Kraft	50	96,05	cN/tex	79,55	82,82	22,59	6,14	330,74
Feinheit	1	10,00	dtex					
Reisszeit	50	10,86	sec	4,23	38,95	1,20	1,84	19,89

ANNEX 4: Industrial Drawings

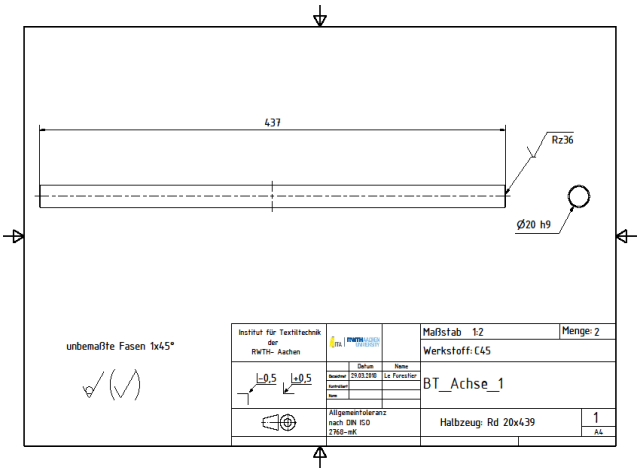

Figure 73 Shaft industrial drawing

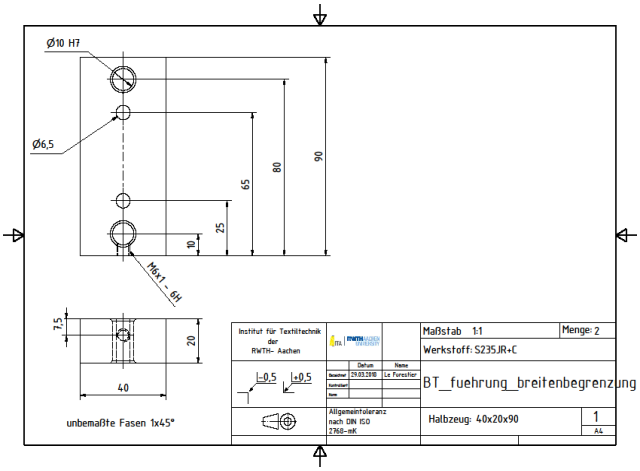

Figure 74 Width limitation bar industrial drawing

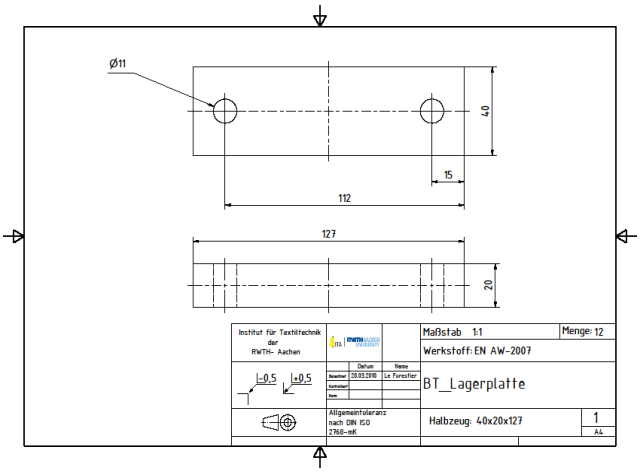

Figure 75 Bearing plate industrial drawing

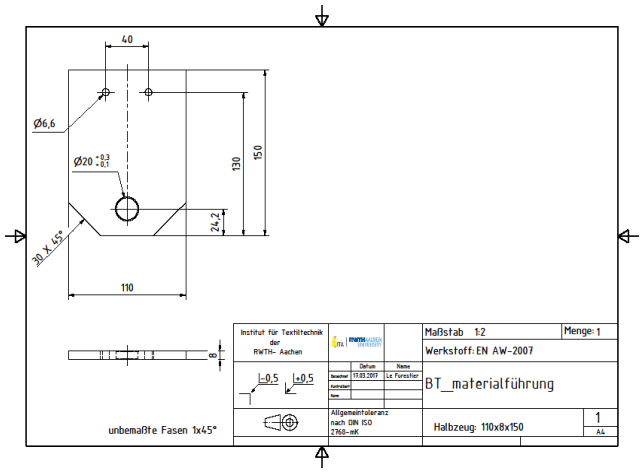

Figure 76 Entrance and exit guidance industrial drawing

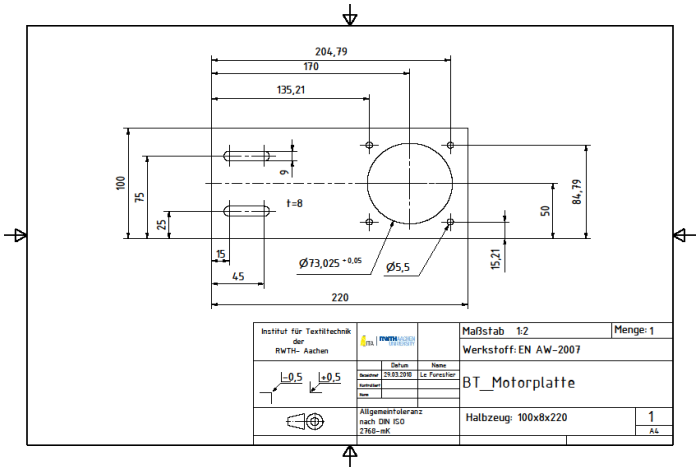

Figure 77 Motor plate industrial drawing

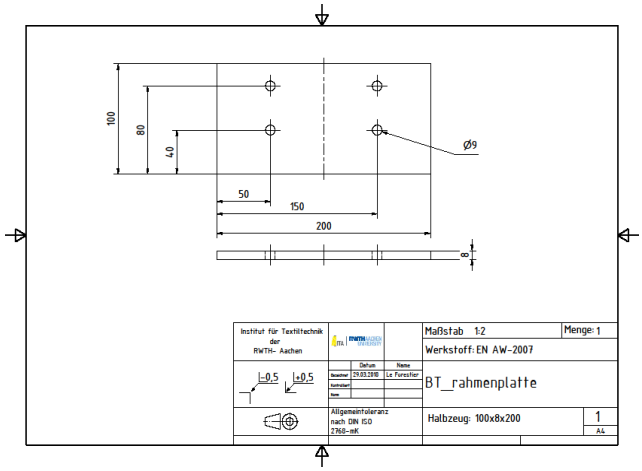

Figure 78 Frame plate industrial drawing

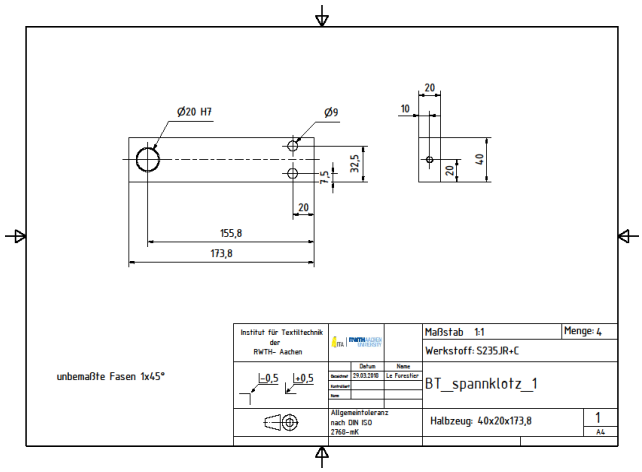

Figure 79 Clamping block industrial drawing

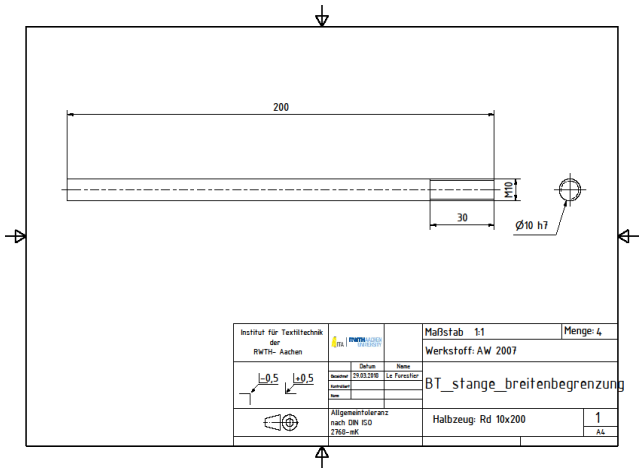

Figure 80 Bar industrial drawing

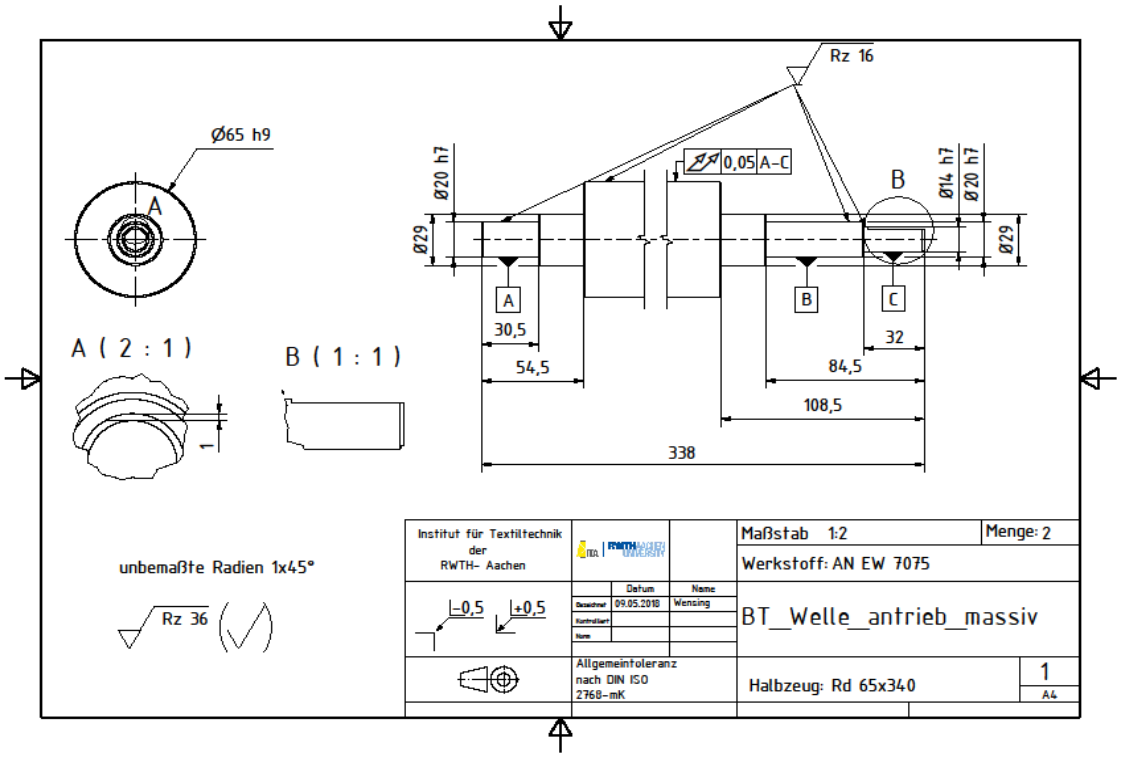

Figure 81 Driving shaft industrial drawing

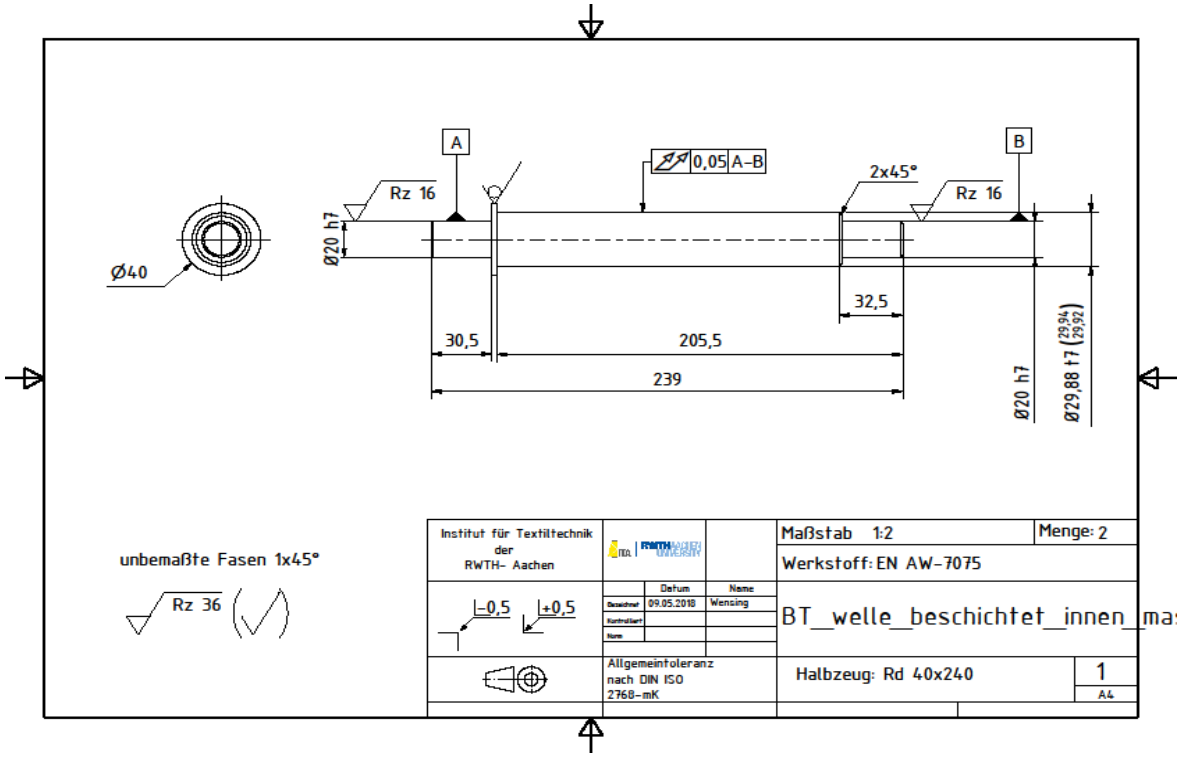

Figure 82 Coated shaft industrial drawing